

Aus dem Lehrstuhl für pharmazeutische Biologie-Biotechnologie
der Ludwig-Maximilians-Universität München

Leitung: Prof. Dr. Ernst Wagner

*Fluorescence labeled PEI-based gene delivery systems for
near infrared imaging in nude mice*

Dissertation
zum Erwerb des Doktorgrades der Medizin
an der Medizinischen Fakultät der
Ludwig-Maximilians-Universität zu München

vorgelegt von

Massimo Concia
aus Varese

2010

Mit Genehmigung der Medizinischen Fakultät
der Universität München

Berichterstatter:	Prof. Dr. Georg Enders
Mitberichterstatter	Prof. Dr. Marc Dellian Priv. Doz. Dr. Anja Ehrhardt
Mitbetreuung durch den promovierten Mitarbeiter:	Dr. Manfred Ogris
Dekan:	Prof. Dr. Dr. h. c. Maximilian Reiser, FACR, FRCR
Tag der mündlichen Prüfung:	04.03.2010

Table of Contents

1 Introduction	1
1.1 Gene therapy	1
1.2 Viral vectors	1
1.3 Non-viral vectors	2
1.4 In-vivo imaging	5
1.4.1 Imaging technologies and their in-vivo applications	5
1.4.2 Bioluminescence	5
1.5 Fluorescence and its in vivo applications	6
1.5.1 Fluorescence and fluorescent dyes	6
1.5.2 Indocyanine green (ICG)	7
1.5.3 Quantum Dots	8
1.6 Aim of the Study	9
2 Materials and methods	10
2.1 Chemicals and reagents	10
2.2 Synthesis of conjugates and polyplexes	10
2.2.1. Synthesis of conjugates	10
2.2.2. Generation of polyplexes	12
2.3 Analysis of transfection complexes	13
2.3.1 Measurement of the particle size	13
2.3.2 Electrophoresis	13
2.4 Cell culture	14
2.5 Animal experiment	15
2.5.1 Animal husbandry	15
2.5.2 Tumor cells implantation	15
2.5.3 Tumor volume measurements	16
2.5.4 Intravenous applications and anesthesia	16
2.5.5 Dissection and organs excision	16
2.6 In vivo imaging procedures	17
2.6.1 In vivo imaging system: imaging adjustments	17
2.6.2 Measurements and data analysis	17
2.6.3 Statistical analysis	17
3 Results	18
3.1 Near infrared fluorescent dyes biodistribution of dyes, conjugates with polycations and pDNA-polyplexes	18

3.1.1 ALEXA 750 and NIR 797 biodistribution of free dyes	18
3.1.1.1 ALEXA 750 free	18
3.1.1.2 NIR 797 free	22
3.1.2 Alexa 750-PEI and Alexa 750-HD O: biodistribution in tumor bearing animals	26
3.1.3 NIR797/PEI: influence of dye/PEI ratio on biodistribution and imaging properties	30
3.1.3.1 NIR 797/PEI conjugates (I)	30
3.1.3.2 NIR 797/PEI conjugates (II)	32
3.2 Near infrared emitting quantum dots as novel tools for bioimaging of polyplexes ..	35
3.2.1 Fluorescent properties of different quantum dots formulations	35
3.2.2 Biodistribution of QD, QD/PEI and QD/pDNA/PEI polyplexes in nu/nu mice	37
3.2.3 Tumor targeting properties of QD labeled polyplexes	43
3.2.3.1 EGF-R targeting in HUH7 Human Hepatocellular Carcinoma (I)	43
3.2.3.2 EGF-R targeting in HUH7 Human Hepatocellular Carcinoma (II)	49
3.2.3.3 EGF-R targeting in HUH7 Human Hepatocellular Carcinoma (III)	54
3.2.3.4 EGF-R targeting in HUH7 Human Hepatocellular Carcinoma (IV)	58
3.2.3.5 Tf-R targeting in N2a Murine Neuroblastoma	60
4 Discussion	67
4.1 Methodological establishments	67
4.2 Fluorescence based in vivo imaging	69
4.2.1 Fluorescent dyes (Alexa 750 and NIR 797) applications	69
4.2.2 Quantum dots applications	70
4.3 Conclusions	70
5a Summary	72
5b Zusammenfassung	73
6 Appendix	74
6.1 Abbreviations	74
7 Acknowledgments	76
8 References	77

*Science may set limits to knowledge,
but should not set limits to imagination.*

Bertrand Russell (1872 - 1970)

1 Introduction

1.1 Gene therapy

Gene therapy is a promising pharmaceutical research field dealing with the insertion of nucleic acids into cells and tissues of an organism to treat neoplastic, metabolic and hereditary diseases^{[1][2][3]}. The nucleic acids used in gene therapy are mostly parts of genes encoding normal versions of mutated, defective or missing proteins responsible for clinical manifestations of many diseases. The insertion and substitution of pathologically altered genes with their normal alternative is the main purpose of this new therapeutic approach. Another possibility is to regulate gene expression on the level of messenger RNA, e.g. by siRNA technology^{[4][5]}. Both approaches need reliable nucleic acid carrier systems which protect the nucleic acids against enzymatic degradation by nucleases and deliver them to the target cells without spreading them to non-target tissues. Designing and testing efficient gene delivering devices is then an essential step in the development of gene therapy strategies.

1.2 Viral vectors

The utilization of viral vectors has been representing an efficient gene delivery device for many years. Viruses seem to be very effective thanks to powerful mechanisms of entering the host's target cells and delivering genetic material into their nuclei^{[6][7]}. Many different viral types have been tested for gene delivery into mammalian organisms. However the viral interaction with the host immune system may cause adverse effects. Neutralizing antibodies may recognize and eliminate viruses causing inflammatory reactions; cells infected by a virus can be recognized as *not self* by the host immune system and eliminated; moreover the presence of viral genome within an organism might lead to severe immune response with adverse effects for the host itself. A further undesirable consequence of virus-mediated transfections is the integration of parts of the viral genome into the host's one with possible activation of oncogenes^[8]. *Adenoviruses*^[9] for example, a family of DNA viruses, show high-rate of gene delivery but most transfected cells are rapidly removed by the immune system^[10]. *Herpes simplex virus* can deliver large amounts of exogenous DNA as well but cytotoxicity and maintenance of transgene expression remain obstacles^[11] in its

application. Other limiting factors are high costs and procedure complexity.

1.3 Non-viral vectors

Non-viral vectors are the alternative to viruses in gene therapy studies because of many favorable characteristics like large-scale production and low immunogenicity. The first experiments using non-viral gene therapy technologies however showed low levels of transfection while general opinion was that viral vectors are more effective despite their many adverse effects. However recent developments in non-viral gene delivery are displaying transfection efficiencies similar to viruses.

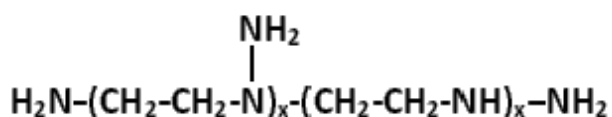
The first and simplest approach to non-viral gene delivery is the application of naked plasmid DNA. Some successful results following intramuscular injection of plasmid DNA have been obtained but the transfection rate was very low. Anyway these experiences contributed to the idea of “protecting” nucleic acids from damage. To this purpose new molecular aggregates, called *lipoplexes* and *polyplexes*, have been synthesized that protect DNA from degradation during the transfection processes. Plasmid DNA or siRNA can be bound to lipids in an organized structure which resembles a micelle or a liposome. Once this organized structure is complexed with DNA it is called a *lipoplex*. Cationic lipids naturally complex with negatively loaded DNA due to their positive charge. In the same way they can electrostatically interact with the cell membrane. As long as endocytosis of the lipoplex occurs, DNA is released into the cytoplasm. These cationic lipids also protect DNA from enzymatic degradation within the cytosol. The most popular application of lipoplexes has been gene transfer into cancer cells. Some studies have shown lipoplexes to be useful in transfecting respiratory epithelial cells, so that they may be utilized in genetic respiratory diseases such as cystic fibrosis^[12] as well as neoplasias^[13].

Polycationic gene delivery systems, called *polyplexes*, are a very promising alternative to lipoplexes. They were at first based on *polylysine* and later on *polyethylenimine* (PEI). PEI was first described by the group of *Jean-Paul Behr* as gene delivering device for mammalian cells^{[14][15]} and is at present the most utilized polycation. PEI contains repetitive *ethylene imine* groups (molecular formula: C₂H₅N) and is available in linear and branched form. *Linear PEI* (PEI lin) contains just secondary amines, in contrast to *branched PEI* (PEI br) which has primary, secondary and tertiary amino groups (*fig. 1* and *2*).

Fig. 1: schematic structure of linear PEI.



Fig. 2: schematic structure of branched PEI.

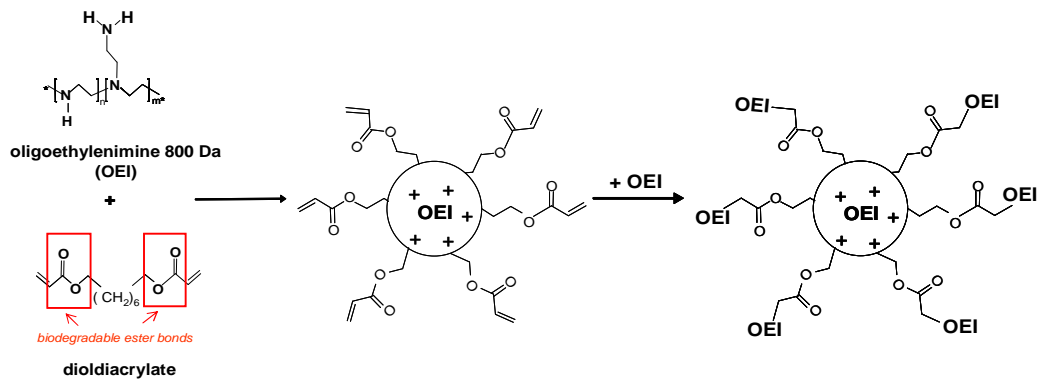


PEI offers high positive charge density and intrinsic buffering capacity that allow good electrostatic binding to negatively charged nucleic acids and efficient compaction of them within the polyplexes. PEI-based polyplexes protect nucleic acids from degradation and enable interactions with negatively loaded cell surfaces triggering the uptake of themselves. PEI enters cells through adhesion to transmembrane heparan proteoglycans^[16] and shows very good transfection capacity in vitro and in vivo^{[17][18][19]}. Many authors^[20] recommend to protect PEI-based gene vectors with molecules masking their positive surfaces to prevent opsonization by the mononuclear phagocytic system and subsequent rapid clearance from circulation. *Polyethylene glycol* (PEG) is a hydrophilic molecule suited for this purpose.

A considerable problem of PEI is its distinctive toxicity observed in vitro^[21] and in vivo^[22] and its unspecific interactions with body structures and fluids^[23]. It can in fact interact with membrane-integrated and circulating proteins and is able to mediate erythrocytes aggregation^[24] and activation of the endothelium particularly within the pulmonary circulation. These toxic properties increase with the density of positive charge and molecular weight of the polycationic chain. The neutralization of positively charged polymers by polyplex formation significantly reduces their toxicity. Besides the acute one the long-term toxicity might be a considerable factor conditioning the clinical applications of these carriers.

Recently other polymers have been synthesized aiming to reduce the unfavorable acute effect of PEI injection. At the *Chair of Pharmaceutical Biotechnology* (LMU, Munich) *oligoethylenimines* (OEI) with low molecular weight cross-linked with degradable linker molecules were designed. The most promising product of this class of molecules was HD O, a OEI 800 Da core modified with *hexane-1,6-diol diacrylate* and surface-modified with OEI 800 Da (*fig. 3*). HD O shares with PEI targeting tumor capacity and is better tolerated in vivo studies^[25] likely owing to its smaller size and biodegradability.

Fig. 3: synthesis and schematic structure of HD O.



1.4 In-vivo imaging

1.4.1 Imaging technologies and their in-vivo applications

Several imaging devices have been developed to check in vivo pharmacodynamic and pharmacokinetic aspects of the interactions between gene carriers and somatic cells. This field has known considerable expansion thanks to well-established imaging technologies including magnetic resonance imaging (MRI), positron emission tomography (PET) and single photon emission tomography (SPECT). Bioluminescence and fluorescence-based labeling of vectors are other powerful strategies for gene delivery^{[26][27][28][29]}. These optical imaging methods are often preferred to MRI and SPECT/PET because they can be performed both in vitro and in vivo studies with simpler study design and cheaper imaging set-ups.

1.4.2 Bioluminescence

Bioluminescence is the emission of light by a living organism as the result of enzymatic reactions. The enzyme *luciferase* is expressed in certain vertebrates and invertebrates and emits visible light by converting the respective substrate to the product. *Firefly* (Fluc) and *Renilla* (Rluc) luciferase genes are responsible for this enzymatic activity and can be transferred to other organisms included in plasmids. The genetic expression of these transgenes and their visible manifestation need *luciferin* as specific substrate and some co-substrates normally contained in cells possessing luciferase enzymatic activity. The interaction between luciferin and luciferase generates visible light which can be detected through imaging devices and expressed as rate of genetic/plasmidic activity. This technology has many attractive applications. It is possible for example to quench the bioluminescence activity of luciferase expressing tumor cells while treating them with siRNA specific for this coding sequence. If we deliver mRNA-specific siRNA into the target cell, the translation of the luciferase gene is blocked and knock-down in photon emission is registered after administration of luciferin.

1.5 Fluorescence and its in vivo applications

1.5.1 Fluorescence and fluorescent dyes

Fluorescence is an optical phenomenon where absorption of a photon by a molecule causes the emission of another photon with longer wavelength. The energy gap between absorbed and emitted photons ends up as molecular vibrations or heat. Fluorescence occurs when molecules or nanostructures relax to their ground state after being electrically excited.

Plenty of biological molecules have strong fluorescent properties due to specific chemical groups (fluorophores) that can be utilized in many different ways. Automated DNA sequencing by chain termination method, DNA detection with ethidium bromide and DNA microarrays for instance are important molecular biology techniques that use fluorescent phenomena. Also in Pathology and Immunology important assays have been developed like fluorescence microscopy of tissues and immunofluorescent tests, commonly used in diagnostics. Concerning cell culture technologies *Fluorescent-Activated Cell Sorting* (FACS) has become a routine investigation method.

In vivo imaging represents a major application of fluorescence for gene therapy. It resembles fluorescence microscopy in that both utilize a low-light camera and collect emission signals through adequate filter combinations. Its object is an animal organism administered with fluorescent labeled molecules and vectors. The aim of this sector is to check and quantify the fluorescence signal intensity coming from the body giving optical data about total-body and organ-specific diffusion, excretion and toxicity. Body imaging presents distinctive features due to the peculiar fluorescence absorption and emission patterns of different organs and tissues. This organism-specific fluorescence is called *auto-fluorescence* and implies that all molecules to be administered have different spectral properties from body tissues and fluids in order to avoid signal loss by overlapping. Other properties of this molecules class are biological stability, preferential accumulation at an intended target site or organ and low toxicity^[30].

The *green fluorescent protein* (GFP) is made up of 238 amino acids and absorbs light between 380 and 488 nm. A cDNA of GFP was first obtained by *Prasher* in 1992^[31]. Afterwards GFP was used as marker for other proteins and became a standard in molecular biology. GFP has great importance in cellular and molecular biology but its applications in vivo imaging are limited because its emission wavelength coincides with some blood pigments such as hemoglobin^[32].

Cy3 and Cy5 of the dye family of *cyanines* can be coupled with different reactive groups with affinity to either nucleic acids or proteins. Cy3 is excited at 550 nm and emits at 570 nm in the red part of the spectrum; Cy5 is excited at 649 nm and emits at 670 nm in the far red part of the spectrum. Both dyes are used in a wide variety of molecular biological applications including comparative genomic hybridization and gene chips. They are also utilized to label proteins for various purposes including proteomics. Owing to their relative distance from the emission patterns of the animal body fluids, Cy3 and Cy5 have some applications in vivo study. However they are not optimal for imaging of rodents due to the strong overlapping spectrum with chlorophyll (emission peaks between 600 and 700 nm) which constitutes the basis of the feeding of these animals. On the contrary near infrared (NIR) dyes are adapted for in vivo imaging of rodents because their emission wavelengths (larger than 700 nm) are located in a biological windows free from overlapping phenomena.

1.5.2 Indocyanine green (ICG)

Indocyanine green (ICG) is a tricyanocyanine dye used intravenously as diagnostic aid for determination of blood volume, cardiac output and hepatic function.

ICG absorption and emission spectra are in the near infrared spectrum (excitation and emission have their maximum at 765 and 830 nm in water). ICG is able to bind to plasma proteins remaining in the blood vessels for long time. It is excreted through the biliary tract and not reabsorbed in the intestine; furthermore it has low-toxicity. Considering its effective binding to plasma proteins ICG is considered a perfusion marker of organs like liver and spleen. Plasmatic ICG concentration after intravenous administration well correlates with liver function. Other important applications of this fluorescent dye are myocardial perfusion studies^[33], oncological staging^{[34][35]} and eye diagnostics (e.g. ICG angiography)^{[36][37]}.

Indocyanine green has very attractive biological properties and its near infrared spectral characteristics are not disturbed by the fluorescence emission of other molecules contained in the animal body compartments. Unfortunately ICG derivatives with amino-reactive groups for binding to PEI are not commercially available at the moment.

1.5.3 Quantum Dots

A *quantum dot* (QD) is a nanometer-sized (ranging from >1.5 to <8 nm) crystalline structure, made up of semiconductors. The electrons movements in a quantum dot are strictly confined in the three dimensions so that their energy cannot vary in a continuous way but only at discrete steps.

Quantum dots usually consist of the semiconductor core (e.g.: *Cd-Se*, *In-Ga-As*, or *Ga-In-P/In-P*) and the shell containing reactive groups that modify the optical and chemical properties of these nanocrystals permitting binding to different biomolecules.

Quantum dots are gaining interest as fluorescent tags for biological molecules thanks to their stronger fluorescence and better photo-stability than organic fluorescent dyes. They also exhibit broader absorption and narrower emission ranges than most fluorescent dyes^{[38][39][40][41][42]}.

While the material, which makes up a quantum dot, determines its intrinsic energy, its emission wavelength is defined by its size. For this reason quantum dots with identical chemical structure but different dimensions emit light of different colors. The wavelength and color of the emitted light is directly proportional to the size of a quantum dot. Like wavelength (i.e. color) of emitted light fluorescence lifetime of a quantum dot is a function of size in that large quantum dots contain more energy levels than “little” ones. These energy levels are also more spaced in large dots and it is more probable that an electron pair is trapped within the crystal for longer time.

1.6 Aim of the Study

The application of gene therapy technologies needs controlling systems to be able to state how efficient the delivery process is. At the *Chair of Pharmaceutical Biotechnology, Department, of Pharmacy, Ludwig-Maximilians-Universität München* (LMU) non-viral gene delivery systems are developed, whose efficiency is tested with methods based on bioluminescence and fluorescence in vitro and in vivo^{[43][44]}. Fluorescence-labeled gene carriers can be efficiently detected in vivo, if the fluorescent markers emit in a different spectral area from other substances (such as hemoglobin, chlorophyll, etc.), whose strong radiation would cover the lower dye emission intensity. In order to avoid such overlapping phenomena fluorescent, dyes emitting in the near infrared region (NIR) are required. These dyes for in vivo purposes should be not toxic and can be administered intravenously.

The aim of this study was to determine what dyes were suitable for our in vivo imaging system, whose emission could be detected and quantitatively analyzed. We wanted to assess what conjugates based on polyethylenimines (PEI) or oligoethylenimines (OEI) were at most adapted for our experiments in vivo using fluorescent dyes. Could EGF and transferrin positively impact the gene delivery in selected tumor cell lines expressing their specific receptors? Was it possible to further improve our results using PEG-shielding? We finally wanted to determine if it is possible to quantitatively measure the accumulation of fluorescence labeled gene carriers in the tumor tissue.

In this study commercially available organic dyes and quantum dots (synthesized by the work group of Dr. Andrey Rogach, LMU) were used with emission spectra between 750 and 800 nm. We tested fluorescence labeled PEI-based gene vectors in immunodeficient mice bearing subcutaneously implanted human or murine tumors cell lines (HUH7, N2a). The gene carriers were additionally coupled to ligands (EGF, transferrin) whose receptors are strongly expressed on the surface of the implanted tumor cells.

2 Materials and methods

2.1 Chemicals and reagents

Branched PEI (brPEI) with an average molecular weight (Mw) of 25 kDa was purchased from *Sigma-Aldrich™* (München, Germany). HD O (Mw 4000 Da; OEI 800 Da core modified with hexane-1,6-diol diacrylate and surface-modified with OEI 800 Da) was synthesized by Dr Verena Ruß, as described in literature^[22]. Murine recombinant EGF (mEGF) was obtained from *Pepro Tech EC Ltd.* (London, United Kingdom). Human transferrin (hTf) with iron was supplied by *Biotech* (Dreieich, Germany). Endotoxin-free pCMVLuc plasmid (*Photinus pyralis* luciferase under control of the CMV enhancer/promoter) was produced by *Plasmid Factory GmbH & Co* (Bielefeld, Germany). *Alexa Fluor® 750 carboxylic acid, succinimidyl ester* was purchased from *Invitrogen Corporation* (Carlsbad, California, USA), *NIR 797 isothiocyanate* from *Sigma-Aldrich Reagents* (Munich, Germany). The quantum dots stock-solutions (Cd-Te core with S-C₃H₆-COO⁻ groups) are produced by Dr Andrei Sussha at the *Faculty of Physics, Photonics and Optoelectronics Group*, LMU, led by Dr Andrey Rogach (emission 650-870 nm, peak emission 790 nm; size: 7 nm). Saline Solution (0.9 %) for intravenous injections was provided by *B.Braun Melsungen AG* (Melsungen, Germany). Dimethylsulfoxide (DMSO) was obtained from *Fluka Chemie GmbH* (Deisenhofen, Germany). All other reagents were purchased from *Sigma-Aldrich* (Munich, Germany).

2.2 Synthesis of conjugates and polyplexes

2.2.1. Synthesis of conjugates

All conjugates were synthesized at the *Chair of Pharmaceutical Biotechnology* (LMU) by Wolfgang Rödl, Dr Arkadi Zintchenko and Dr Verena Ruß. PEG20-brPEI25 (with molar ratio PEG/PEI=2:1) and hTf-PEG3.4-brPEI25 conjugates linked with a hetero-bifunctional 3.4 Da PEG derivative were synthesized and purified as previously described^[45]. hTf-brPEI25 conjugate (molar ratio Tf/PEI 1/1 M/M) was synthesized as described by *Kircheis et al*^[46]. mEGF-PEG3,4-brPEI25 (murine EGF conjugated to branched PEI 25 kDa via a 3,400 Da PEG-spacer) was synthesized as described by

Wolschek et al^[47]; mEGF-brPEI25 conjugate has been produced as described by Blessing et al^[48].

Alexa 750/brPEI25 conjugate was synthesized as follows: 256 nmol PEIbr25 were dissolved in 1 ml HEPES-buffered saline (HBS) at 10 mg/ml (pH=7.4). While vortexing the PEI solution 768 nmol *Alexa Fluor® 750 carboxylic acid, succinimidyl ester* (Mw 1300; ex/em=746/775 nm) were slowly added: molar ratio Alexa 750/PEIbr25 = 3:1. The reaction was incubated 2 hours at room temperature (RT) with continuous stirring. The conjugate was separated from unreacted labeling reagents using *Sephadex G25, BioGel* gel filtration (HR 10/30, HBS, 1:1 with H₂O; 0.5 ml/min). Branched PEI concentration was determined by trinitrobenzenesulphonic acid (TNBS) assay; Alexa 750 concentration calculated from the absorption at 700 nm (molar extinction coefficient Alexa ϵ = 240,000/mol*cm). The final molar ratio Alexa/PEI was 1/1 M/M.

Alexa 750/H DO conjugate was obtained following the same protocol, mixing Alexa 750 dye and H DO with a molar ratio dye/polycation = 3:1 Two different fractions of Alexa 750/HD O conjugate were obtained differing in their Alexa 750 concentration: #1 45 μ M, #2 12 μ M Alexa. Fraction 1 showed a final degree of Alexa 750 labeling of 1/2.4 (Alexa 750-HD O, M/M) and fraction 2 of 1/5.6 (Alexa 750-HD O, M/M).

NIR 797-brPEI25 conjugates were synthesized as follows:

Conjugate A:

80 μ l of NIR 797 [1,1'-Bis(4-sulfobutyl)-11-(4-isothiocyanatophenylthio)-3,3,3',3'-tetramethyl-10,12-trimethylenindotricarbocyanine monosodium salt, Molecular Formula: C₄₅H₅₀N₃NaO₆S₄, Mw 880.14, fluorescence: λ_{ex} 795 nm; λ_{em} 817 nm in 0.1 M phosphate pH 7.0] in dimethyl sulfoxide (DMSO, 25 mg/ml) were added to 1 ml of the brPEI25 solution (10 mg/ml) in 0.1 M carbonate buffer (pH=9). The reaction mixture was incubated for four hours at 37°C. Labeled polymers were separated from unreacted dye by size exclusion chromatography (*Sephadex G25 HR 10/30*, 20 mM HEPES, pH=7.4, 0.15 M NaCl) and desalted by ultrafiltration. Branched PEI concentration was determined by TNBS assay for primary amino groups; NIR 797 concentration was calculated from the absorption at 700 nm (molar extinction coefficient NIR: ϵ = 48500/mol*cm). The final degree of NIR labeling NIR/PEI = 0.98/1.

Conjugate B:

400 μ l of NIR 797 [1,1'-Bis(4-sulfobutyl)-11-(4-isothiocyanatophenylthio)-3,3,3',3'-tetramethyl-10,12-trimethylen-eindotricarbocyanine monosodium salt, Molecular Formula: C₄₅H₅₀N₃NaO₆S₄, Mw 880.14, fluorescence: λ_{ex} 795 nm; λ_{em} 817 nm in 0.1 M phosphate pH 7.0] in dimethyl sulfoxide (DMSO, 25 mg/ml) were added to 1 ml of the

branched PEI25 solution (10 mg/ml) in 0.1 M carbonate buffer (pH=9). The reaction mixture was incubated for four hours at 37°C. Labeled polymers were separated from unreacted dye by size exclusion chromatography (*Sephadex G25 HR 10/30*, 20 mM HEPES, pH=7.4, 0.15 M NaCl) and desalted by ultrafiltration. Branched PEI concentration was determined by TNBS assay for primary amino groups; NIR 797 concentration was calculated from the absorption at 700 nm (molar extinction coefficient NIR $\epsilon = 48500/\text{mol}\cdot\text{cm}$). The final degree of NIR labeling NIR/PEI = 6/1.

2.2.2. Generation of polyplexes

Polyplexes were generated with a final DNA concentration of 200 $\mu\text{g}/\text{ml}$ at an N/P ratio (molar ratio nitrogen in PEI to phosphate in pDNA) of 6 in HBG (HEPES buffered glucose; 20 mM HEPES pH 7.1, 5% glucose w/v) as described in literature^{[49][50]}, and rapidly mixed by pipetting. Polyplexes were allowed to stand for at least 20 min at room temperature before use. Previous studies^{[51][52]} revealed that generating PEI-based polyplexes at an N/P ratio of 6 is most favorable for in vivo, resulting in efficient transfection and minimized toxicity^[53].

N/P ratio 6 was calculated as follows: for each P in DNA an average molecular weight of 330 Da was calculated; the average molecular weight of one N-containing repeating unit in PEI (-CH₂-CH₂-NH) was calculated as 43 Da. For a known concentration of DNA corresponding PEI concentration was calculated as follows: $[\text{PEI}] = [\text{DNA}] \cdot 43 \cdot 6 / 330$

Standard pDNA-PEI polyplexes were generated in HBG at a final DNA concentration 200 $\mu\text{g}/\text{ml}$ as follows: pDNA was diluted in a reaction tube to 400 $\mu\text{g}/\text{ml}$ in HBG. In a separate vial PEI solution was diluted in the same volume to a final concentration of 313 $\mu\text{g}/\text{ml}$. Thereafter PEI solution was pipetted to the DNA solution and immediately pipetted up/down several times to obtain optimal mixing of both components.

To obtain pDNA-PEI polyplexes with fluorescently labeled PEI, PEI was replaced by Alexa 750/brPEI25 and NIR 797/brPEI25 conjugates (see 2.2.1).

Quantum dots were delivered as stock dispersions $1.2 \cdot 10^{-6}$ M. The standard application dose was defined optically through fluorescence emission testing of dilution series of the stock solution and put at 2.01 μl *stock solution*/100 μl injection volume.

QD/pDNA-PEI polyplexes were generated as follows: pDNA was diluted in a reaction tube to 800 $\mu\text{g}/\text{ml}$ in HBG. In a separate vial QD suspension was diluted to the final

concentration of $7.5 \cdot 10^{-4}$ nmol/ml. The QD suspension was then added to the DNA solution and mixed together quickly. PEI solution was diluted in the same volume as DNA-QD mix and subsequently pipetted to the first solution and quickly pipetted up/down to obtain small particles.

QD/PEI conjugates were generated as follows: QD suspension was diluted in a vial to $3.75 \cdot 10^{-4}$ nmol/ml. In a separate vial PEI solution was diluted in the same volume to a final concentration of 313 μ g/ml. Thereafter the PEI solution was pipetted to the QD suspension and immediately pipetted up/down several times to obtain an optimal mixing and small particles.

2.3 Analysis of transfection complexes

2.3.1 Measurement of the particle size

Particle size and zeta potential of transfection complexes were measured by laser-light scattering using *Malvern Zetasizer 3000 HS* (by *Malvern Instruments*, Worcestershire, United Kingdom). Polyplexes generated in HBG at 20 μ g/ml DNA concentration were allowed to stand 30 min prior to measurement.

2.3.2 Electrophoresis

1% agarose gels were prepared by dissolving 1.2 g agarose (by *Invitrogen Corporation*, Carlsbad, California, USA) in 120 ml tris-borate EDTA (TBE) buffer (by *Sigma-Aldrich Reagents™*; Munich, Germany) and boiling the solution up to 100°C. After cooling down to 70°C the gel was poured into the electrophoresis unit *Sub-Cell GT Cell* (by *Bio-Rad Laboratories*, Hercules, California, USA). 19 μ l of solution to be analyzed were mixed with 3 μ l of xylene cyanol loading buffer solution from *PEQLAB Biotechnologie GMBH* (Erlangen, Germany), inserted into the gel wells and separated under electric field (120 mV, 2 A) for 120 minutes. Electrophoresis gels were then scanned with *Odyssey® Infrared Imaging System* (by *LI-COR Corporate Offices*, Lincoln, Nebraska, USA) to detect near infrared fluorescence after excitation with 700 and 800 nm laser. The resulting images were edited with *Odyssey® software version 3.0* (by *LI-COR Corporate Offices*). After being scanned for fluorescence the gel was stained in a TBE buffer solution containing *ethidium bromide* (500 ng/ml TBE) for 30 min, and then illuminated with an ultraviolet lamp to view the DNA bands. Photographs were taken

with an UV-imaging device by *Raytest GmbH* (Straubenhardt, Germany), and edited using *AIDA Image Analyzer Software Version 3.21* (*Raytest GmbH*).

2.4 Cell culture

Cell culture media and fetal calf serum (FCS) were purchased from *Invitrogen GmbH* (Karlsruhe, Germany). All cultured cells were grown at 37°C in 5% CO₂ humidified atmosphere. *Human Hepatocellular Carcinoma HUH7* cells (JCRB 0403; Tokyo, Japan) were cultured in DMEM/HAM's F12 medium (1:1) supplemented with 10% heat-inactivated FCS and L-alanyl-L-glutamine 1.6 mmol/500 ml medium (*Biochrom*, Berlin, Germany). *Murine neuroblastoma N2a* cells (ATCC CCL-131) were grown in *Dulbecco's modified Eagle's medium* (DMEM) supplemented with 10% FBS with 10% heat-inactivated FCS and L-alanyl-L-glutamine 1.6 mmol/500 ml medium at 37°C in 5% CO₂ humidified atmosphere.

Animal experiment*

2.5.1 Animal husbandry

4 weeks old female nu/nu mice were delivered by *Elevage Janvier* (Le Genest-Saint-Isle, France). The animals were housed under pathogen-free conditions in individually ventilated cages (type 2L by *Techniplast IVC Systems*, Buguggiate, Italy), 5 mice/cage under controlled light (12 hours light/12 hours darkness), temperature (21–22°C), humidity (60%). They were fed with autoclaved chlorophyll-free experimental mouse chow (product code: E_15000-04 by *Ssniff Spezialdiäten*, Soest, Germany) and fresh water ad libitum. Each cage was fitted with wood shavings made from debarked aspen wood (by *ABEDD® LAB & VET Service GmbH*, Vienna, Austria), equipped with a wooden rodent tunnel (size 2; *ABEDD® LAB & VET Service GmbH*, Vienna, Austria) and a red transparent plastic lodge (by *Techniplast IVC Systems*, Buguggiate, Italy). After being delivered all animals were habituated for a week to the new environment conditions before starting any treatment.

2.5.2 Tumor cells implantation

As described in 2.4 the tumor cells (HUH7 or N2a) were harvested after reaching 70–80% confluence. Cell culture medium was removed and the tumor cells were washed twice with phosphate-buffered saline (PBS). They were then incubated with trypsin/EDTA for 5 minutes at 37°C and separated from their support. After inactivating trypsin solution with culture medium containing fetal bovine serum (FBS) the cells were suspended with fresh medium and centrifuged (5 min, 1300 rpm, 4°C). The supernatant was then discarded and the cells resuspended in PBS and centrifuged again at the same conditions. After this second centrifugation 1µL of cells suspension was taken and put into a Rosenberg's counting chamber to be counted. According to the tumor type 1×10^6 N2a cells/mouse and 5×10^6 HUH7 cells/mouse were collected and suspended in 100 µL PBS at 4°C. The cell suspension was injected with a 25 G needle (by *B. Braun Melsungen AG*, Melsungen, Germany) into the left/right or bilateral loin region.

* All experimental procedures with living animals in our laboratories were approved by the *Upper Bavarian Government (Regierung Oberbayern)* complying with the *Guidelines of the Council of Europe* (24.9.86) and the *German Animal Protection Law (Tierschutzgesetz, 18.5.05)*.

2.5.3 Tumor volume measurements

The sizes of the implanted tumors were measured every other day with a digital caliper (by *HELIOS-PREISSER Vertriebszentrum*, Gammertingen, Germany). Tumor's length, width and height were registered. About 0.3 cm³ of tumor volume was considered optimal for starting in vivo assays.

2.5.4 Intravenous applications and anesthesia

Mice were immobilized in a restrainer and their tail submersed in water warmed to 40°C for 2 minutes to dilate the superficial tail veins. The solution (12.5 µL/g mouse) was injected intravenously using an U-40 sterile insulin syringe with a 29 G needle (*Beckton Dickinson*, Franklin Lakes, NJ, USA) and the animal put into the anesthesia chamber of *IVIS® Lumina imaging system 100 Series* (by *Xenogen Corp*, Alameda, California, USA). Anesthesia was induced with 2% isoflurane gas (*cp-pharma Handelsgesellschaft mbH*, Burgdorf, Germany) in oxygen.

For standard-dose applications pDNA-PEI and QD/pDNA-PEI polyplexes were injected at 2.5 mg/kg DNA dose (corresponds to PEI dose of 1.95 mg/kg) and QD/PEI polyplexes at final PEI dose of 1.95 mg/kg. In certain experiments fluorescently labeled PEI alone was injected. Labeled PEI was diluted to a final concentration of 0.156 µg/ml in HBG and injected intravenously at a PEI dose of 1.95mg/kg (standard dose) or 1.3 mg/kg (reduced dose). QD alone were applied at a dose of 0.75 nmol/kg (10⁵ particles/l).

2.5.5 Dissection and organs excision

Fluorescent emission images of anesthetized mice were taken at different points in times after intravenous injection of fluorescent labeled polycations and polyplexes. All animals were then euthanized by inhalation of CO₂. Afterwards they were fixed onto a plastic support with pins and dissected; their organs were excised and put on a Petri dish. Fluorescence emission images of dead animals were taken after opening their abdominal cavity and exposure of their organs.

2.6 In vivo imaging procedures

2.6.1 In vivo imaging system: imaging adjustments

The anesthetized animals were placed into the *IVIS[®] Lumina imaging system 100 Series* (by *Xenogen Corp*, Alameda, California, USA). During the imaging process the mice were kept under anesthesia by 2% isoflurane gas in oxygen. Most images were obtained using the ICG/ICG (excitation/emission: 710-760/810-875) filter combination (mode: fluorescence; exposure time: 1 sec; binning: high; block filter: on; tray position: A/D).

Physical Units for fluorescence Imaging:

Photons/sec: imaging data are displayed in terms of absolute photon emission from the source (a 150-W quartz-tungsten halogen lamp).

Efficiency: non uniformity in the illumination profile is corrected for by dividing images by a stored reference image (normalization).

2.6.2 Measurements and data analysis

Fluorescence imaging data were edited in photons/sec using *Living Image 260.1-IGOR Pro 4.09 Software* (by *Xenogen Corp*, Alameda, California, USA). All signal emission values were inserted into a file sheet using *Microsoft[®] Excel 2006* (by *Microsoft[®] Corporation*, Redmond, Washington, USA).

2.6.3 Statistical analysis

For statistical analysis of imaging data paired and unpaired t-tests and one-way analysis of variance (ANOVA) were performed using *Prism 5 for Windows* (by *GraphPad Software, Inc.*, San Diego, CA, USA) and *WinStat for Microsoft[®] Excel 2006*.

A *p value* < 0.05 was considered to be significant.

3 Results

3.1 Near infrared fluorescent dyes: biodistribution of dyes, conjugates with polycations and pDNA-polyplexes

3.1.1 Alexa 750 and NIR 797: biodistribution of free dyes

3.1.1.1 Alexa 750 free

This was a preliminary experiment to evaluate the usability of Alexa 750 for in vivo imaging with the IVIS system, describing distribution patterns of free Alexa 750, its fluorescent signal intensity, its emission decay and toxicity after iv application in living animals.

Animals: 5 *nu/nu* mice, male; 5 weeks old; tumor free.

Considering previous literature experience^[29] we administered 5 nmol/animal of Alexa 750 dissolved in HBG (HEPES buffered glucose) solution (12.5 μ l/g mouse) into the animals' tail vein.

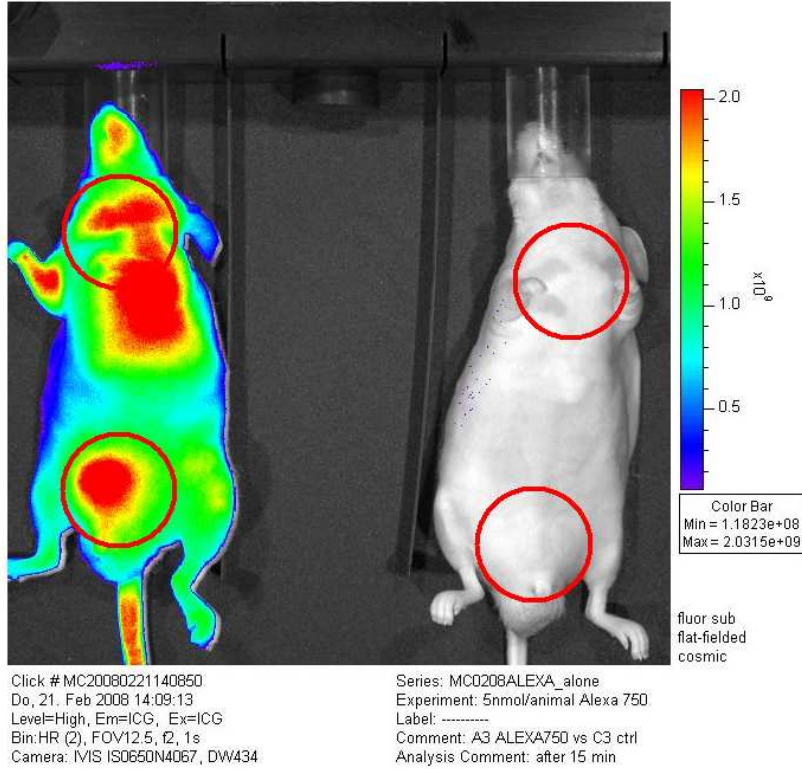
Application scheme:

Mice 1,2,3,4	5 nmol Alexa 750 in HBG
Mouse 5 (ctrl)	HBG buffer

Body fluorescence emission signals were checked 15 minutes and 24 hours after systemic injection. All animals were then sacrificed and their organs were excised, checked for fluorescence emission and then frosted in order to be analyzed separately. We tried to detect fluorescence in organ homogenates but we could not register any signal.

Fig. 1a,b: 2 animals treated with 5 nmol Alexa 750 alone (left) and the control mouse 15 minutes and 24 hours after iv application (filter ex/em: ICG/ICG). Regions of interest marked with red circles (n=4; ctrl=1).

a: ventral signal after 15 minutes



b: ventral signal after 24 hours

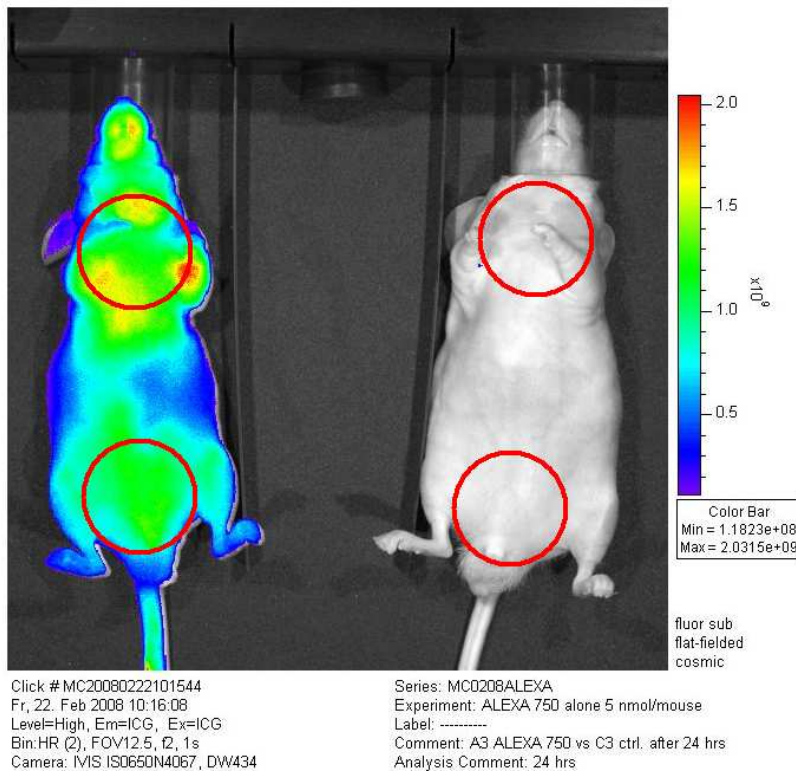


Fig. 3: fluorescence emission signal in photons/sec from thorax/neck (thyroid) 15 minutes and 24 hours after iv application of 5 nmol Alexa 750 free (n=4; ctrl=1).

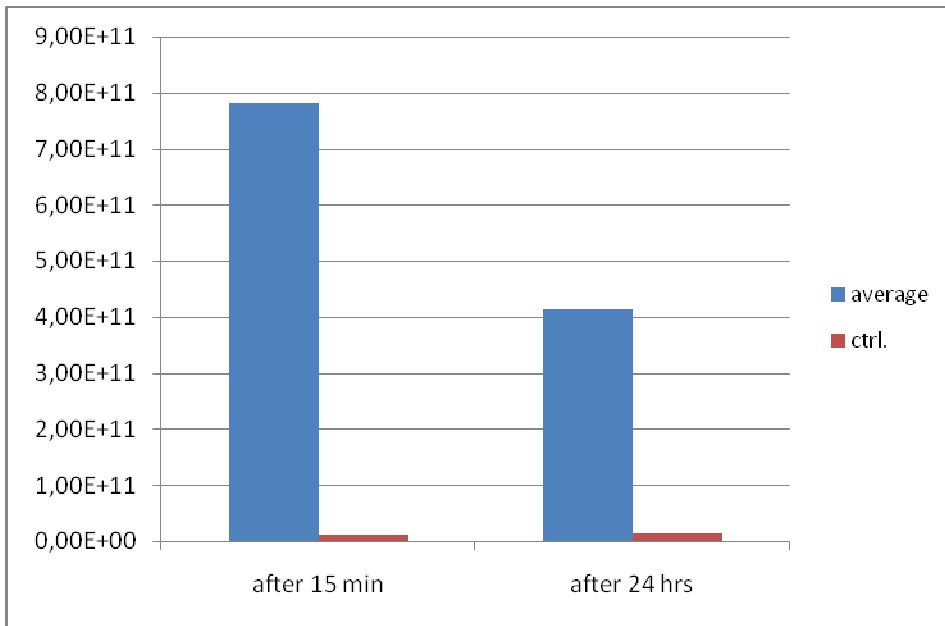


Fig 4: fluorescence emission signal in photons/sec from pelvis/bladder 15 minutes and 24 hours after iv application of 5 nmol Alexa 750 free (n=4; ctrl=1).

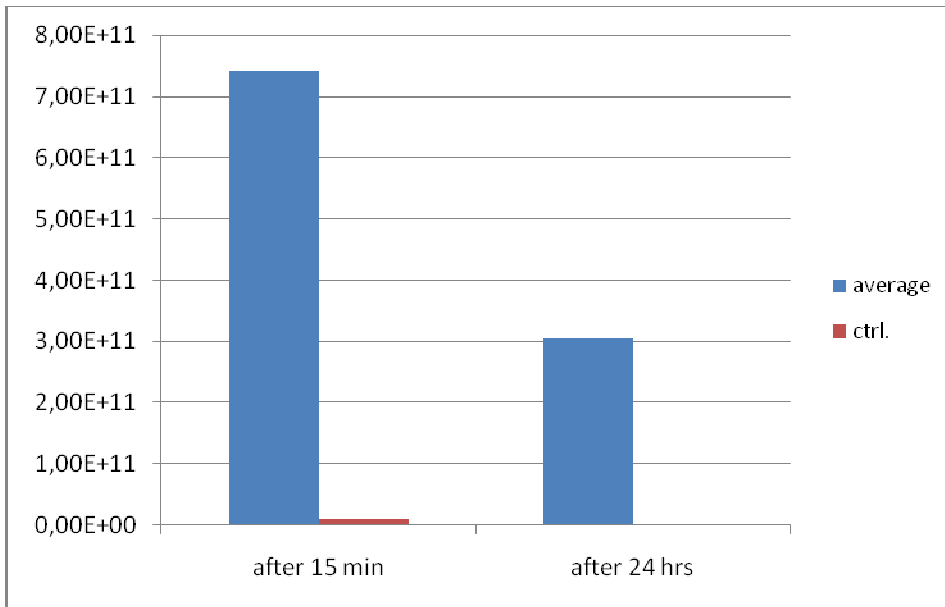
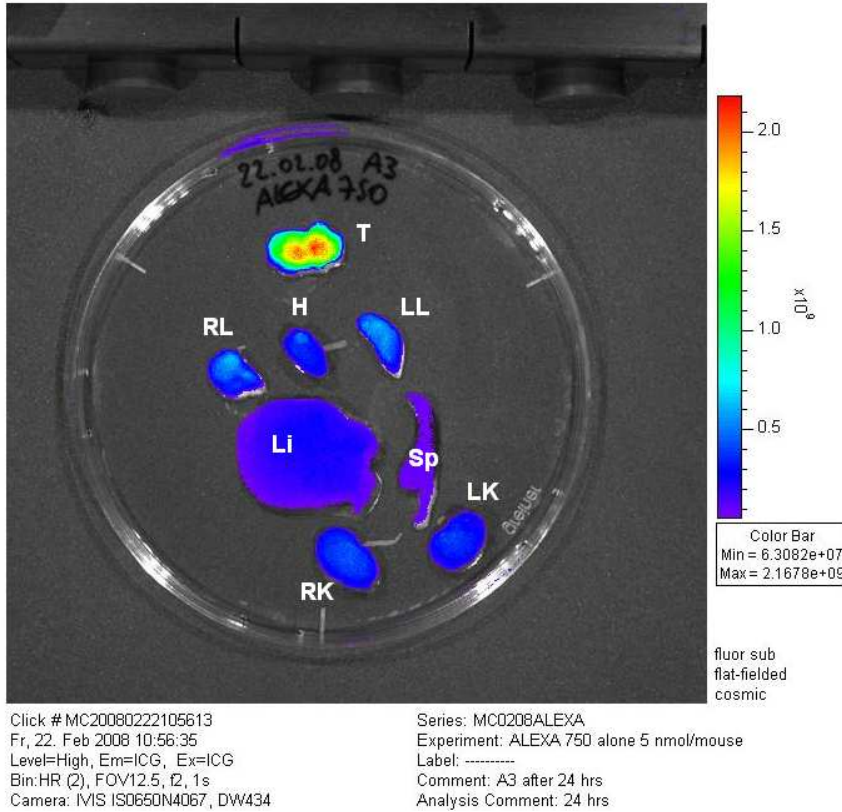
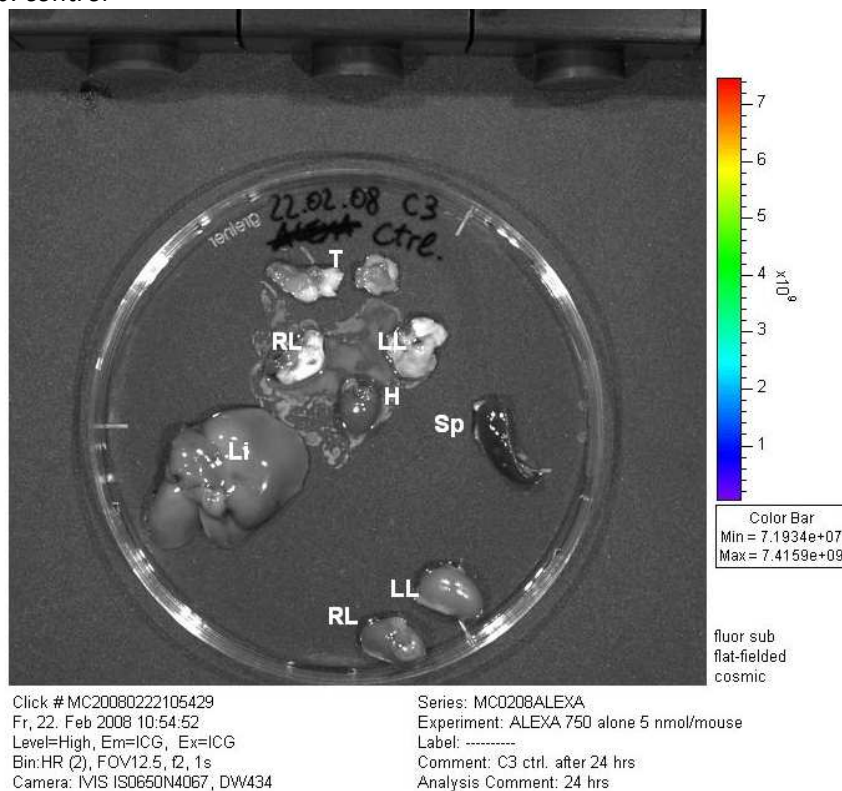


Fig. 5a,b: excised organs of mouse treated with 5 nmol Alexa 750 free and the control mouse 24 hours after iv application (filter ex/em: ICG/ICG; n=4; ctrl=1).
 T=thyroid; RL, LL=right, left lung; H=heart; Li=liver; Sp=spleen; RK, LK=right, left kidney.

a: Alexa 750 free



b: control



At both time points (15 min, 24 hrs) after injection of 5 nmol Alexa 750 bladder, thyroid and lungs showed the most intense signals (*fig. 4a-b*). Ex vivo imaging data visualized strong thyroid dye accumulation after organ excision (*fig. 5a-b*). All fluorescence signal values decreased in similar way after 24 hrs (*fig. 3 and 4*). No acute/subacute toxic effects were observed because free Alexa 750 did not cause aggregation of red cells in the blood stream.

3.1.1.2 NIR 797 free

We repeated the same experiment with NIR 797 (same dosage: 5 nmol/animal) to compare its properties with Alexa 750. The goal was evaluating the usability of NIR 797 for in vivo imaging with the IVIS system, describing distribution patterns of free NIR 797, its fluorescent signal intensity, its emission decay and toxicity after iv application in living animals.

Animals: 3 *nu/nu* mice, female; 8 weeks old; bearing HUH7 cells tumors.

We administered 5 nmol/animal of NIR 797 dissolved in HBG buffering solution (12.5 μ l/g mouse) into the animals' tail vein.

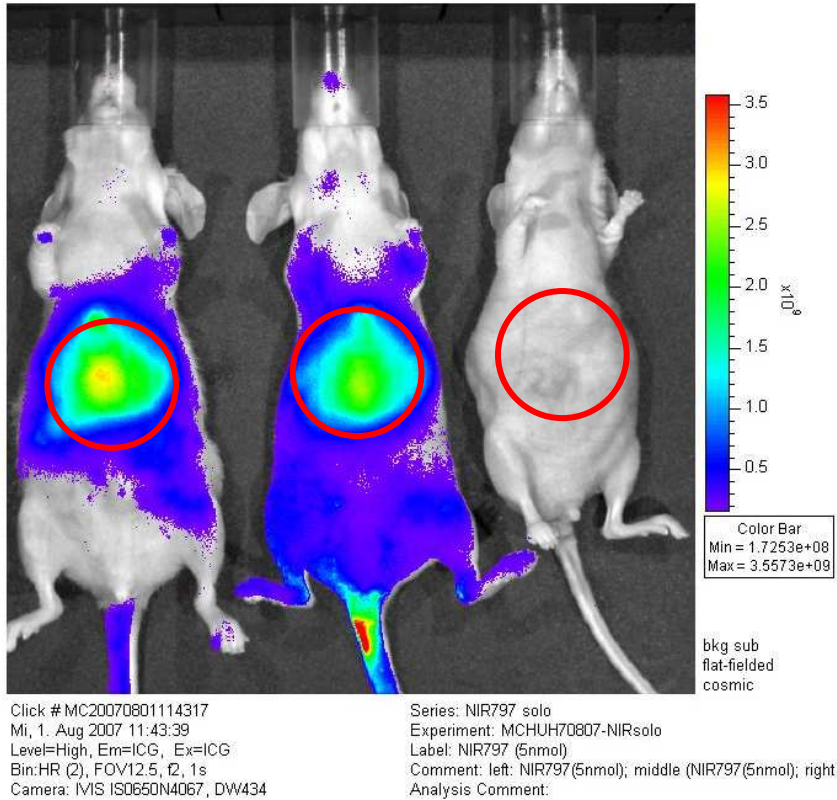
Application scheme:

Mice 1,2	5 nmol NIR 797 in HBG
Mouse 3 (ctrl)	HBG buffer

Body fluorescence emission signals were checked 15 minutes, 6, 24 and 48 hours after the systemic injection.

Fig. 1a,b: ventral and left-side images of 2 animals treated with 5 nmol NIR 797 alone (left) and the control mouse 15 minutes after iv application (n=2, ctrl=1; filter ex/em: ICG/ICG). Regions of interest marked with red circles.

a: ventral (liver) signal after 15 minutes



b: left side (tumor) signal after 15 minutes

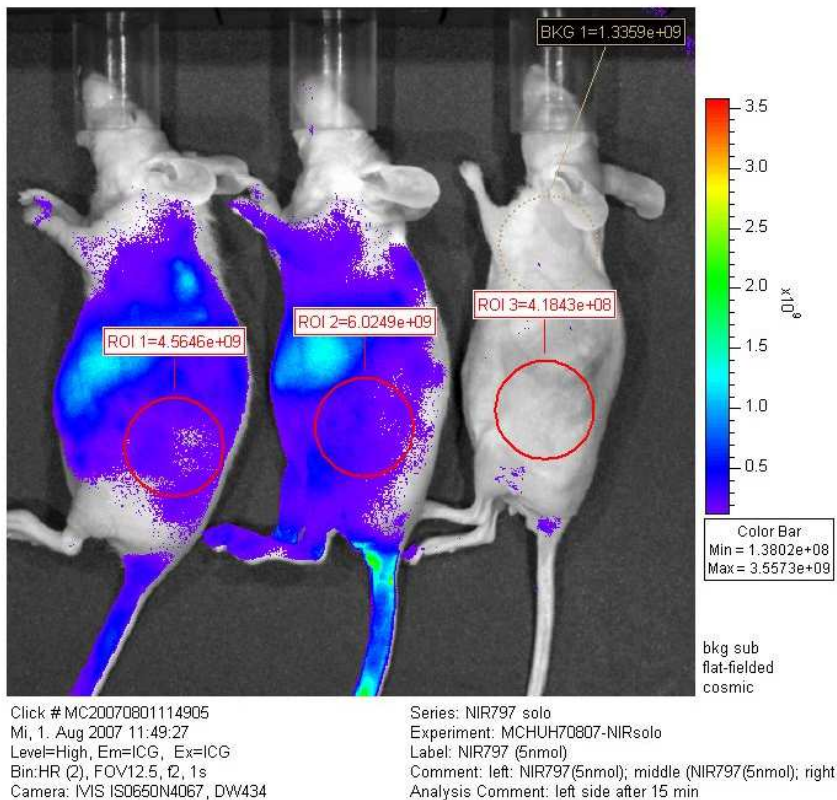


Fig. 2: ventral (liver) fluorescence emission signals in photons/sec 15 minutes, 6, 24 and 48 hours after iv application of 5 nmol NIR 797 free (n=2; ctrl=1).

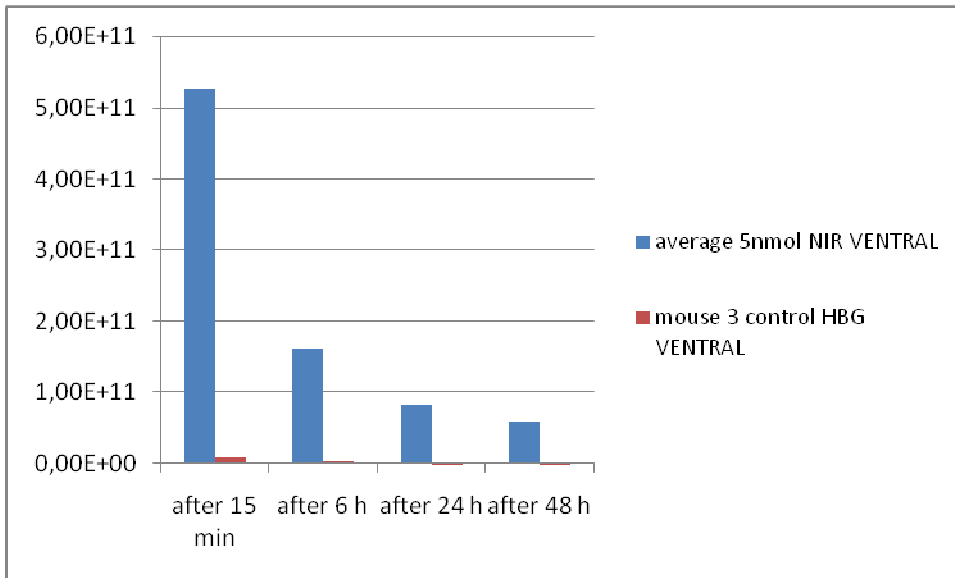


Fig 3: dorsal fluorescence emission signals in photons/sec 15 minutes, 6, 24 and 48 hours after iv application of 5 nmol NIR 797 free (n=2; ctrl=1).

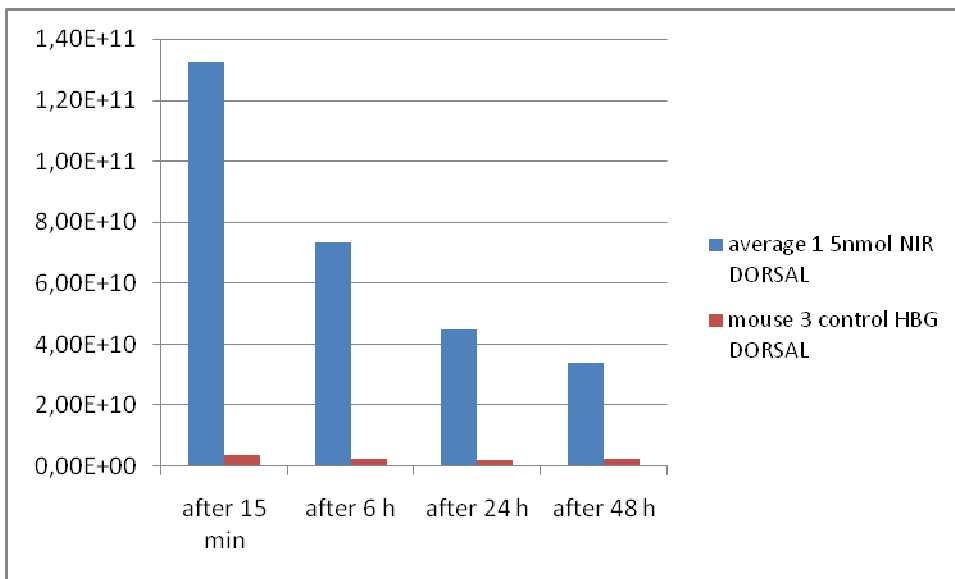
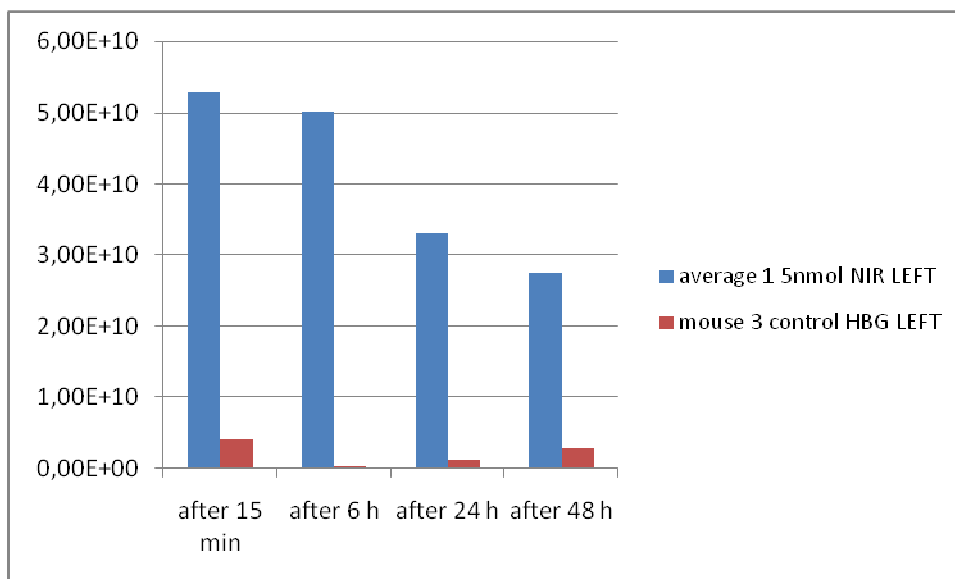


Fig. 4: *left side (tumor) fluorescence emission signals in photons/sec 15 minutes, 6, 24 and 48 hours after iv application of 5 nmol NIR 797 free (n=2; ctrl=1).*



Unlike Alexa 750 NIR 797 tended to accumulate within the liver in presence of scarce thyroid and moderate lungs depots (*fig. 1a-b*). NIR 797 had slightly lower emission signals compared to Alexa 750 at any time point and observation area. All fluorescence values decreased in a similar way while control mouse emission values did not change (*fig. 2, 3 and 4*). Low fluorescent signals could be checked within the tumor tissue (*fig. 1b and 4*). No acute/subacute toxic effects were observed, thus confirming the absence of cells aggregation in presence of free dyes. We stated a distinctive tropism for hepatic tissue of non conjugated NIR 797. Considering the results obtained by application of free Alexa 750 and NIR 797, we planned following experiments with PEI-conjugated Alexa 750 and NIR 797 in order to check modifications of their pharmacokinetic properties and toxicity.

3.1.2 Alexa 750/PEI* and Alexa 750/HD O: biodistribution in tumor bearing animals

After the distribution of free fluorescent dyes (Alexa 750 and NIR 797) the next step was describing the distribution patterns of Alexa 750/PEI and Alexa 750/HD O conjugates, their fluorescent signal intensities, emission decay and toxicity. We aimed at checking any modification in distribution and particularly verifying if the predominant accumulation in thyroid/lungs and bladder for Alexa 750 and liver for NIR797 persists and toxicity occurs after dye/PEI (or OEI) complexing.

Animals: 7 *nu/nu* mice, female; 6 weeks old; bearing HUH7 cells tumors.

Respecting the standard applications dose for PEI/OEI (in presence of 200 µg/ml DNA or RNA: N/P ratio=6) we injected 0,378 nmol Alexa 750 conjugated to PEI into each animal. Two different Alexa 750-HD O conjugates were applied differing in their dye molarity: conjugate 1 (#1): 45 µM Alexa 750, dye/HD O=1/2.4 M/M; conjugate 2 (#2): 12 µM Alexa 750, dye/HD O=1 /5.6 M/M).

Application scheme:

Mice A1, A4	Alexa750/PEI
Mice B1, B2	Alexa750-/HD O #1
Mice B3, B4	Alexa750-/HD O #2
Mouse A2	ctrl (HBG buffering solution)

Body fluorescence emission signals were measured 15 minutes, 24 and 48 hours after the systemic injection.

*In this and the following chapters branched PEI 25 25kDa is simply indicated as PEI. mEGF and hTf are indicated as EGF and Tf.

Fig. 1: mouse treated with Alexa 750/HD O (0.378 nmol, left) vs the control animal (right). Fluorescence signal is not present in the tumor area.

(n: Alexa 750/PEI=2, Alexa 750/HD O #1=2, Alexa 750/HD O #2=2, ctrl=1)

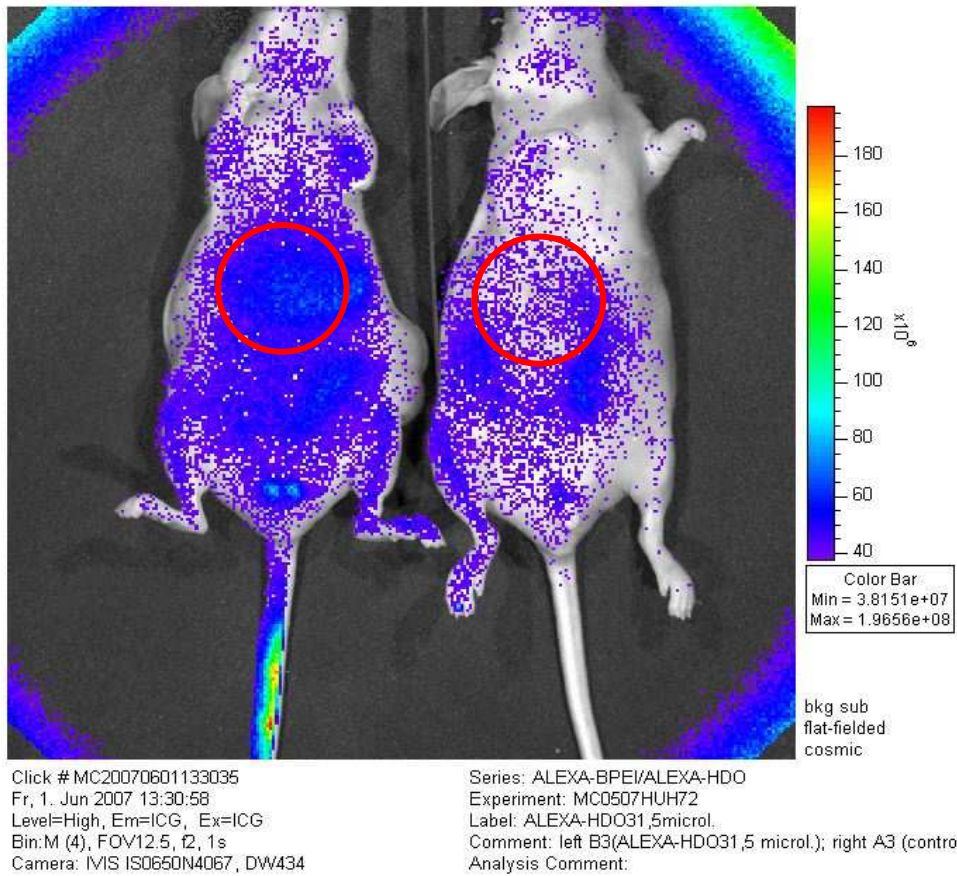
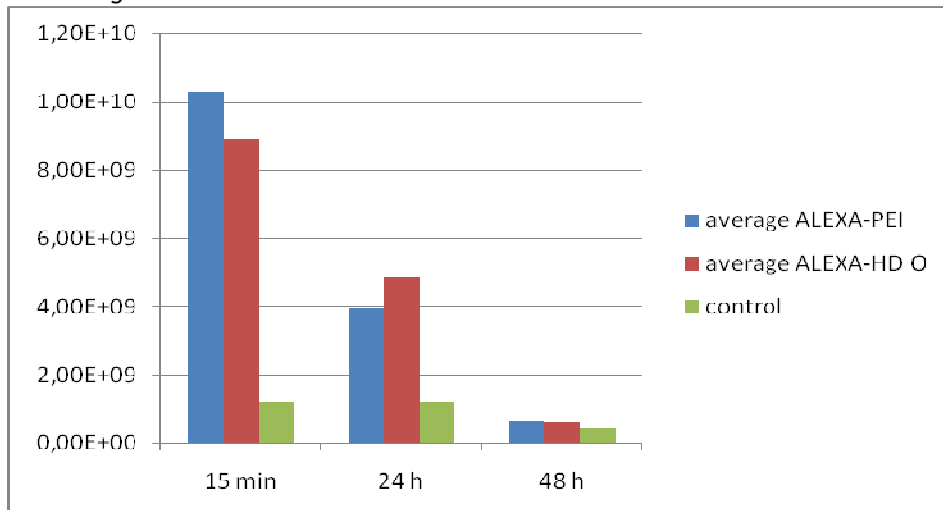
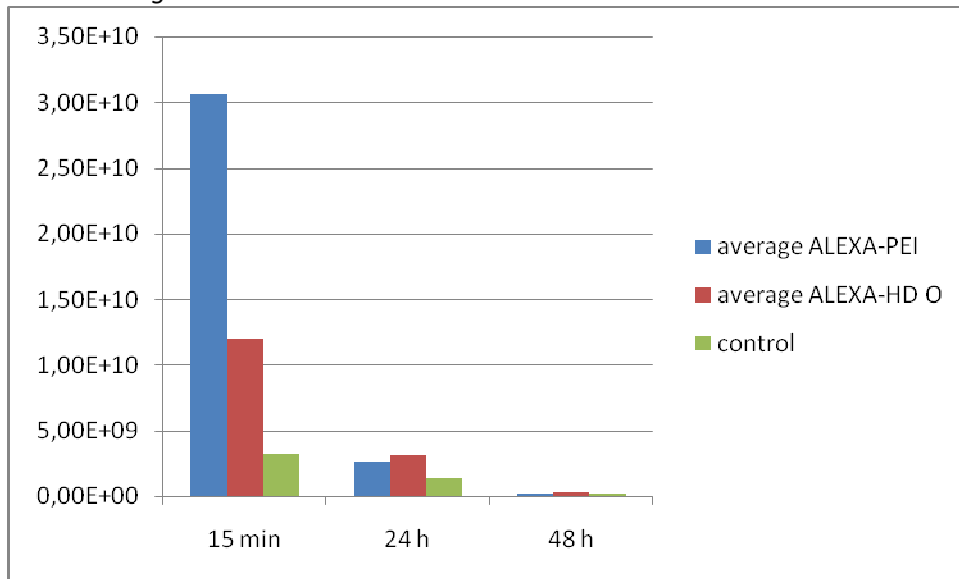


Fig 2a,b,c: fluorescence emission signal in photons/sec from a)liver, b)bladder, c)kidneys 15 minutes, 24 and 48 hours after application of 0,378 nmol Alexa 750/PEI and Alexa 750/HD O (n: Alexa 750/PEI=2, Alexa 750/HD O=2 #1, Alexa 750/HD O=2, ctrl=1)

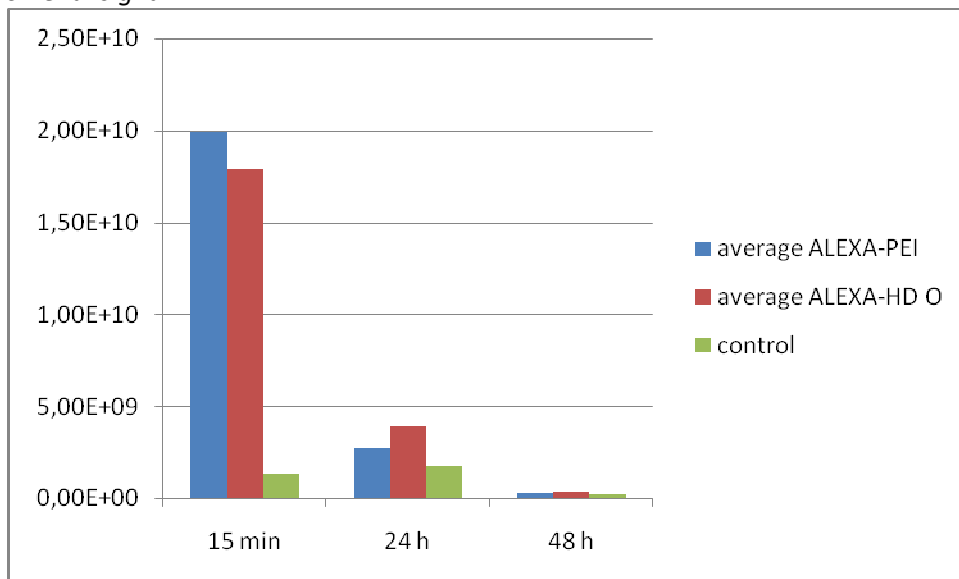
a: liver signal



b: bladder signal



c: renal signal



All fluorescence signals decreased in a similar way after 24 hours while emission values did not significantly change in the control mouse (*fig. 2a,b,c*). Bladder and kidneys signal at early time points (15 min) were stronger than the liver's but decayed faster. This was likely due to the high rate of conjugates elimination through the kidneys filtration during the first hours after systemic application. No signals were observed in the tumor (*fig. 1*). The thyroid/lungs accumulation 15 minutes after administration, detected using free Alexa 750, was not observed anymore. The increased particles size had modified the kinetic properties of the free dye. Unlike PEI-based conjugates Alexa/HD O spread through joints and connective tissue due to its inferior size. These data demonstrated that stronger dye labeling for our PEIs or OEIs was necessarily to detect emission intensities comparable to those of Alexa 750 free. Our group had much more experience with PEI-based conjugates in vitro and in vivo than with OEI so we decided to continue our tests using just PEI.

3.1.3 NIR797/PEI: influence of dye/PEI ratio on biodistribution and imaging properties

After the distribution of free fluorescence dyes (Alexa 750 and NIR 797) and of Alexa 750/PEI and HD O conjugates the next step was describing the distribution in vivo of NIR 797/PEI conjugates.

3.1.3.1 NIR 797/PEI conjugates (I)

This first assay with NIR 797/PEI conjugates describes spreading and accumulation patterns of NIR/PEI conjugates at different dye/PEI labeling ratios with or without nucleic acid, their fluorescent signal intensity, emission decay and toxicity after iv application in living animals. Our intention was to check any modification in distribution and particularly verify if predominant accumulation in liver persists. We wanted also to observe if toxicity phenomena occur after dye/PEI conjugation.

Animals: 3 *nu/nu* mice, female; 8 weeks old; tumor free.

We tested two differently labeled NIR 797/PEI conjugates synthesized in our laboratory:

conjugate A: dye/PEI ratio = 0.98:1

conjugate B: dye/PEI ratio = 6:1

Conjugate B showed a much stronger labeling. Better fluorescent signal were to be expected.

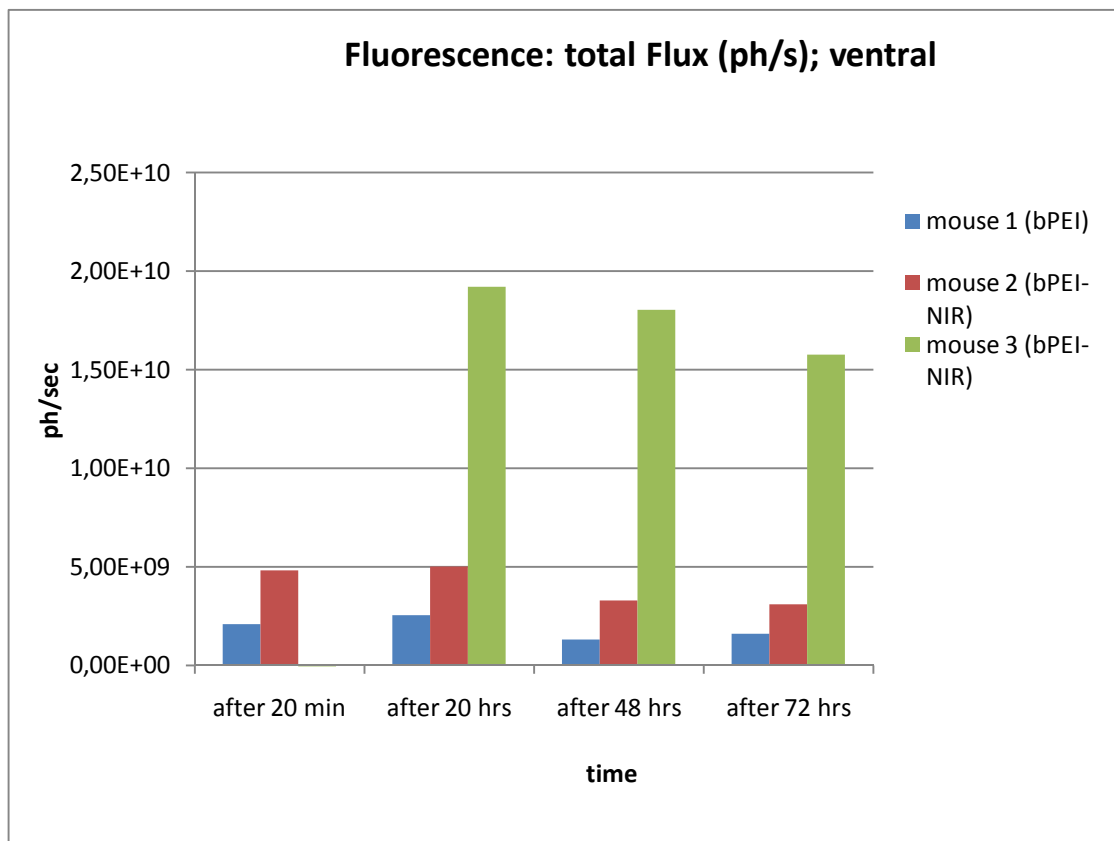
Application schema:

Mouse 1	unlabeled PEI (control)
Mouse 2	NIR797/PEI conjugate A
Mouse 3	NIR797/PEI conjugate B

Body fluorescence emission signals were measured 20 minutes, 20, 48 and 72 hours after the systemic injection.

Fig. 1: fluorescence emission signal in photons/sec from abdomen (liver) 15 minutes, 20, 48 and 72 hours after iv application of two differently labeled NIR/PEI formulations: conjugate A, (dye/PEI ratio=0.98:1, mouse 2) vs conjugate B (dye/PEI ratio=6:1, mouse 3) vs control (unlabeled PEI, mouse 1).

abdomen (liver)



Conjugate B (dye/PEI ratio=6:1; mouse 3 in *fig. 1*) had better imaging properties than B (dye/PEI ratio=0.98:1; mouse 2 in *fig. 1*) owing to stronger labeling, as expected. Mouse 1 (control), administered with unlabeled PEI, displayed the lowest signal intensity. Fluorescence signal emission was detected mostly in the liver, as observed using non-conjugated NIR 797. In this case the dye distribution pattern was not modified by conjugation with PEI unlike using Alexa 750. In this and in following assay the signal intensity was lower than using free NIR 797, because of the lower amount (< 1 nmol) of injected NIR 797 as requested by conjugating with PEI.

3.1.3.2 NIR 797/PEI conjugates (II)

This second assay on NIR 797/PEI conjugates describes the distribution patterns of NIR 797/PEI conjugates and NIR 797/PEI-DNA polyplexes, their fluorescent signal intensity, emission decay and toxicity after iv application in living animals.

As in the previous experiment we intended to verify changes in distribution properties and toxicity, even those after complexing with DNA.

Animals: 5 nu/nu female mice, 12 weeks old; tumor-free

The following experiment was performed utilizing conjugate B of previous report (dye/PEI ratio = 1:6).

Application scheme:

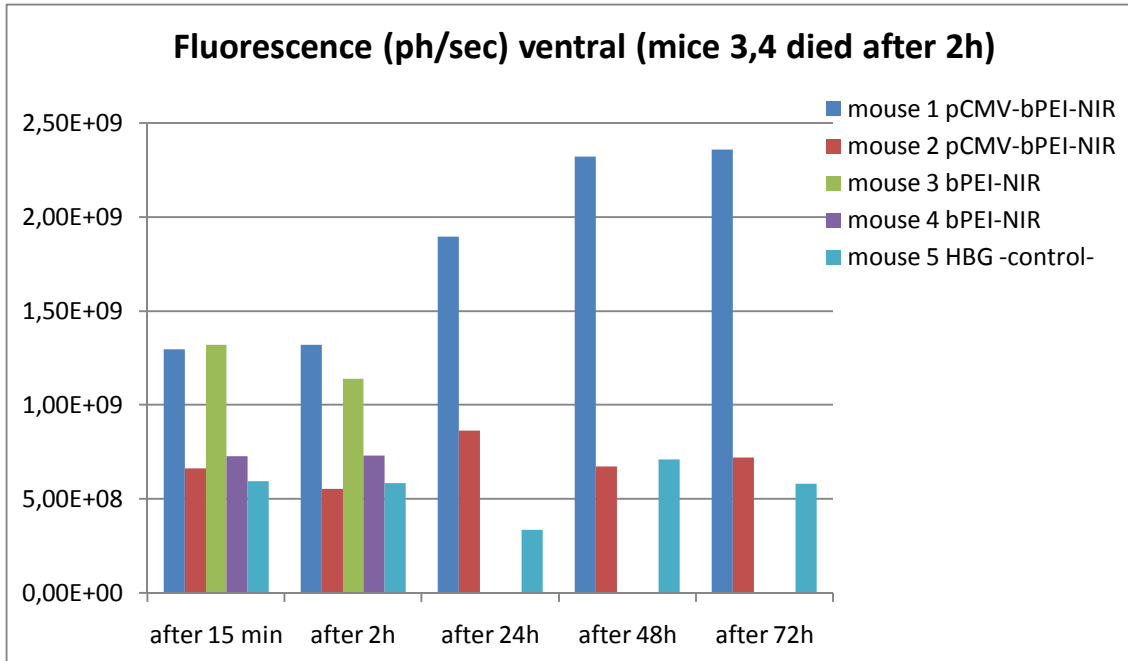
Mouse 1	pCMV-PEI + HBG
Mouse 2	pCMV-PEI + HBG
Mouse 3	NIR 797/PEI + HBG
Mouse 4	NIR 797/PEI + HBG
Mouse 5	HBG (control)

Body fluorescence emission signals were checked 15 minutes, 20, 48 and 72 hours after the systemic injection.

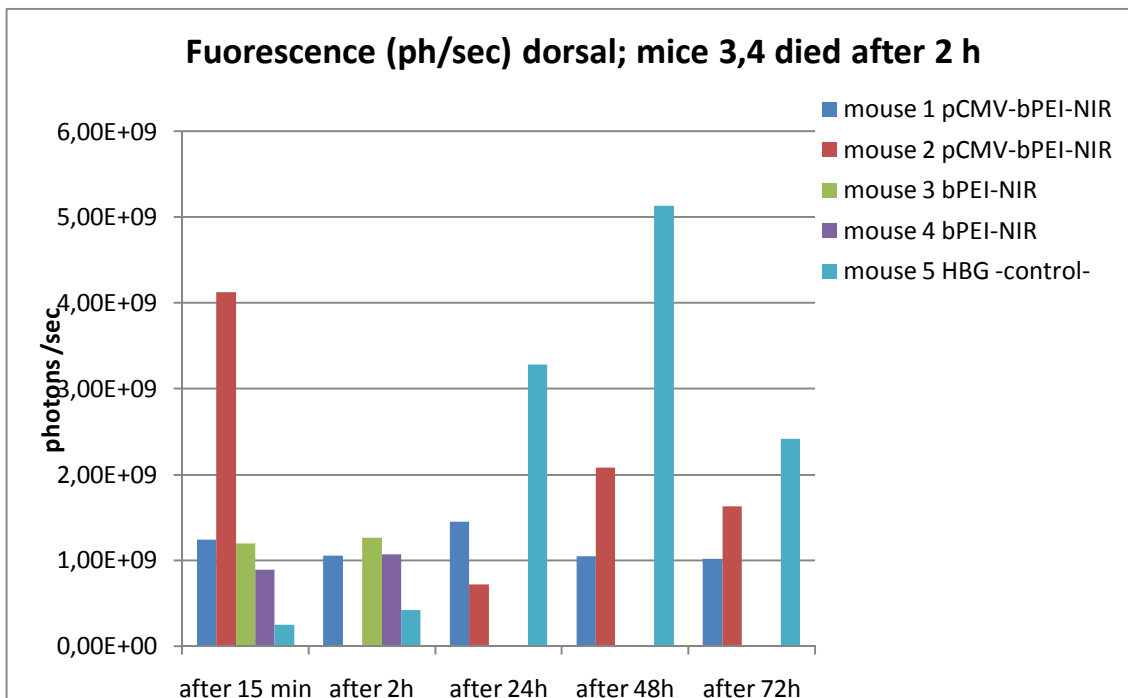
Mice 3 and 4 died 2 hours after iv application.

Fig 1a,b: fluorescence emission signal (photons/sec) from abdomen and dorsal region 15 minutes, 20, 48 and 72 hours after iv application of NIR 797/PEI-DNA polyplexes vs NIR 797/PEI conjugates vs HBG (control).

a: abdomen (liver)



b: dorsal region (kidneys)



NIR 797/PEI-DNA polyplexes and NIR 797/PEI conjugates showed comparable fluorescent emission mostly in the liver (*fig. 1a*). The distribution pattern of these conjugates was similar to that of free NIR 797. This represented a major difference between this dye and Alexa 750, whose distribution had considerably changed after conjugation with PEI and OEI. We attested the acute/subacute toxicity of NIR 797/PEI conjugates. The cause of this phenomenon could have been the absence of DNA negative charge, which interacted with the positively loaded carrier, avoiding a too strong erythrocyte aggregation within the pulmonary circulation during the first hours after injection. Animals older than 8 weeks are anyway particularly susceptible to adverse effects.

3.2 Near infrared emitting quantum dots as novel tools for bioimaging of polyplexes

We decided to test quantum dots (QD) because of their strong fluorescence and very low production cost in co-operation with the *Department of Physics* of the LMU.

3.2.1 Fluorescent properties of different quantum dots formulations

The first experiment consisted in testing fluorescence properties of different quantum dots (QD) formulations compared to a standard preparation of anionic QD with a *Cd-Te core* and a shell containing $S-C_3H_6-COO^-$ groups.

We also tried to assemble zwitterionic particles endowed with a neutrally charged shell containing cystein with similar fluorescence excitation/emission like our standard preparation. The advantage of utilizing neutral nanocrystals consists in eliminating unspecific interactions with blood and tissue compounds. Unfortunately their fluorescence intensity was too weak for *in vivo* applications (*fig. 1* and *2*). The signal intensity of the anionic (acid) QD standard formulation is 10-fold higher than the zwitterionic (neutral) QD.

Fig. 1a,b: dilution series of zwitterionic vs anionic quantum dots. QD concentrations are:
 - 1.2, 0.6, 0.3, 0.15, 0.075, 0.0375 mmol/l (left: zwitterionic Cd-Te QD)
 - 0.6, 0.3, 0.15, 0.075, 0.0375, 0.0188, 0.0094, 0.0047 mmol/l (right: anionic Cd-Te QD).

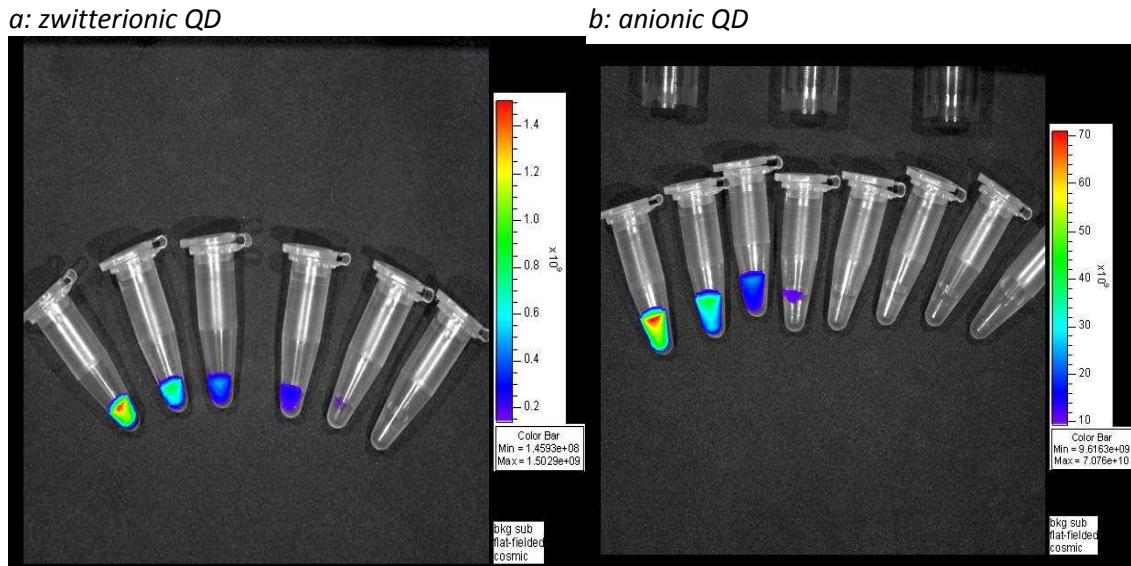
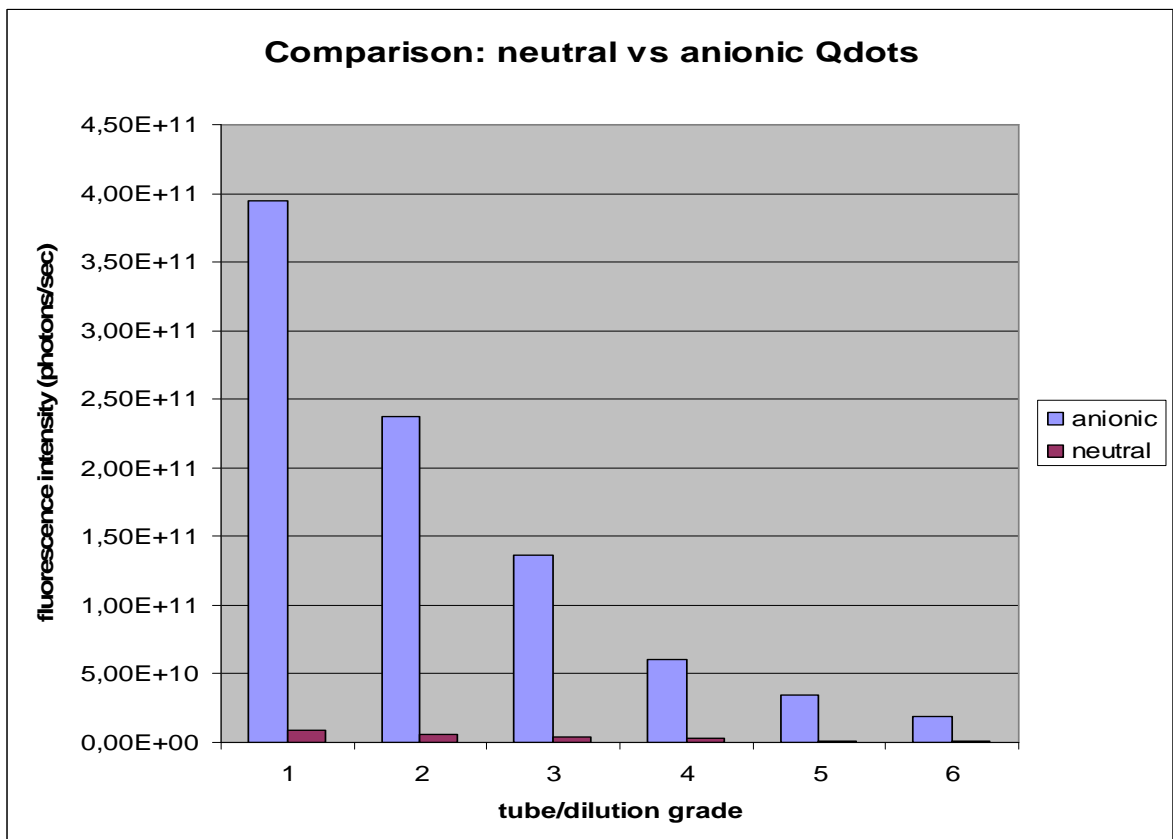


Fig. 2: dilution series of zwitterionic (red bars) vs anionic quantum dots (blue bars). For both groups QD concentrations are: 1.2, 0.6, 0.3, 0.15, 0.075, 0.0375 mmol/l corresponding to tubes 1 to 6.



3.2.2 Biodistribution of QD, QD/PEI and QD/pDNA/PEI polyplexes in *nu/nu* mice

The first experiment with QD was a distribution study and toxicity evaluation of anionic QD, conjugated with PEI and PEI-DNA (pCMV) polyplexes. We aimed at checking the fluorescent properties of these dyes to compare them with the organic dyes (Alexa 750 and NIR 797) and verifying signal modifications after complexing of QD with PEI and PEI-DNA.

Animals: 6 (2 males and 4 females) *nu/nu* mice, 5 weeks old; tumor-free

Application scheme:

Mouse 1	QD + PEI-DNA
Mouse 2	QD + PEI-DNA
Mouse 3	QD + PEI
Mouse 4	QD + PEI
Mouse 5	QD
Mouse 6	HBG buffer (ctrl)

Body fluorescence emission was checked 15 minutes and 6 hours after systemic injection. Thereafter All animals were sacrificed and their organs excised, in order to separately measure their specific fluorescence emission.

Fig. 1a,b: *in vivo* fluorescence emission signal (photons/sec) 20 minutes and 6 hours after iv application of free QD (left) vs control (middle); n: QD/PEI-DNA=2, QD/PEI=2, QD free=1, ctrl=1.

a: after 20 minutes

b: after 6 hours

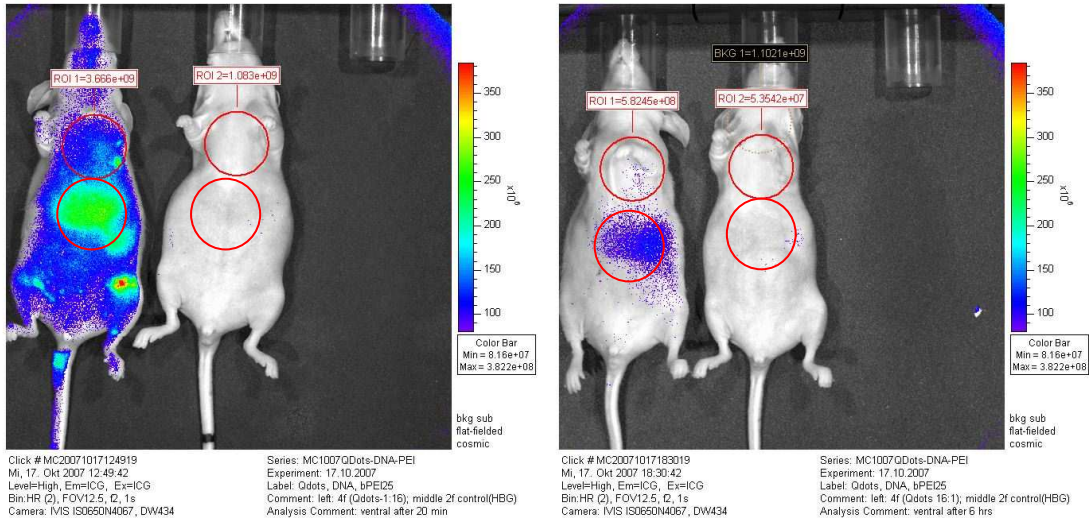


Fig. 2c,d: *in vivo* fluorescence emission signal (photons/sec) 20 minutes and 6 hours after iv application of QD/DNA-PEI polyplexes (left) vs control (middle) vs QD/PEI (right); n: QD/PEI-DNA=2, QD/PEI=2, QD free=1, ctrl=1.

c: after 20 minutes

d: after 6 hours

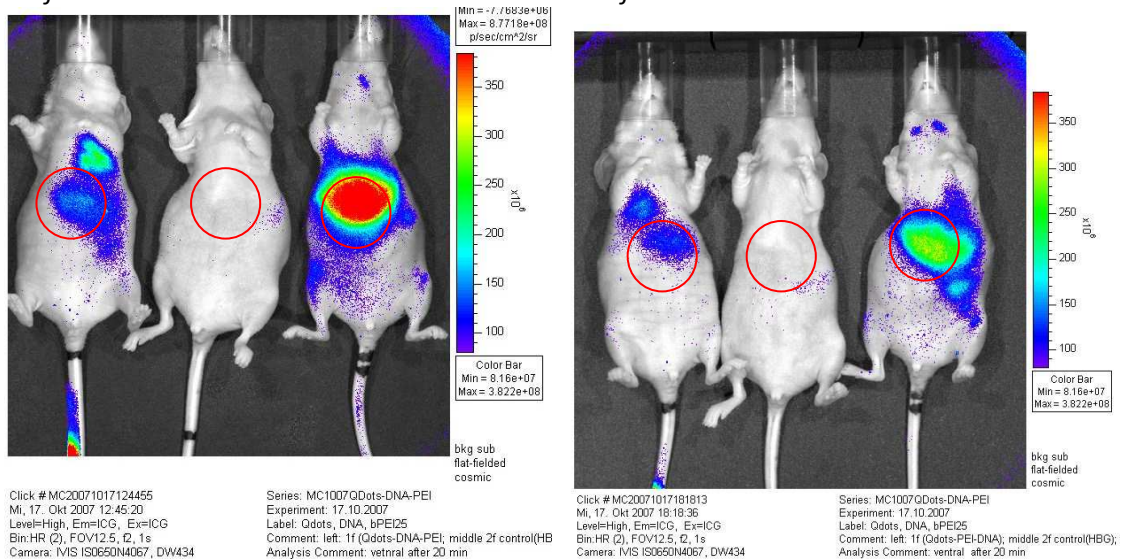


Fig. 3: fluorescence emission signal (ph/sec) 20 minutes and 6 hours after iv application of QD/DNA-PEI polyplexes vs QD/PEI vs free QD vs control from the abdominal region (liver).
 n: QD/PEI-DNA=2, QD/PEI=2, QD free=1, ctrl=1.

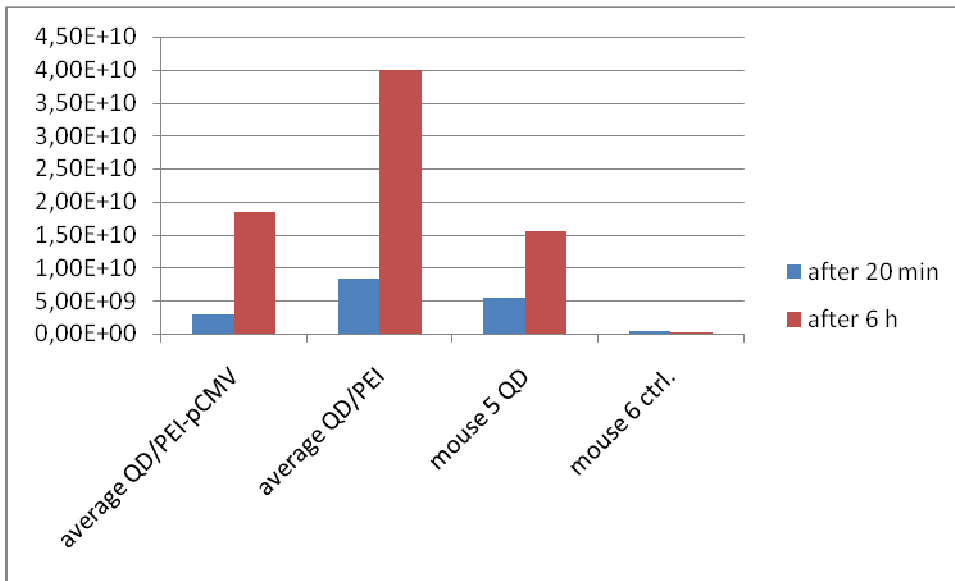


Fig. 4: ex vivo fluorescence emission signal (ph/sec) of excised organs 6 hours after iv application of QD/DNA-PEI polyplexes vs QD/PEI conjugates vs QD alone vs control.
 n: QD/PEI-DNA=2, QD/PEI=2, QD free=1, ctrl=1.

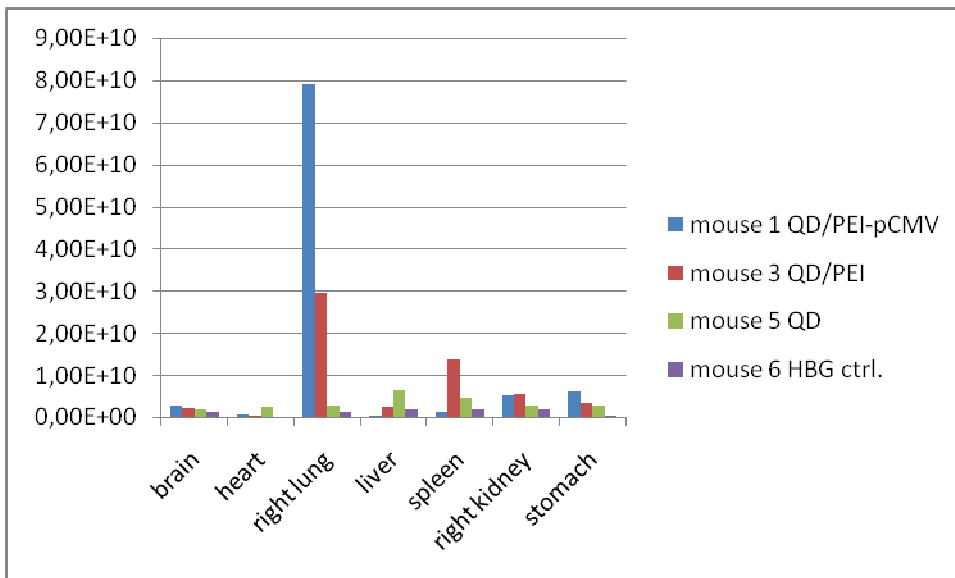
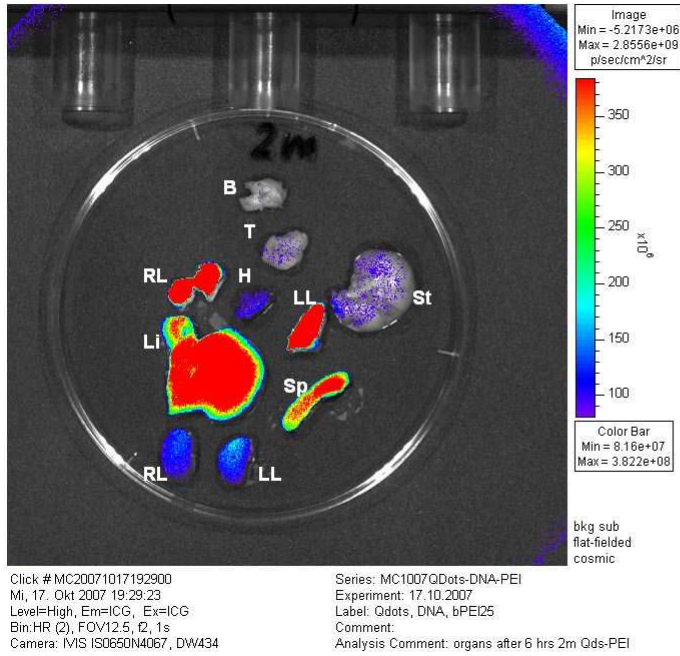
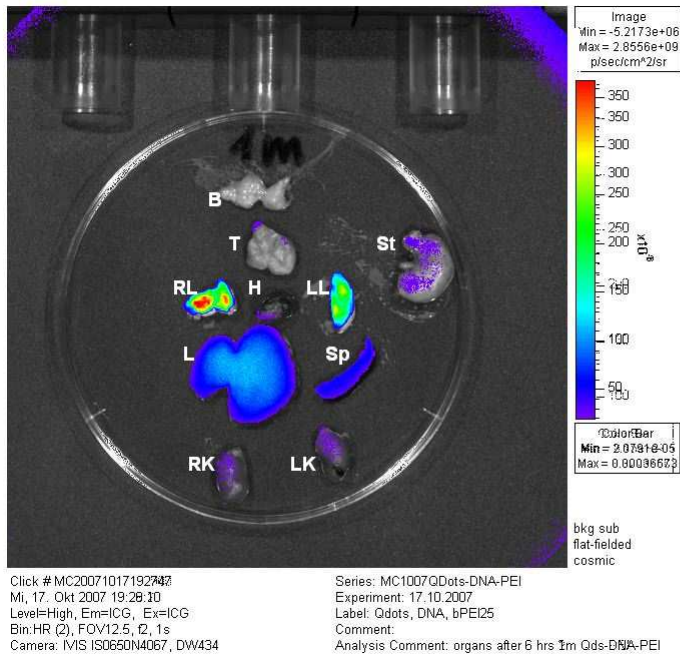


Fig. 5a,b,c,d: *ex vivo* fluorescence emission signal (photons/sec) of excised organs of 4 mice after application of QD/PEI conjugates vs QD/DNA-PEI polyplexes vs free QD vs control. B=brain; T=thyroid; RL, LL=right, left lung; H=heart; St=stomach; Li=liver; Sp=spleen; RK, LK=right, left kidney; n: QD/PEI-DNA=2, QD/PEI=2, QD free=1, ctrl=1.

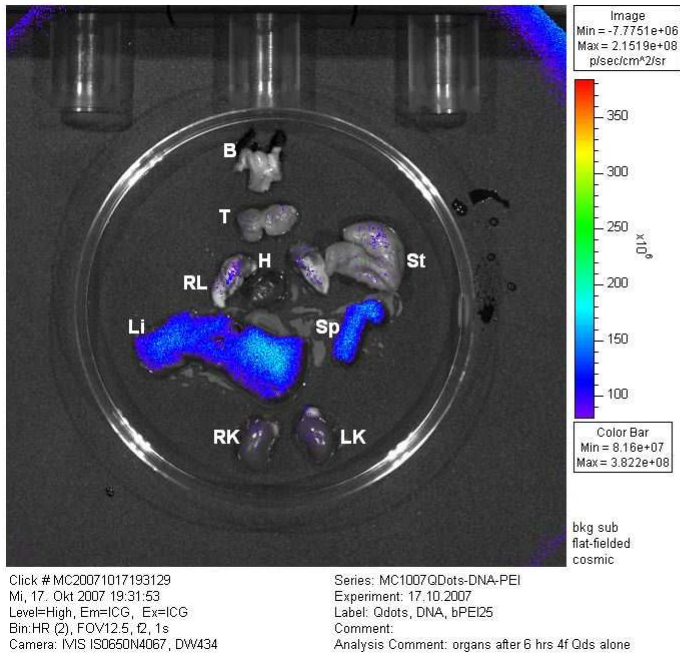
a: QD/PEI



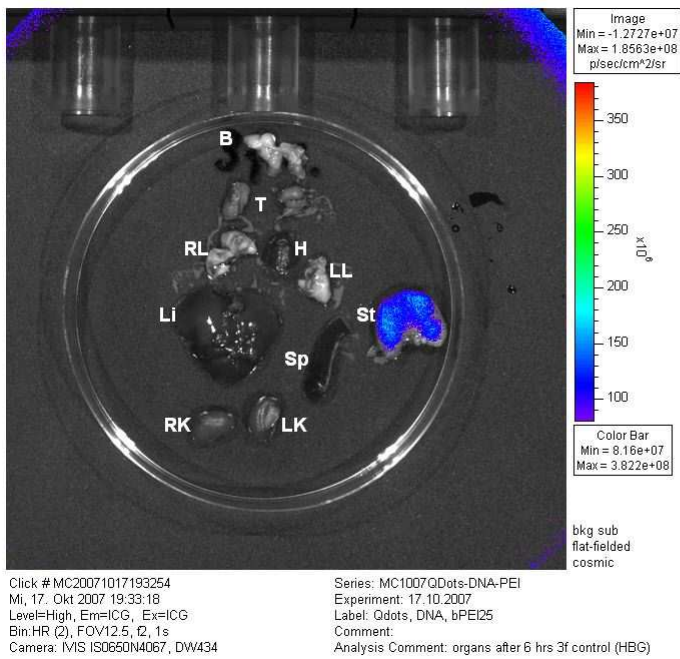
b: QD/PEI-DNA



c: free QD



d: control (fluorescence only present in stomach, containing feeding material)



Mice administered with QD/PEI displayed the most intense signal: all animals belonging to this group showed the highest liver accumulation intensity (*fig. 2c,d* and *5a*). Fluorescent signal were detected in lungs for the QD/PEI-DNA group (*fig. 2c,d, 4* and *5b*), in bones and joints for the QD “free” group (*fig. 1a*). Negatively charged nucleic acid (DNA) within the polyplexes impacted body diffusion patterns of the carriers while enhancing lungs accumulation probably because of increased size. Free quantum dots accumulated in bone marrow and joints due to their small size (a similar result had been observed using small-sized OEI labeled with Alexa 750 in comparison to Alexa 750-PEI conjugates). QD fluorescence was slightly less intense than free Alexa 750 and comparable to free NIR 797 but the concentration of administered QD was much lower (0.75 nmol QD vs 5 nmol organic dye). Moreover QD are much cheaper and can be produced by a partner laboratory. Therefore we concluded to continue our *in vivo* tests using QD and to utilize them for DNA delivering studies with implanted tumors.

3.2.3 Tumor targeting properties of QD labeled polyplexes

3.2.3.1 EGF-R targeting in HUH7 Human Hepatocellular Carcinoma (I)

This was the first assay with tumor bearing animals and QD. We chose first Human Hepatocellular Carcinoma HUH cells which overexpress receptors for EGF (EGF-R). We aimed at targeting it with our fluorescently labeled vectors carrying EGF on their surface using PEI, PEI-EGF conjugates and PEI-EGFP Luc(DNA) polyplexes.

Animals: 15 female *nu/nu* mice, 7 weeks old; 4 mice bearing HUH7 Luc cells tumors and 11 mice tumor free (not implanted).

Application scheme:

Mice A1, A2, A3 (tumor free)	QD free
Mice B2, C1, C2 (tumor free)	QD/PEI
Mice B1, B3 (tumor bearing)	PEI st. dose
Mice D1, D2, D3 (tumor free)	QD/PEI/EGFP Luc PEI st. dose
Mice E2, E3 (tumor bearing), Mouse E1 (tumor free)	QD/PEI-EGF PEI-EGF: 2/3 of st. dose)
Mouse C3 (ctrl)	not treated

Considering previous experience we used 2/3 of standard PEI dose for QD/PEI-EGF complexes to reduce their size avoiding pulmonary embolism. Particles size was measured 30 minutes after separate dilution in HBG and careful mixing of the reagents.

- QD/PEI average size: 117 nm
- QD/PEI/EGFP Luc average size: 204 nm
- QD/PEI-EGF average size: 186 nm

We considered these values suitable for iv application into living animals. Body fluorescence was detected 15 minutes, 6 and 24 hours after systemic injection. After 24 hours the mice were sacrificed and their organs (lungs, liver, heart, spleen, kidneys and tumor) were excised and checked for fluorescence emission.

Fig. 1: mouse A1 (free QD, left) 15 minutes after injection vs ctrl (right). Filter ex/em: ICG/ICG. Regions of interest (liver, lungs) marked with red circles.

n: QD free =3, QD/PEI =5, QD/PEI-EGF-DNA=3, QD/PEI-EGF=3, ctrl=1

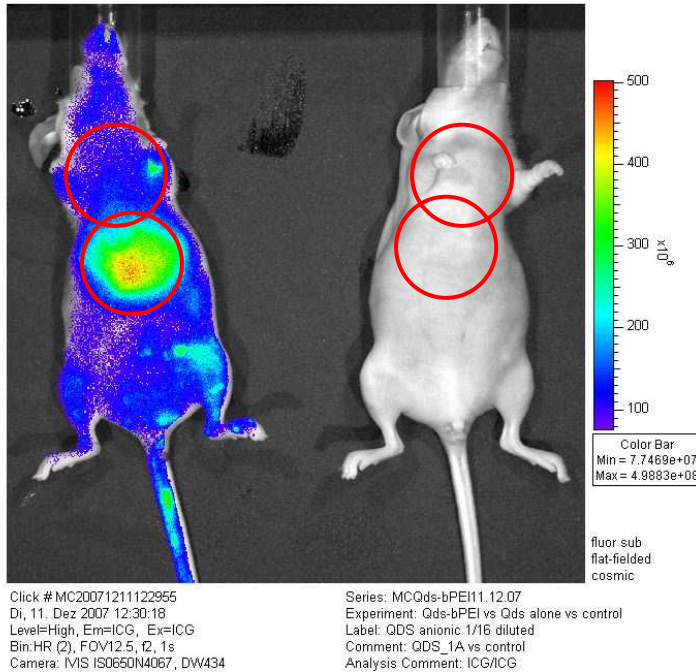


Fig. 2: mice C1 and C2 (QD/PEI) 15 minutes after injection vs ctrl (right). Filter ex/em: ICG/ICG. Regions of interest (liver, lungs) marked with red circles.

n: QD free =3, QD/PEI =5, QD/PEI-EGF-DNA=3, QD/PEI-EGF=3, ctrl=1

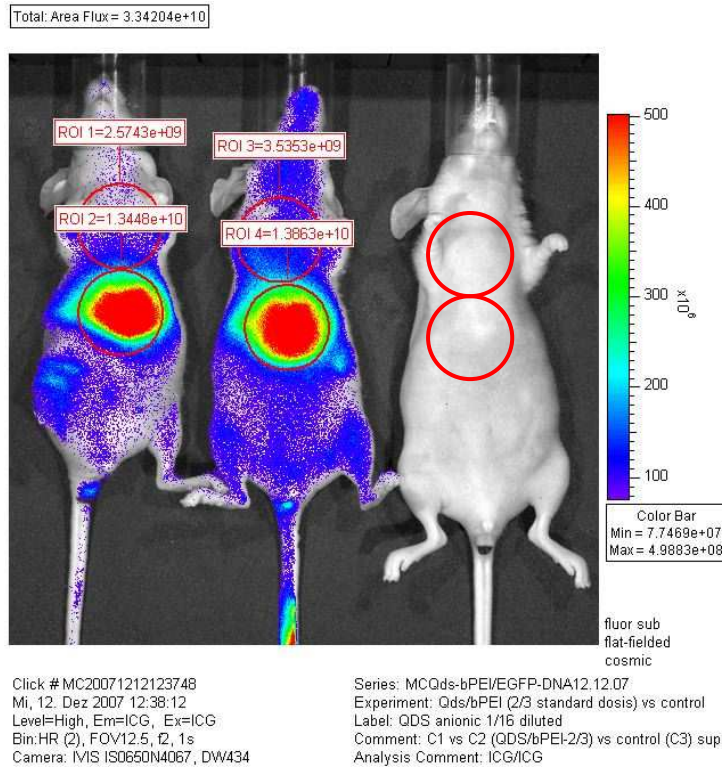


Fig. 3: mouse D1 (QD/PEI/EGFP Luc 15 minutes after injection vs ctrl. Filter ex/em: ICG/ICG. Regions of interest (liver, lungs) marked with red circles.

n: QD free =3, QD/PEI =5, QD/PEI-EGF-DNA=3, QD/PEI-EGF=3, ctrl=1

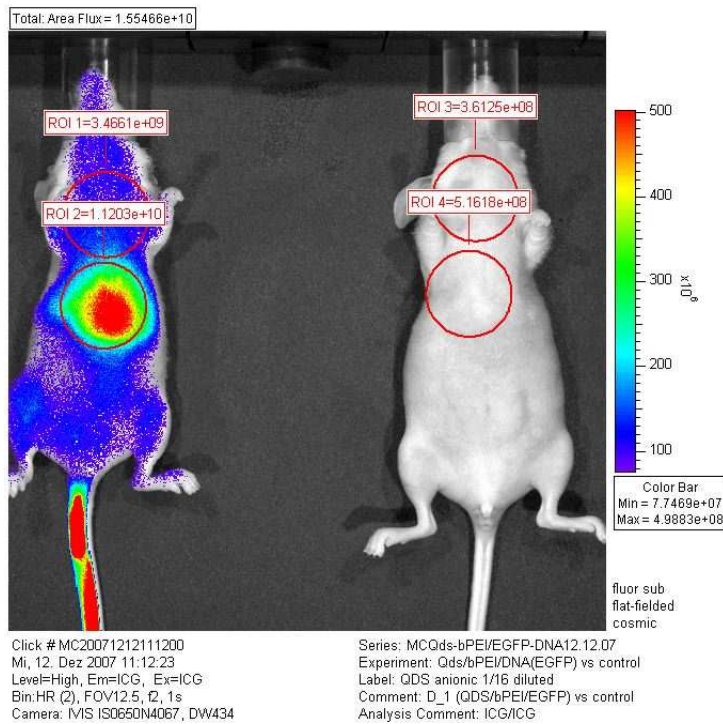


Fig. 4: mouse E3 (QD/PEI-EGF) 15 minutes after injection vs ctrl. Filter ex/em: ICG/ICG. Regions of interest (liver) marked with red circles.

n: QD free =3, QD/PEI =5, QD/PEI-EGF-DNA=3, QD/PEI-EGF=3, ctrl=1

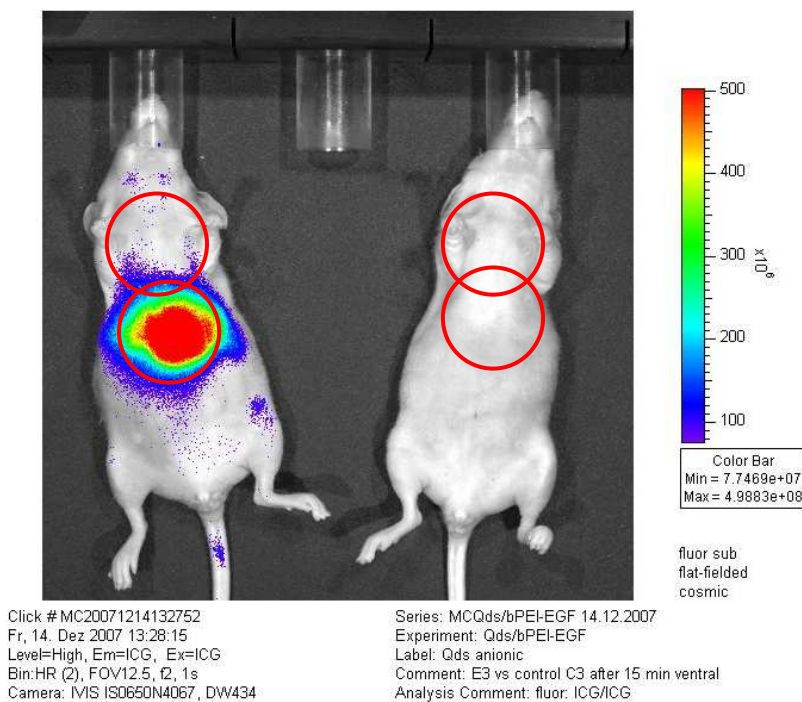
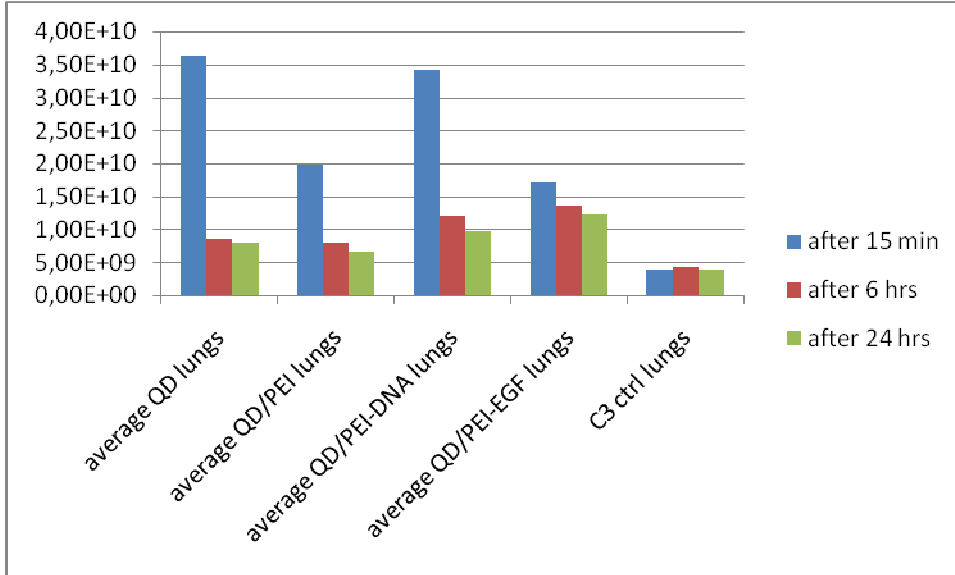


Fig. 5a,b: *in vivo* fluorescence emission signal (ph/sec) 15 minutes, 6 and 24 hours after iv injection of free QD vs QD/PEI vs QD/PEI-EGFP Luc vs QD/PEI-EGF vs ctrl in lungs and liver.
n: QD free =3, QD/PEI =5, QD/PEI-EGF-DNA=3, QD/PEI-EGF=3, ctrl=1.

a: lungs



b: liver

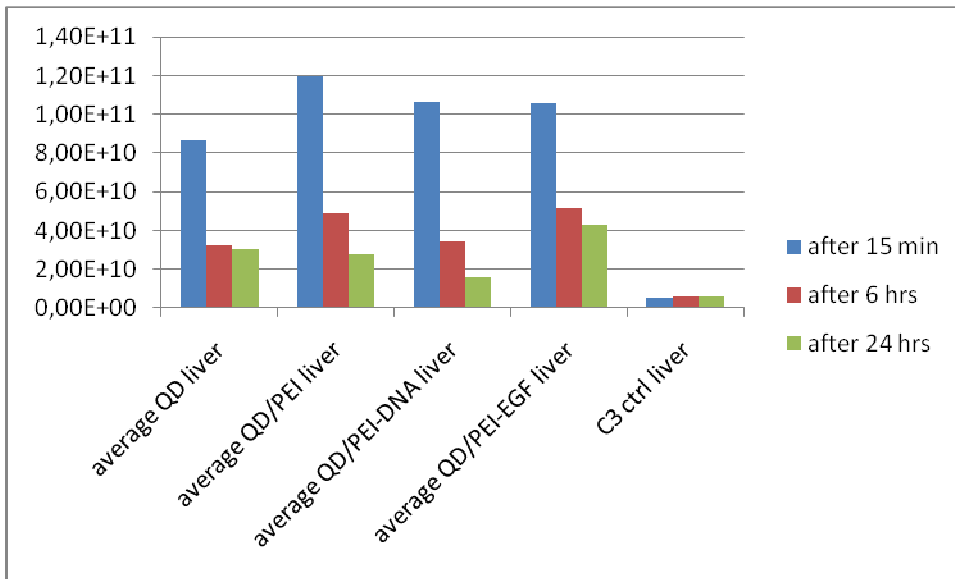


Fig. 6: excised organs of mouse E2 (QD/PEI-EGF).

RL, LL=right, left lung; H=heart; Li=liver; Sp=spleen; RK, LK=right, left kidney, Tu=tumor.

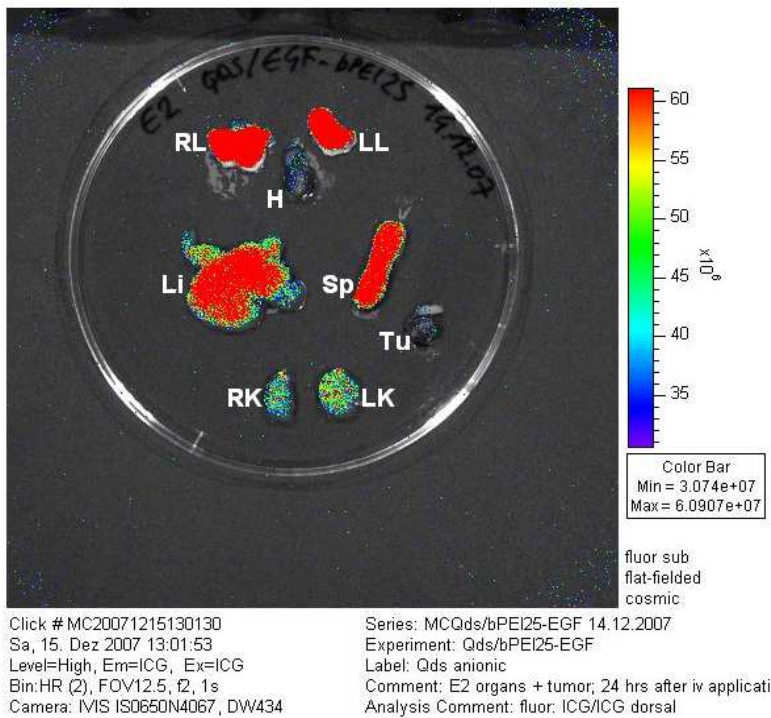


Fig. 7: excised organs of mouse E3 (QD/PEI-EGF). Fluorescent tumor signal (right down).

Two little tumor masses are presented on the skin region upside.

RL, LL=right, left lung; H=heart; Li=liver; Sp=spleen; RK, LK=right, left kidney, Tu=tumor.

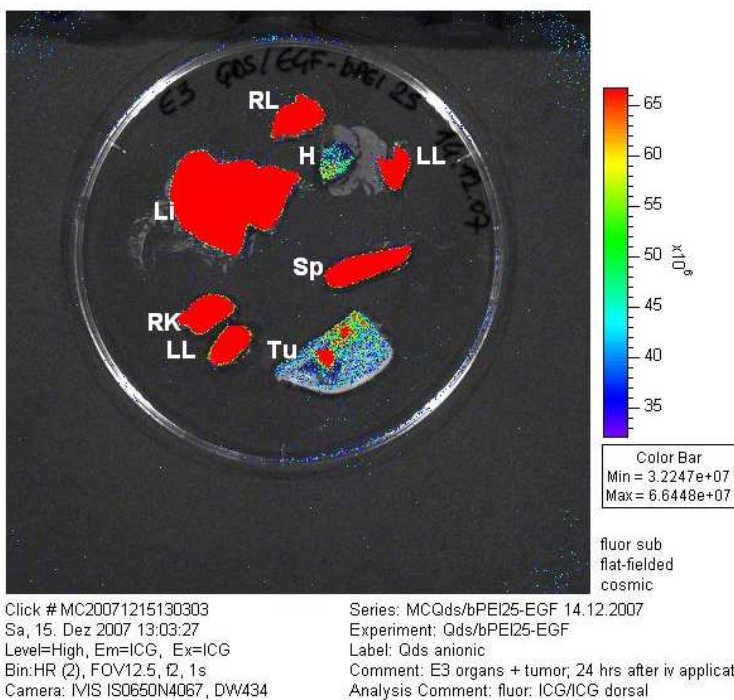


Fig. 8: excised organs of mouse C3 (control).
 T=thyroid; RL, LL=right, left lung; H=heart; Li=liver; Sp=spleen; RK, LK=right, left kidney.

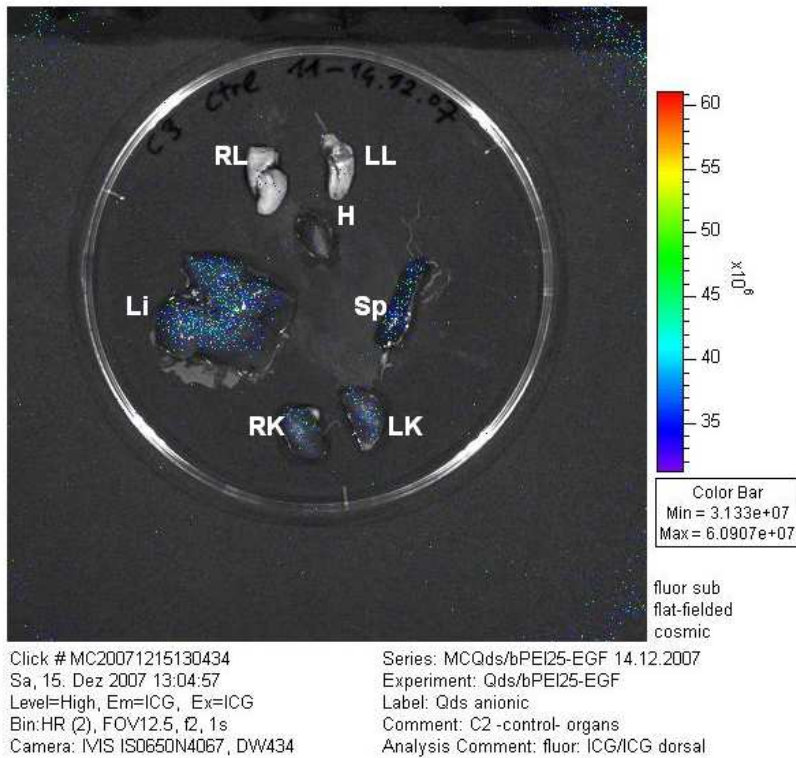
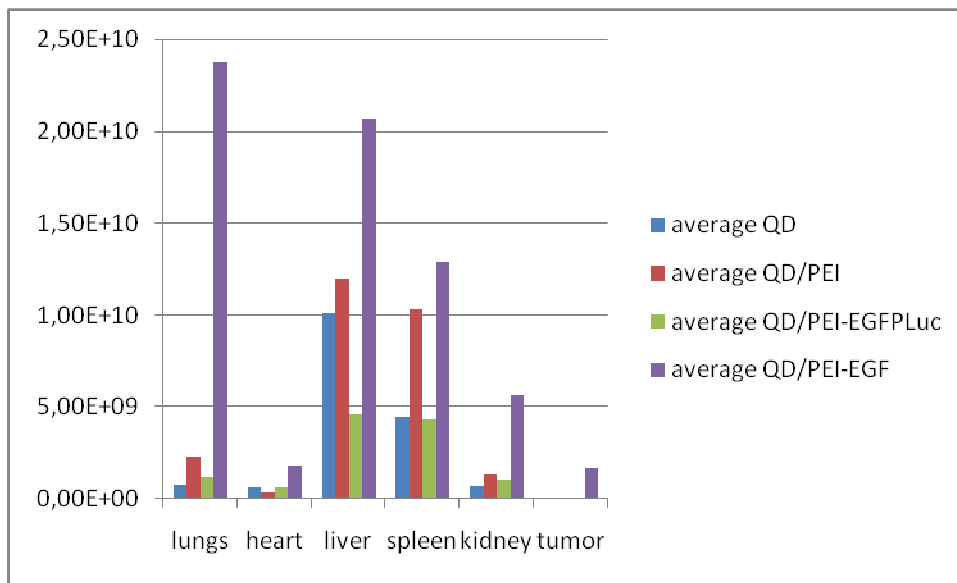


Fig. 9: ex vivo organ-specific fluorescence signals (ph/sec). Only mice B1, B3 (QD/PEI), E2, and E3 (QD/PEI-EGF) had visible tumors. n: QD free =3, QD/PEI =5, QD/PEI-EGF-DNA=3, QD/PEI-EGF=3, ctrl=1.



In all groups the fluorescence in liver was higher than in lungs due to standardized particle size. Hepatic intensities in vivo were in general stronger than pulmonary fluorescence (*fig. 5a,b*). Only mice administered with QD/PEI-EGF showed a comparable signal for liver and lung ex vivo (*fig. 9*). For all animals fluorescence emission values decreased over time (*fig. 5a,b*). In Mice E1, E2, E3 (QD/PEI-EGF) a clear accumulation in excised lung was observed (*fig. 6 and 7*). EGF-PEI caused higher pulmonary emission than other conjugates though 2/3 of standard PEI dose had been taken. In excised organs a fluorescent signal from tumor tissue was detectable however too weak for detection in vivo (*fig. 7 and 9*). To improve this signal we planned to perform a test using QD/PEI-EGF conjugated with PEG-shielding.

3.2.3.2 EGF-R targeting in HUH7 Human Hepatocellular Carcinoma (II)

Last experiment showed for the first time visible fluorescent signals in the excised tumor tissue. We tried to obtain a measurable fluorescence signal difference in vivo tumor and background protecting our QD/PEI-EGF conjugates with PEG.

Animals: 5 nu/nu females, 8 weeks old; bearing HUH7 cells tumors

Application scheme:

Mice A1, A2, B2, B3	QD/PEI-EGF-PEG
Mouse B1 (ctrl)	not treated

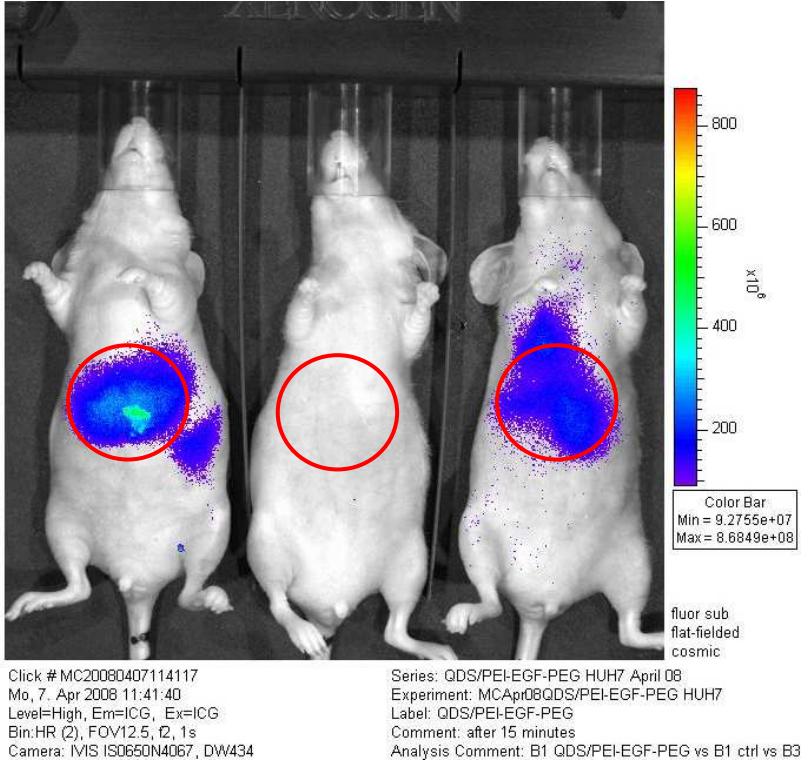
Particles size was measured 30 minutes after separate dilution in HBG and careful mixing of the reagents.

QD/PEI-EGF-PEG	size: 199.5 nm
----------------	----------------

This value was considered adapted for iv applications into living animals avoiding lungs aggregations.

Fig. 1a,b: fluorescent image (supine) 15 minutes and 24 hours after QD/PEI-EGF-PEG iv application (right and left) vs ctrl (middle). Filter ex/em: ICG/ICG. Regions of interest (liver) marked with red circles; n: QD/PEI-EGF-PEG=4, ctrl=1.

a: after 15 minutes



b: after 24 hours

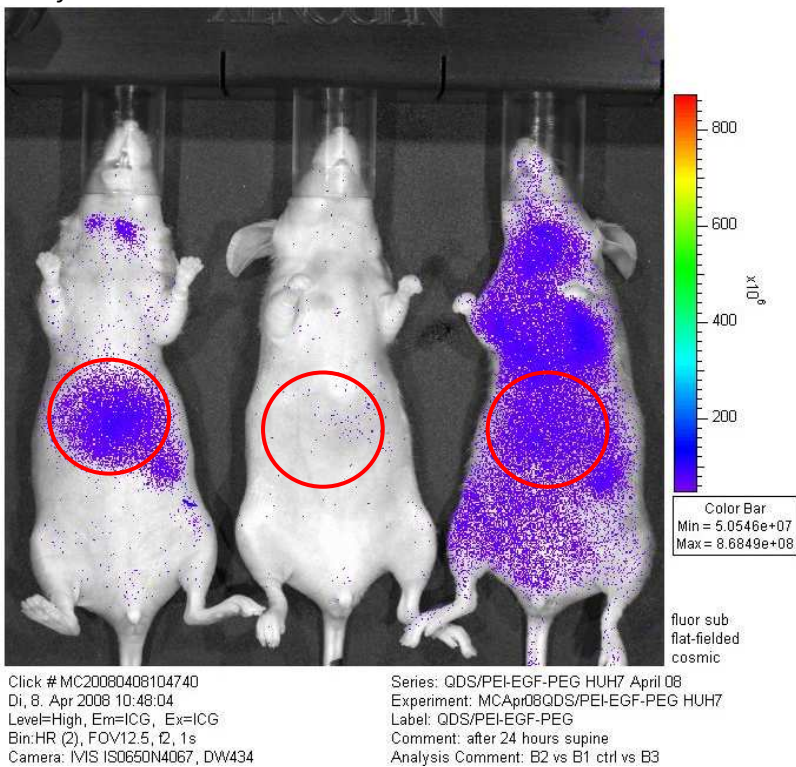
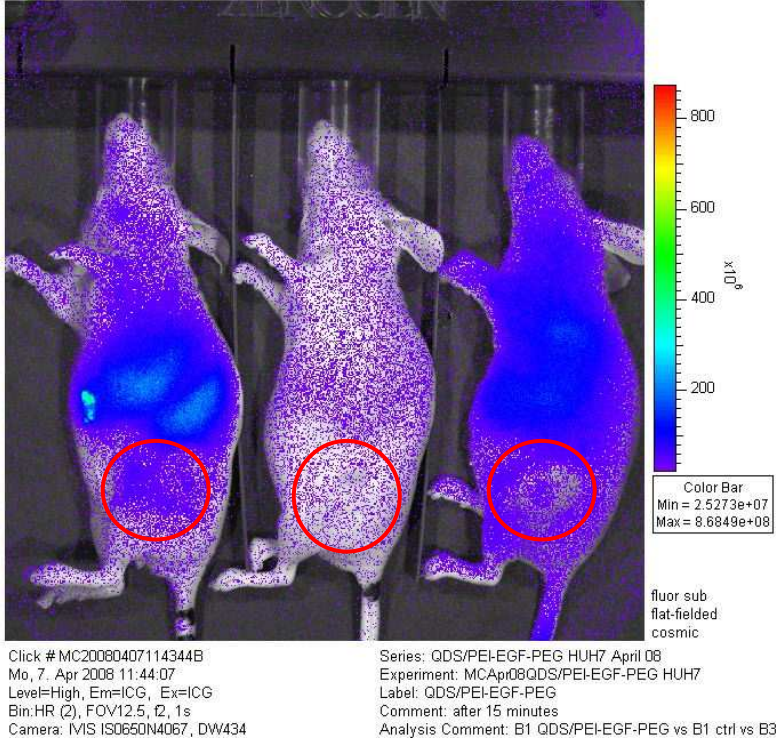


Fig 2a,b: fluorescent image (left side) 15 minutes and 24 hours after QD/PEI-EGF-PEG iv application (right and left) vs ctrl (middle). Filter ex/em: ICG/ICG. Regions of interest (tumor) marked with red circles; n: QD/PEI-EGF-PEG=4, ctrl=1.

a: after 15 minutes:



b: after 24 hours:

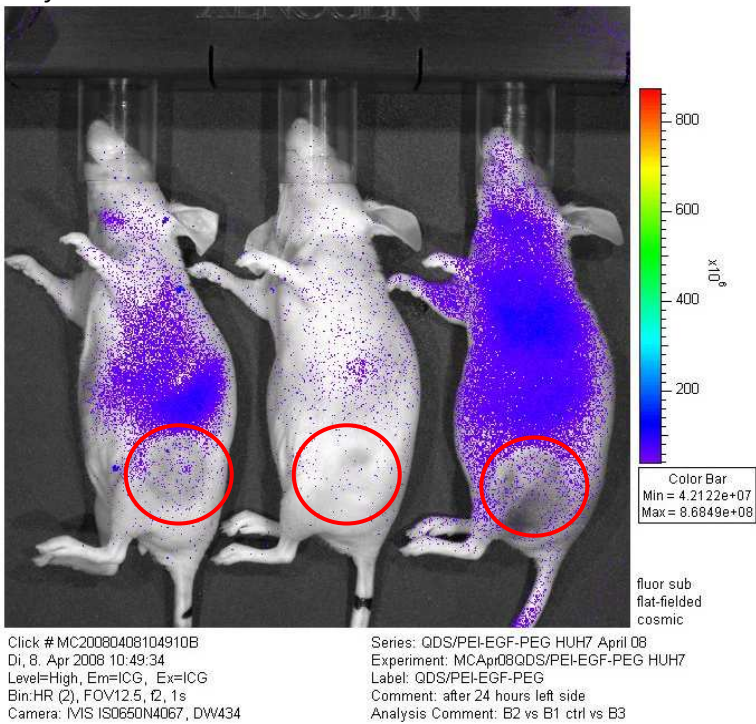


Fig. 3: excised organs of mouse A2 (QD/PEI-EGF-PEG)
 T= thyroid; RL, LL=right, left lung; H=heart; Li=liver; Sp=spleen; Tu=tumor

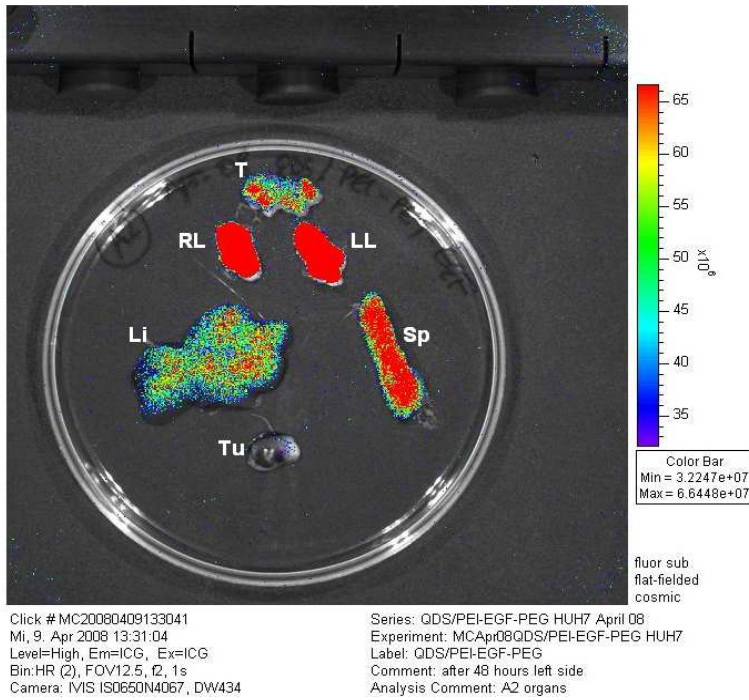
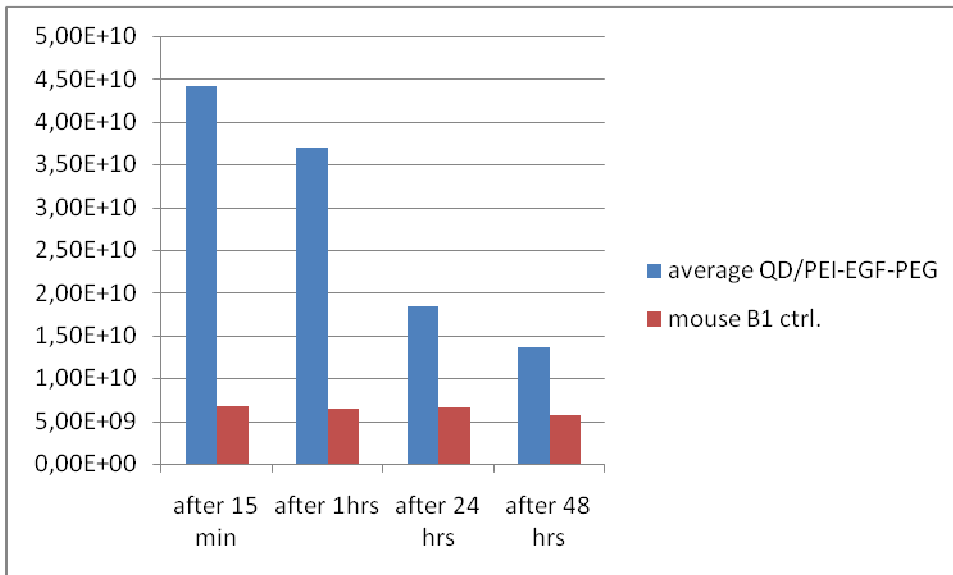
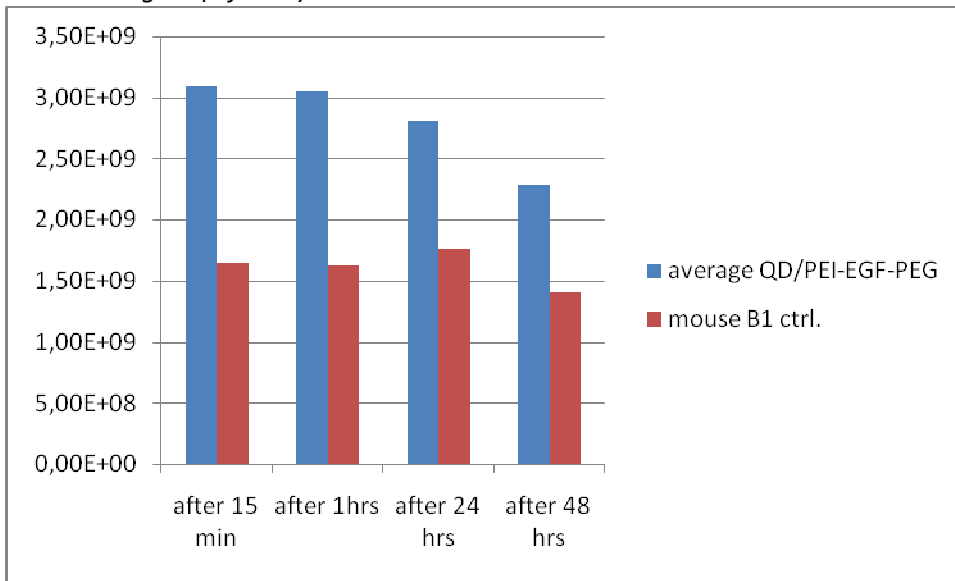


Fig. 4a,b: in vivo fluorescence imaging data 15 minutes, 1, 24 and 48 hours after iv application of QD/PEI-EGF-PEG conjugates vs ctrl (abdominal and tumor region).
 n: QD/PEI-EGF-PEG=4, ctrl=1.

a: Abdomen:



b: Tumor region (left loin):



The data showed stronger dye diffusion through the tumor tissue compared to the results of a prior experiment with QD/PEI-EGF (*fig. 4a,b*). PEG-shielding enhanced the accumulation of QD/PEI conjugates in the tumor tissue. *Fig. 1-2a,b* show optical differences in fluorescence emission between hepatic and tumor tissue (right down) between the two animals. This was probably due to inhomogeneity in tumor vascularization and size. Some more experience was needed to assess the positive impact of PEG on diffusion through tumor masses. Therefore we planned another comparison between QD/PEI-EGF and QD/PEI-PEG conjugates.

3.2.3.3 EGF-R targeting in HUH7 Human Hepatocellular Carcinoma (III)

After observing the first measurable signals from tumor tissue using QD/PEI-EGF-PEG conjugates we aimed at verifying the positive impact of PEG-shielding comparing distribution and tumor targeting properties of QD/PEI-EGF and QD/PEI-PEG conjugates labeled with anionic quantum dots (QD).

Animals: 9 *nu/nu* females, 9 weeks old; bearing HUH7 cells tumors

Application scheme:

Mice C1,C2,C3,C4	QD/PEI-EGF
Mice B1,B2,B3,B4	QD/PEI-PEG
Mouse A (ctrl)	

Particles size was measured 30 minutes after separate dilution in HBG buffer and careful mixing of the reagents.

QD/PEI-EGF	size: 198.4 nm
QD/PEI-PEG	size: 138.2 nm

Mice B3 and B4 died 24 hours after the iv administration of QD/PEI-PEG conjugates. Mice B1 and B2 which had been administered with the same solution survived although (as shown in pictures below) the amount of injected conjugates that effectively reached the circulatory system was much greater in mice B3 and B4 due to the better quality of intravenous application thus suggesting effective subacute toxicity of QD/PEI-PEG conjugates.

Fig. 1: fluorescent image 15 minutes after QD/PEI-EGF iv application (C1 vs ctrl vs C2). Filter ex/em: ICG/ICG. Regions of interest (liver) marked with black circles. n: QD/PEI-EGF=4, QD/PEI-PEG=4, ctrl=1.

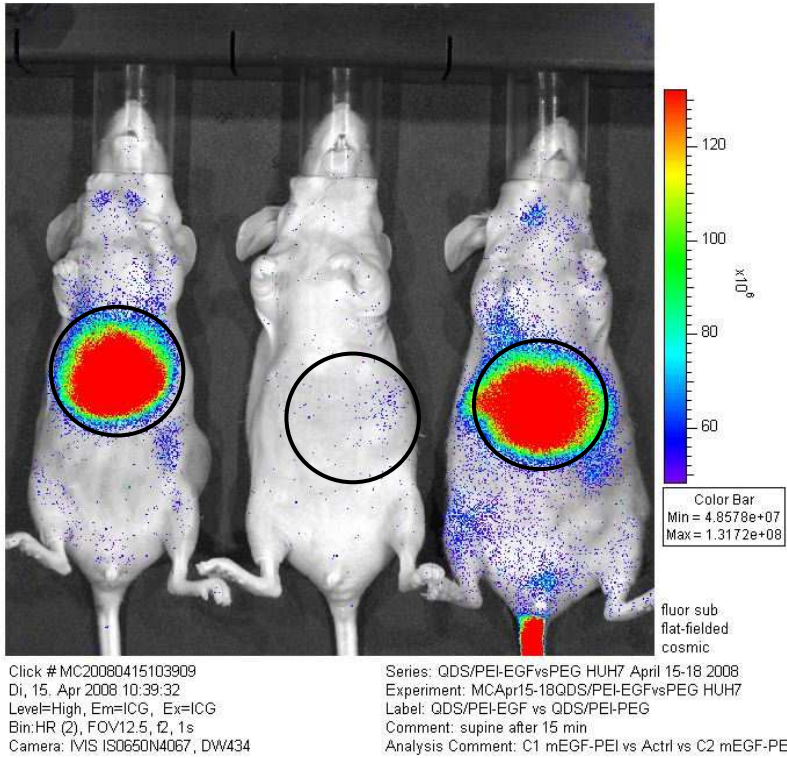


Fig. 2: fluorescent image 15 minutes after QD/PEI-PEG iv application (B3 vs ctrl vs B4). Filter ex/em: ICG/ICG. Regions of interest (liver) marked with black circles. n: QD/PEI-EGF=4, QD/PEI-PEG=4, ctrl=1.

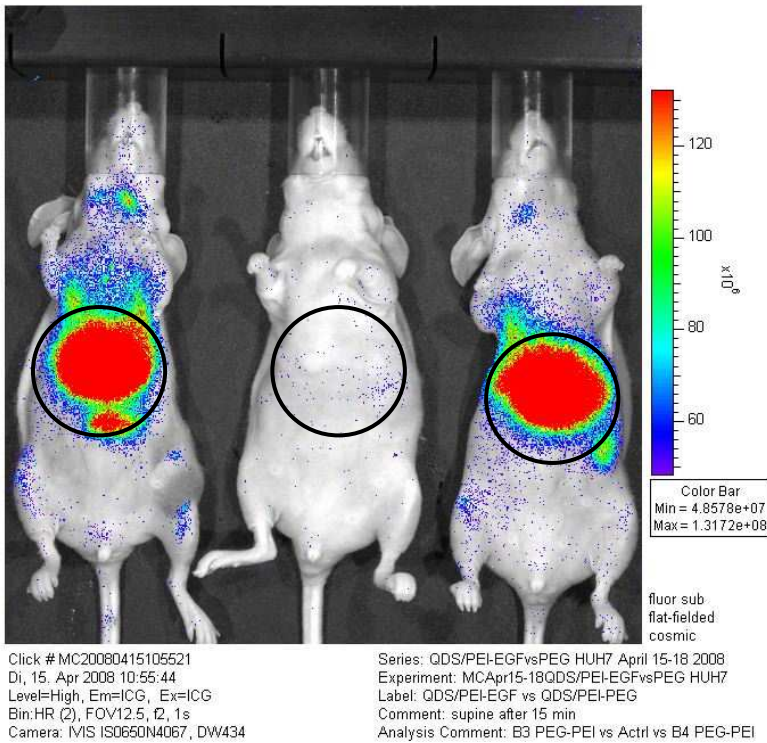


Fig. 3: fluorescent image of the left side 15 minutes after QD/PEI-EGF iv application (C1 vs ctrl vs C2). Filter ex/em: ICG/ICG. Regions of interest (tumor) marked with black circles.
 n: QD/PEI-EGF=4, QD/PEI-PEG=4, ctrl=1.

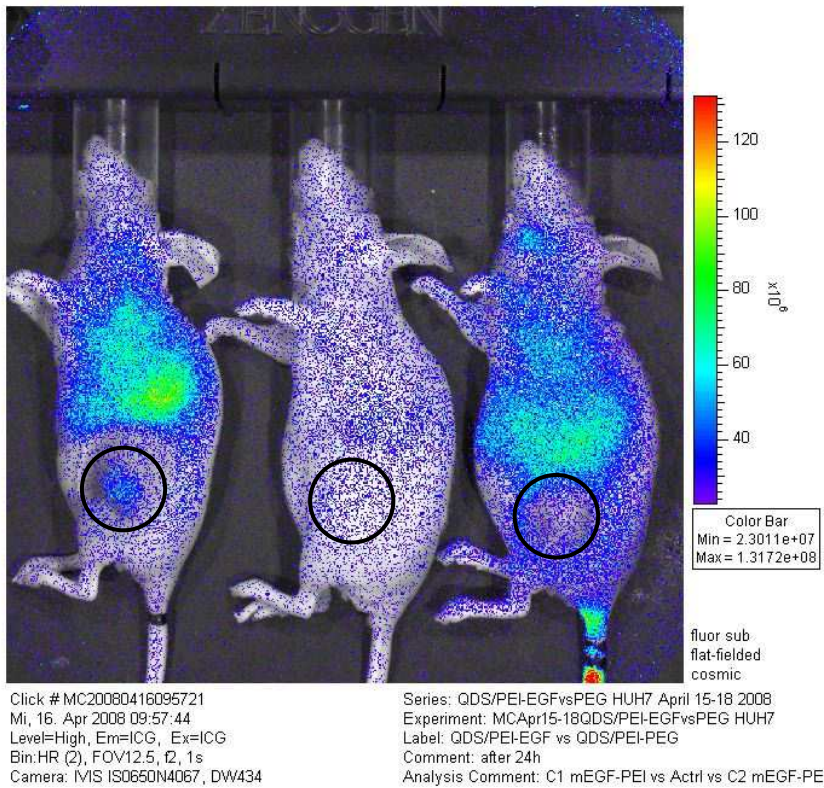
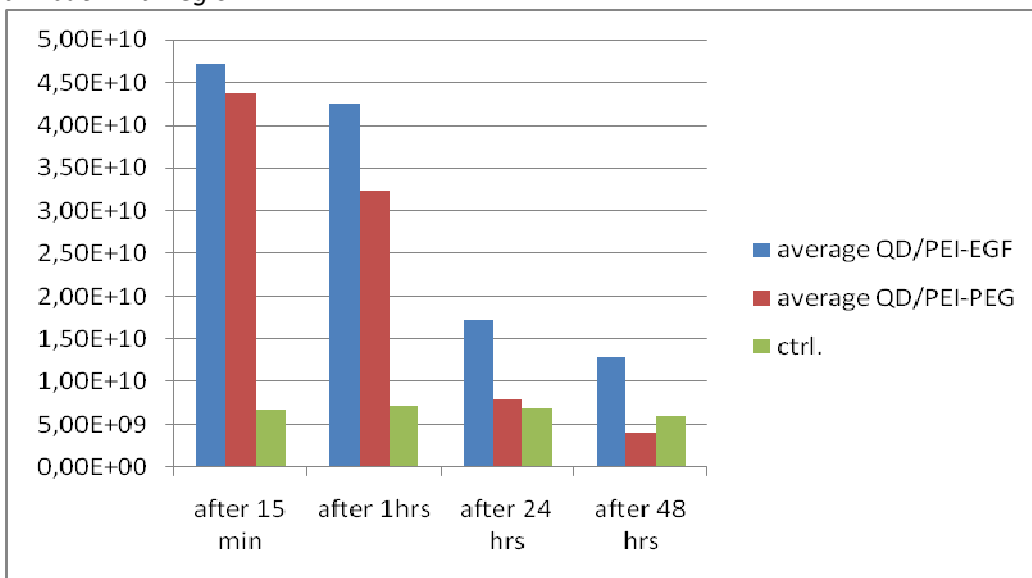
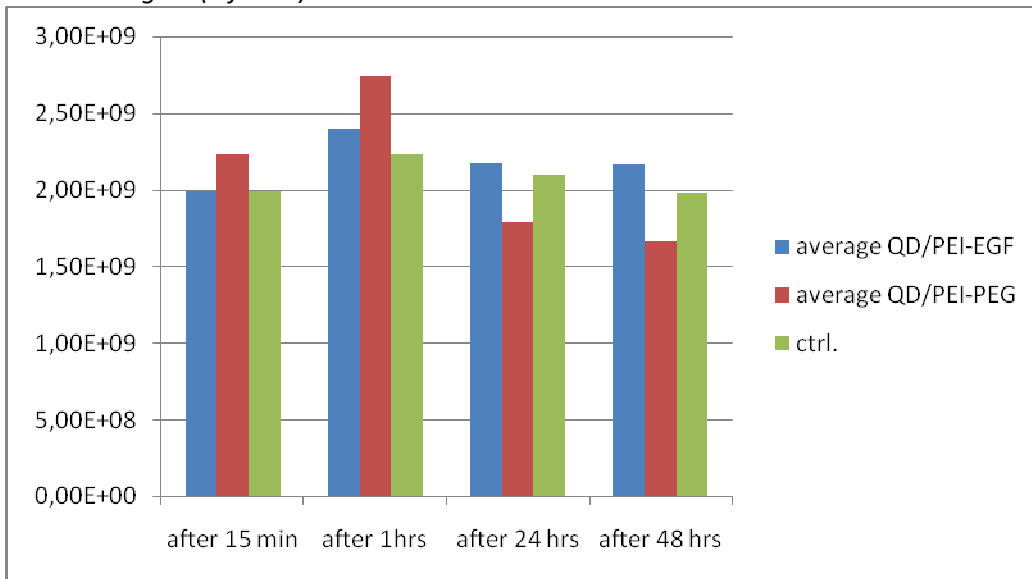


Fig. 4a,b: in vivo fluorescence imaging data 15 minutes, 1, 24 and 48 hours after iv application of QD/PEI-EGF vs QD/PEI-PEG conjugates vs ctrl (abdominal and tumor region).
 n: QD/PEI-EGF=4, QD/PEI-PEG=4, ctrl=1.

a: Abdominal region:



b: Tumor region (left loin):



The intensity of dye diffusion through the tumor tissue was comparable to the results using QD/PEI-PEG-EGF conjugates in previous test. Both QD/PEI-EGF and QD/PEI-PEG conjugates spread within liver, spleen, thyroid and lungs in a very similar way (*fig. 1,2*). Just mouse C1 (QD/PEI-EGF) showed a stronger optical tumor signal in images taken after 24 and 48 hours as shown above (*fig. 3*). PEG-shielding positively impacted dye diffusion throughout the tumor tissue 1 hour after application.

3.2.3.4 EGF-R targeting in HUH7 Human Hepatocellular Carcinoma (IV)

All fluorescence imaging data obtained using QD-labeled conjugates and polyplexes of the last three assays (I,II,III) performed using PEI-DNA vs PEI-EGF vs PEI-EGF-PEG vs PEI vs ctrl are collected and compared in graphs below, sorted on the basis of the body region of interest.

Fig. 1: in vivo fluorescence imaging data from abdomen of all animals treated with:

- Free QD 3 mice
- QD/PEI st. dose 5 mice
- QD/PEI-EGFP Luc 3 mice
- QD/PEI 2/3 st. dose 3 mice
- QD/PEI-EGF 4 mice
- QD/PEI-PEG 4 mice
- QD/PEI-EGF-PEG 4 mice
- Buffering solutions (ctrl) 3 mice

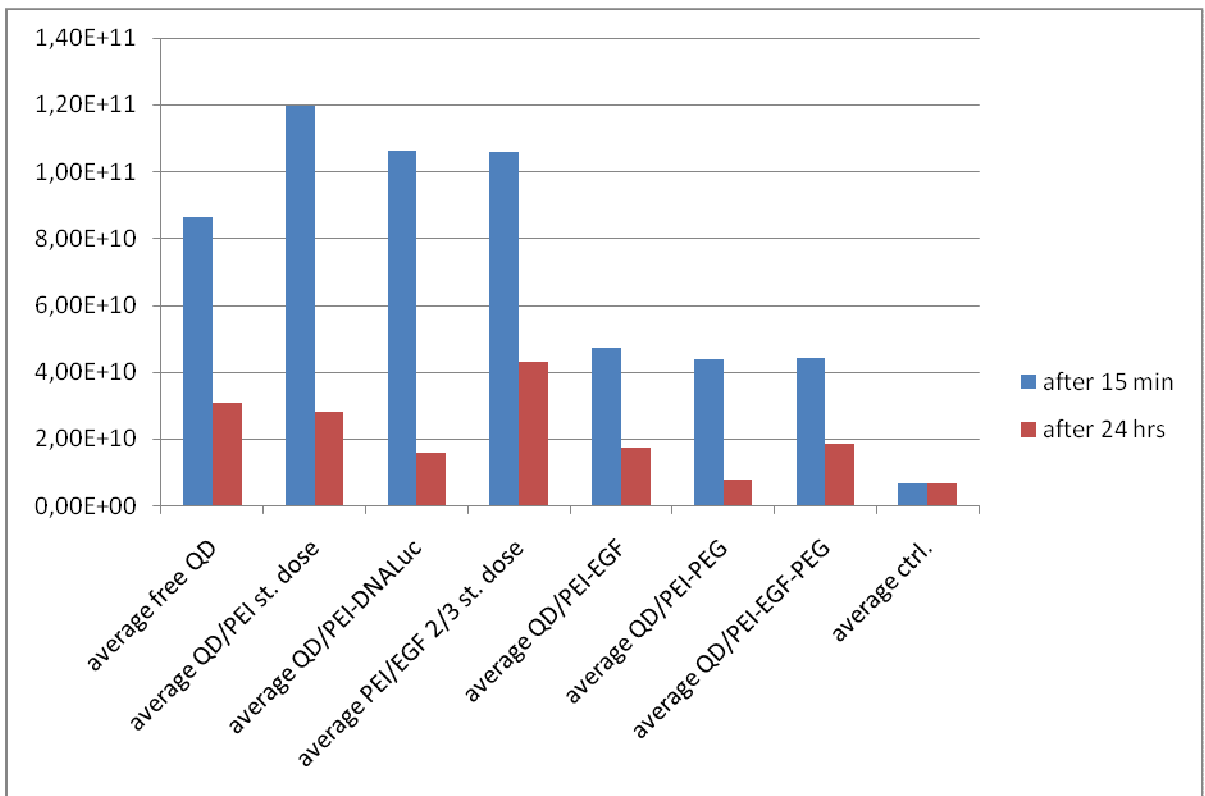
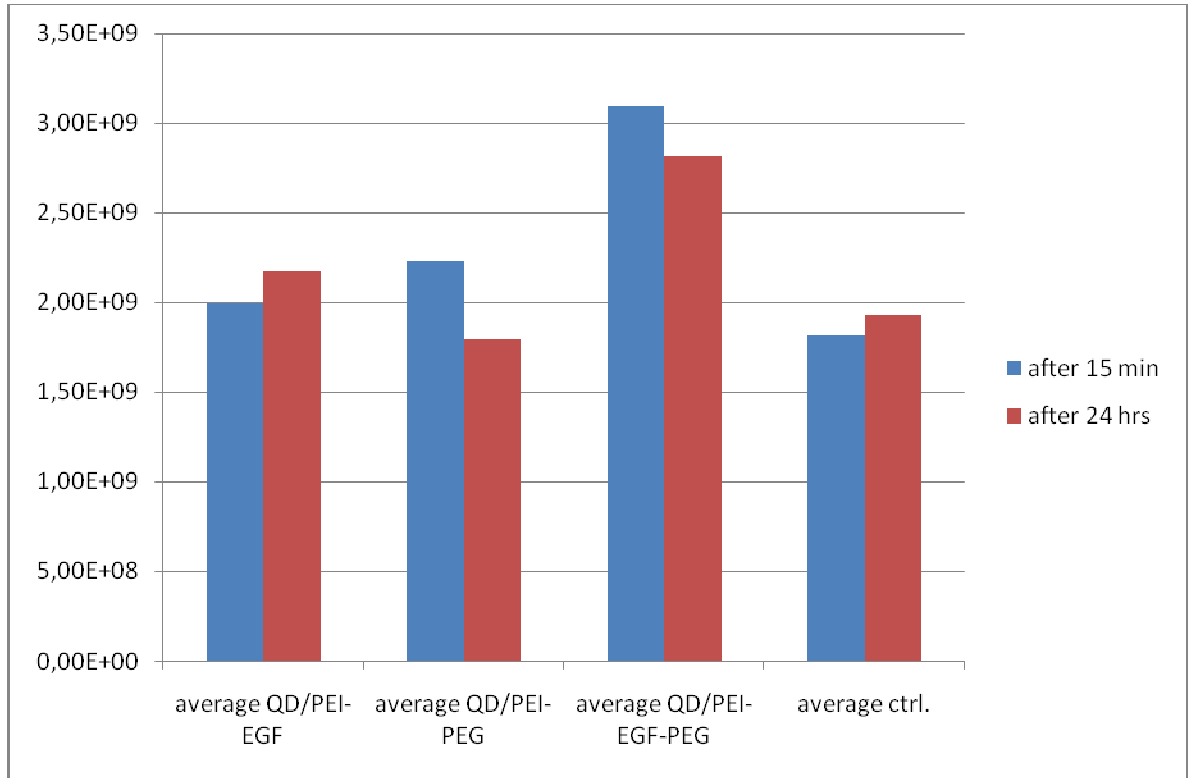


Fig. 2: *in vivo* fluorescence imaging data from tumor of all animals treated with:

- QD/PEI-EGF 4 mice
- QD/PEI-PEG 4 mice
- QD/PEI-EGF-PEG 4 mice
- Buffering solutions (ctrl) 3 mice



In vivo fluorescence emission patterns of QD/PEI, QD/PEI-EGF and QD/PEI-PEG were basically similar. We did not observe whole body diffusion patterns, as detected after application of non-conjugated quantum dots, but hepatic accumulation after 15 minutes slowly decreasing over time, and a modest accumulation in the tumor tissue. Occasionally tumor specific signals were very strong and comparable to that of the liver (considering a region with the same surface). Slightly more intense fluorescence was registered after PEG-shielding. EGF-PEI conjugates caused higher pulmonary emission and slower decrease of lungs fluorescence 24 hours after iv injection. In respect of biocompatibility QD/PEI-PEG particles seemed to be more toxic than the others.

3.2.3.5 Tf-R targeting in N2a Murine Neuroblastoma

N2a is the second tumor cell line, well-established for in vivo imaging, that we used. It over-expresses receptors for human transferrin (hTf or Tf), so that conjugates containing transferrin are preferentially delivered into this tissue. We planned a distribution and tumor targeting study of QD-labeled conjugates with PEI, PEG-PEI and Tf-PEG3.4-PEI mixed with PEG20-PEI (termed Tf-PEG-PEI). Our aim was defining the impact of transferrin on distribution properties, verifying the positive effect of PEG-shielding of the conjugates and comparing the results obtained with those using EGF in HUH7 tumor cells.

Animals: 13 nu/nu males, 5 weeks old; bearing N2a tumors

Application scheme:

Mice 1,2,3,4	QD/Tf-PEG-PEI*
Mice 5,6,7,8	QD/PEG-PEI
Mice 9,10,11,12	QD/Tf-PEI

30 minutes after separate dilution in HBG and mixing of the reagents particles size was measured.

QD/ Tf-PEG3.4-PEI/PEG20-PEI*	average size: 326 nm
QD/PEG-PEI	average size: 169 nm
QD/Tf-PEI	average size: 259 nm

On the basis of previous experience we considered these dimensions suitable for iv application into living animals in order to avoid lungs entrapment.

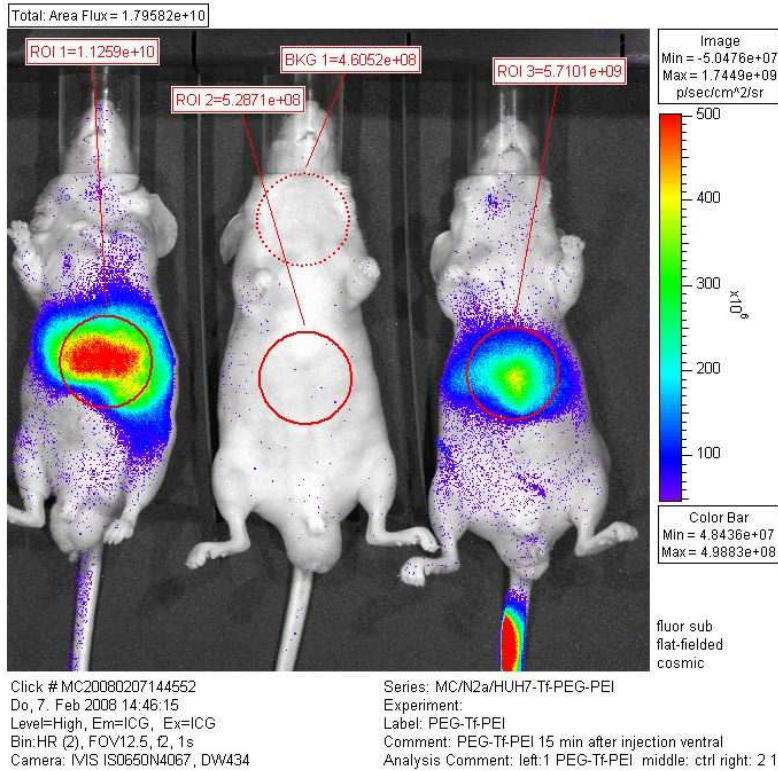
Body fluorescence emission signal was checked 15 minutes, 2, 24, and 48 hours after systemic injection. After 48 hours all animals were sacrificed and their livers and tumors were excised and checked for fluorescence emission.

Mice 4 and 5 died 20 hours after the iv application.

*Repeated measurements of Tf-PEG3.4-PEI complexed with anionic QD showed very large dimensions (diameter>2000 nm). To obtain soluble particles, mixtures of PEG-PEI (50%) and hTf-PEG3.4-PEI (50%) were used and the complexes termed QD/Tf-PEG-PEI.

Fig. 1a,b: *in vivo* fluorescence emission signal 15 minutes after iv application of QD/Tf-PEG-PEI conjugates (left and right) vs HBG buffer (middle). Filter ex/em: ICG/ICG); n: QD/Tf-PEG-PEI =4, QD/PEI-PEG=4, QD/Tf-PEI=4, ctrl=1. Regions of interest marked with red circles.

a: QD/Tf-PEG-PEI ventral signal:



b: QD/Tf-PEG-PEI dorsal signal:

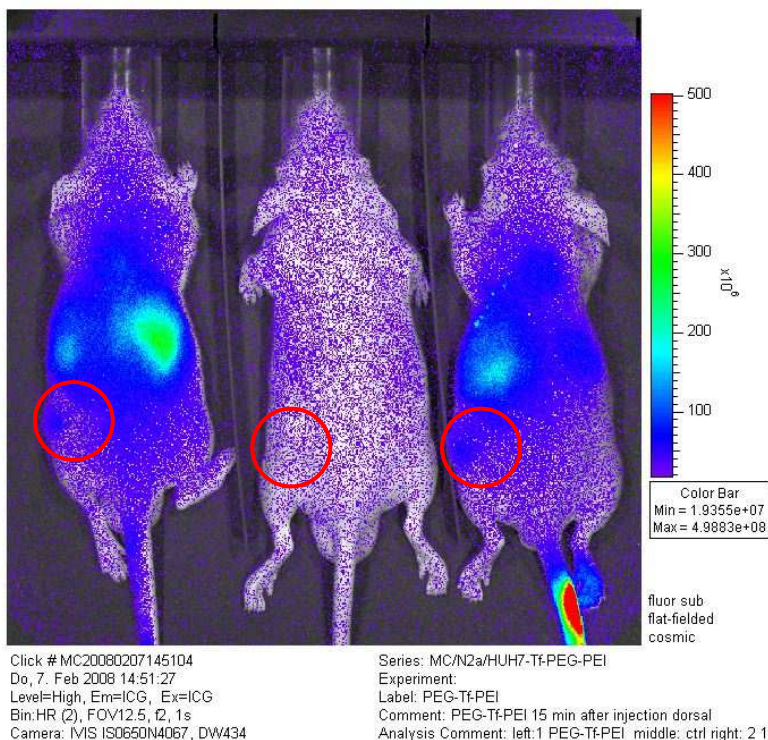
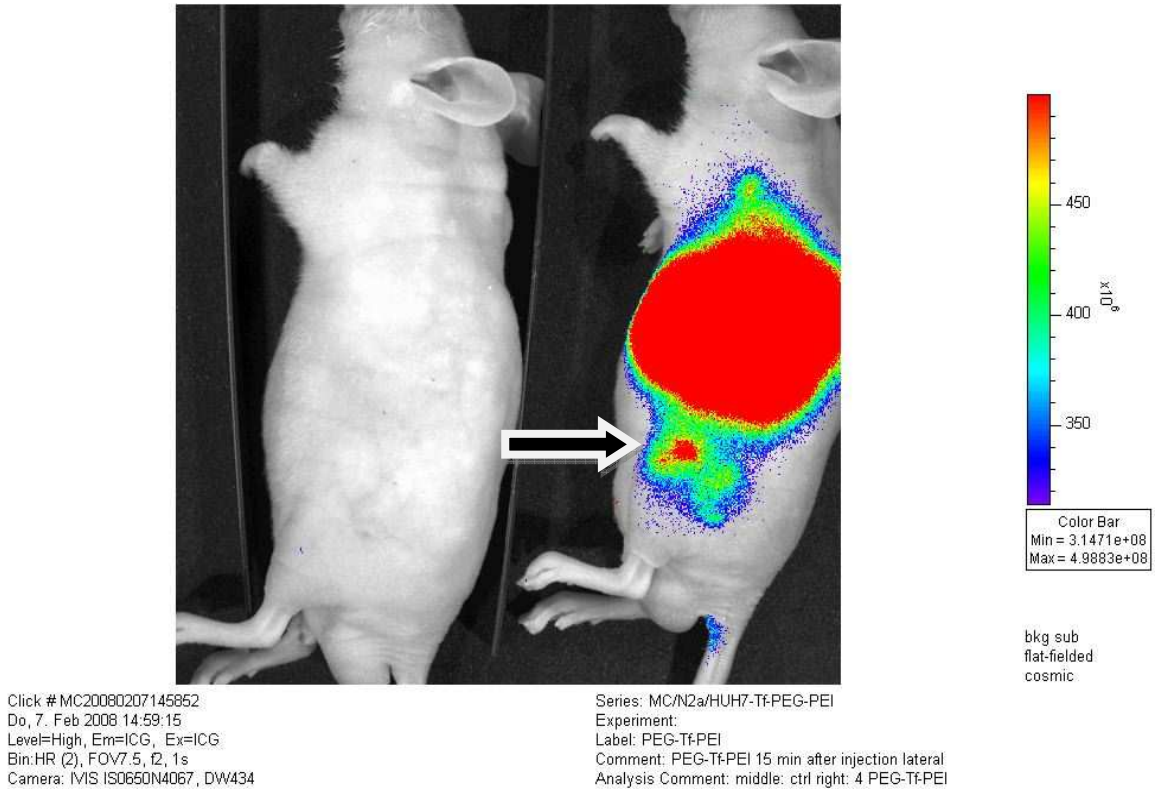


Fig. 2: *in vivo* fluorescence emission signal 15 minutes after iv application of QD/Tf-PEG-PEI conjugates (right) vs HBG buffer (left). Filter ex/em: ICG/ICG.
 n: QD/Tf-PEG-PEI =4, QD/PEI-PEG=4, QD/Tf-PEI=4, ctrl=1.

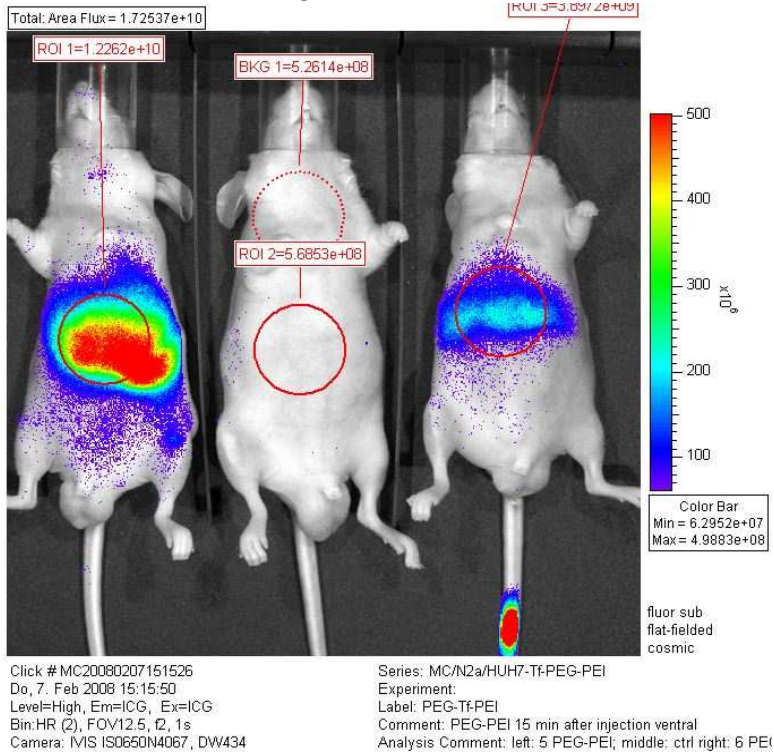
Left lateral image



The image above displays the left side view of a mouse administered with QD/Tf-PEG-PEI conjugates after successful tumor targeting. The fluorescence signal from the core of the hypodermic tumor mass optically reached the same intensity as hepatic tissue.

Fig. 3a,b: *in vivo* fluorescence emission signal 15 minutes after iv application of QD/PEG-PEI conjugates (left and right) vs HBG buffer (middle). Filter ex/em: ICG/ICG); n: QD/Tf-PEG-PEI =4, QD/PEI-PEG=4, QD/Tf-PEI=4, ctrl=1. Regions of interest marked with red circles.

a: QD/PEG-PEI ventral image



b: QD/PEG-PEI left side signal

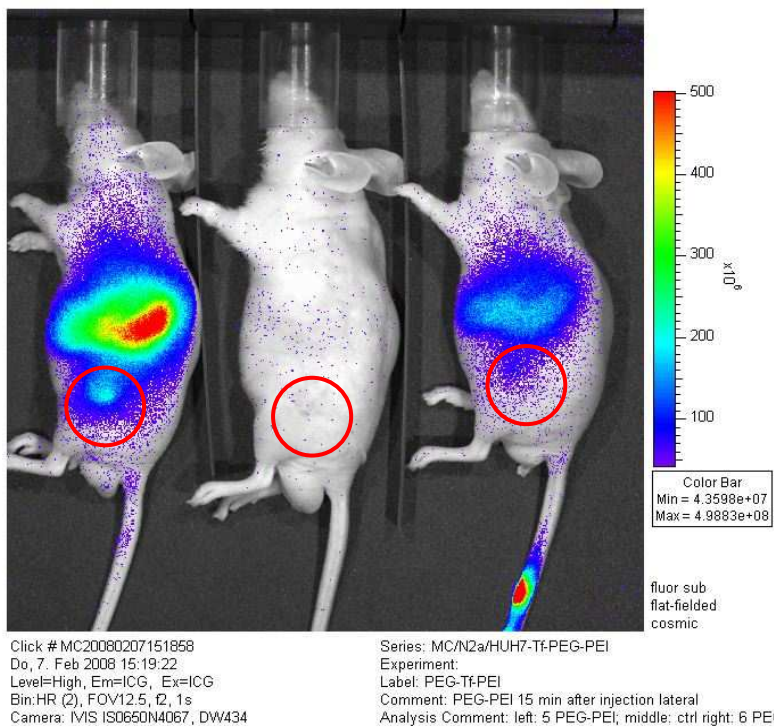
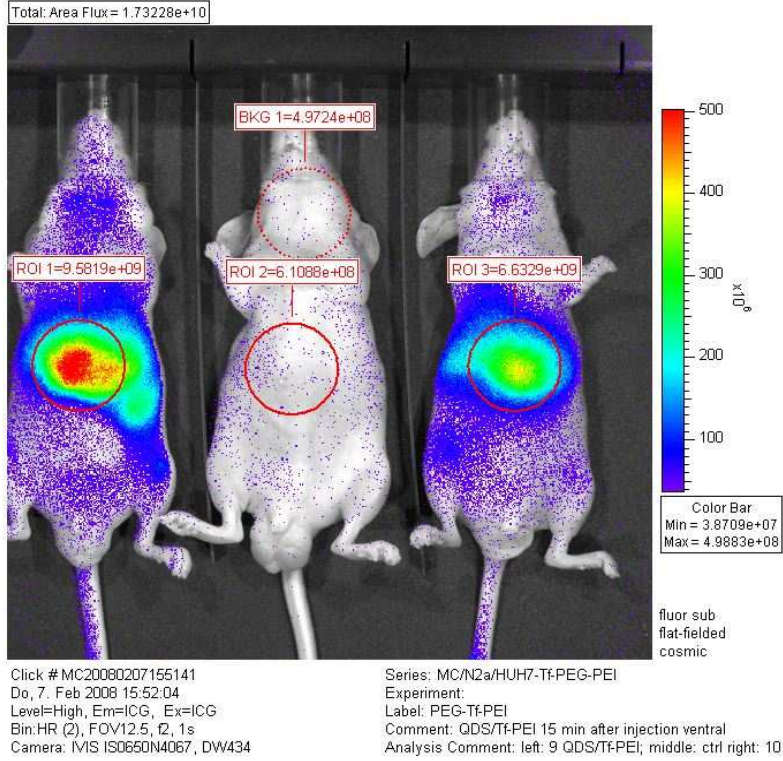


Fig. 4a,b: *in vivo* fluorescence emission signal 15 minutes after iv application of QD/Tf-PEI conjugates (left and right) vs HBG buffer (middle); Filter ex/em: ICG/ICG); n: QD/Tf-PEG-PEI =4, QD/PEI-PEG=4, QD/Tf-PEI=4, ctrl=1. Regions of interest marked with red circles.

a: QD/Tf-PEI ventral image



b: QD/Tf-PEI left side image

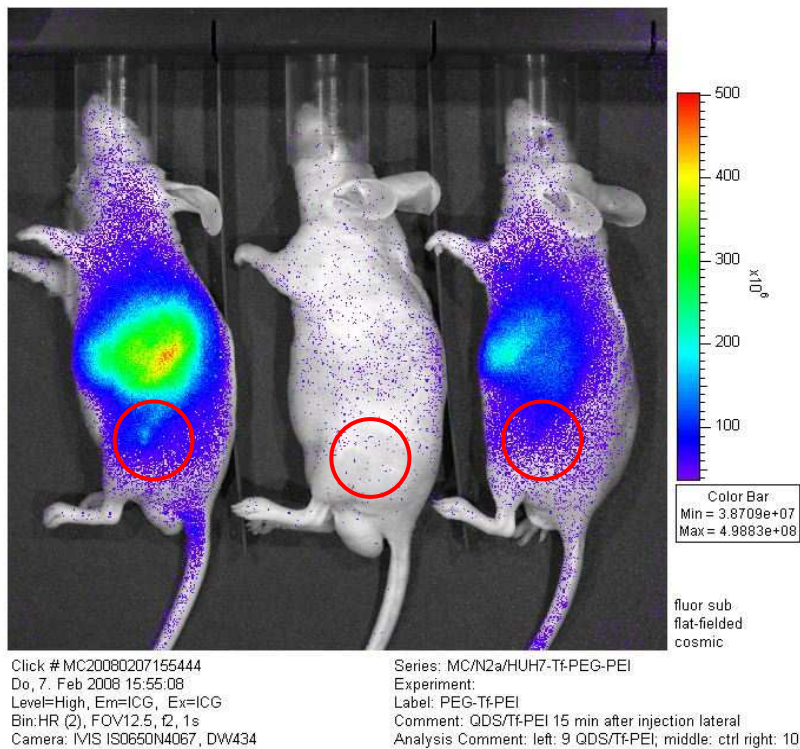
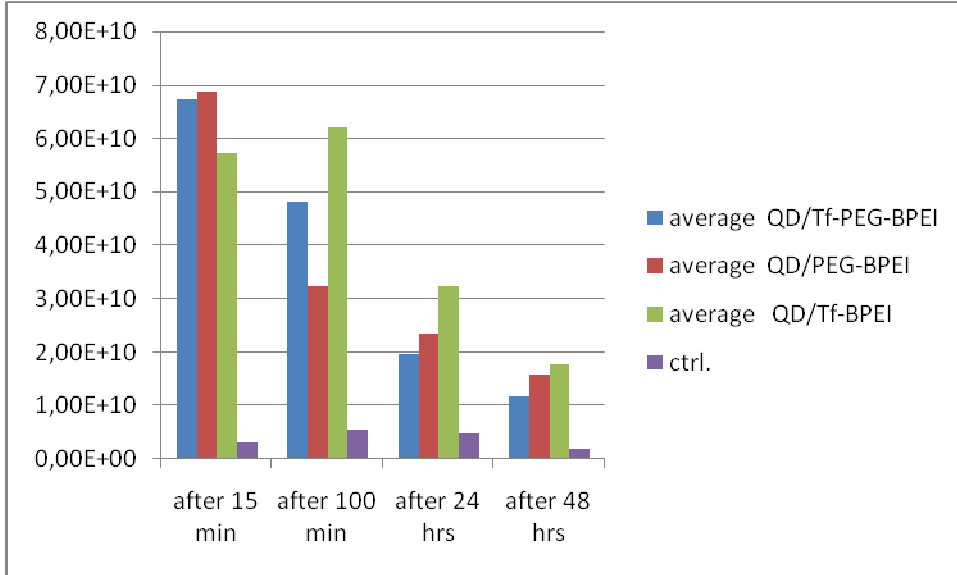
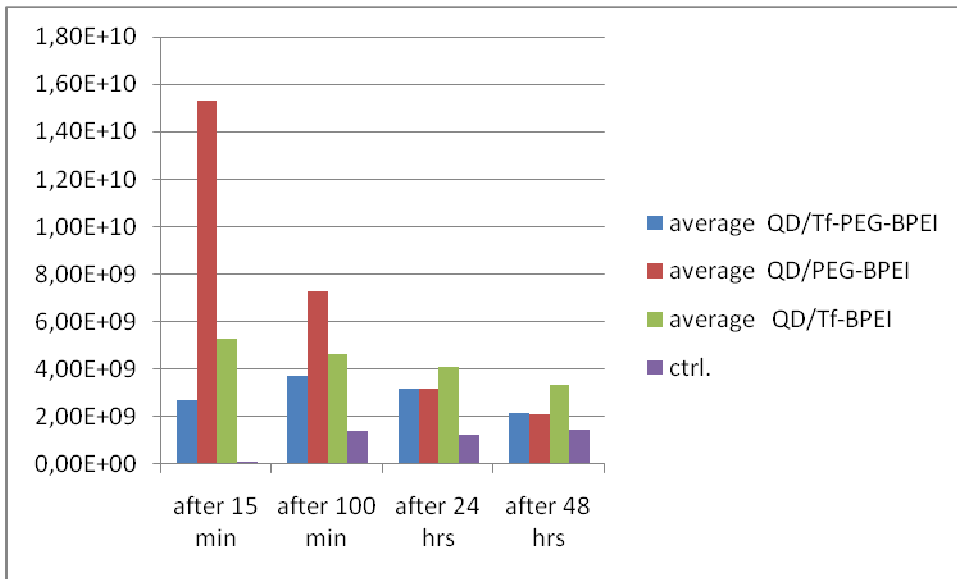


Fig. 5a,b: *in vivo* fluorescence imaging data in photons/sec 15, 100 minutes and 24, 48, and hours after iv administration of QD/Tf-PEG-PEI vs QD/PEG-PEI vs QD/Tf-PEI conjugates vs ctrl (liver and tumor region); n: QD/Tf-PEG-PEI =4, QD/PEI-PEG=4, QD/Tf-PEI=4, ctrl=1.

a: liver



b: tumor



Liver fluorescence decreased 1 hour after systemic administration in comparison to the first measurement 15 minutes after injection. The peak of hepatic accumulation of QD/Tf-PEI conjugates was reached after 2-3 hours observation time and decreased only after 6 hour (*fig. 5a*). The emission of the tumor tissue of QD/PEG-PEI was much higher than in the other groups and gradually decreased over time (*fig. 5b*). This result was also evident in our in vivo images (*fig. 3b*). The other tumor masses displayed good emission signals as well (*fig. 2, 4b*). Imaging results with N2a tumors were similar to those with HUH7 cells. Fluorescence intensity (measured in photons/sec) was comparable in both groups and PEG-shielding positively impacted the results in the same way. We detected strong hepatic emission and an evident signal from tumor tissue in all groups.

4 Discussion

In this study organic fluorescent dyes and quantum dots emitting in the near infrared (NIR) spectral region were utilized for labeling PEI-based non viral gene carriers to observe their bio-distribution in living mice after systemic application.

4.1 Methodological establishments

Our in vivo models consisted of *nu/nu* mice with subcutaneously implanted tumors. Initial experiments were carried out in animals with fur (*Albino Jackson, A/J* mice) but fluorescence from the abdominal organs could not be visualized with satisfying quality because of scattering of emitted fluorescent dye by the fur. Removing superficial hair was possible when implanting subcutaneous tumors into the hind leg^[54] but not applicable to the whole mouse as this would cause unnecessary stress to the animals. *Nu/nu* mice are characterized by almost complete absence of body hair and lack the *FOXN1* gene function, thus determining severe immunodeficiency, almost absent T cell production and no possibility of rejection response towards non-self antigens such as implanted tumor cells and tissues. These are essential requirements for implanting xenograft (like human HUH7 Hepatocellular Carcinoma) and tumors deriving from different mouse strains (N2a Murine Neuroblastoma from A/J mice), that we had already utilized for bioluminescence assays. *FOXN1* gene disruption shows variable phenotypical expressivity within different animals^[55] so that the time between setting of tumor cells and formation of tumor masses as well as velocity of tumor growth is variable. A partial solution to this problem is careful selection of the animals age (between 5 and 8 weeks) in order to minimize variability in tumor growth. Employing younger animals (5-6 weeks) also reduces acute toxic reactions towards PEI-based gene carriers^[21].

We used two tumor cells lines, well-established for in vitro and in vivo gene targeting experiments. Both HUH7 and N2a cells overexpress receptors for biological molecules that can be included in PEI-based conjugates and polyplexes, i.e. EGF-R in HUH7 and Tf-R in N2a. Tumor histology and vascularization have primary impact on tumor targeting after systemic application. Although a broad range of tumor cell lines could be efficiently transfected with PEI-based systems in vitro, only a few of them were amendable to tumor transfection in vivo^[56]: only tumor cell lines leading to tumors with hyper-vascularized structure and leaky vasculature were efficiently transfected

after systemic injection of polyplexes. We utilized N2a and HUH7 model: both tumors are well vascularized and exhibit leaky blood vessels. In HUH7 tumors large blood vessels are found and blood lakes can be observed. In N2a necrotic cores are present when tumors exceed volume of approximately 0.9 cm^3 .

The application of many fluorescent dyes for in vivo imaging is limited by light absorption by abundant components like hemoglobin in blood and chlorophyll contained in the animals feeding, where the latter also emits within the near infrared range. The choice of hairless animals and proper adjustments in image exposure and analysis to eliminate background fluorescence significantly improved the signal-to-noise ratio. The quality of fluorescence signal was further improved by feeding our nu/nu mice with chlorophyll-free mouse chow in order to diminish abdominal auto-fluorescent phenomena.

The biodistribution of fluorescently labeled gene carriers or free dyes was mostly visualized 15 minutes, 120 minutes, 24 hours and 48 hours after the intravenous administration of them. Diffusion throughout the mouse organism, organ accumulation (i.e. in liver, lungs and thyroid) and renal excretion were observed 15 and 120 min after injection. The observation after 24 hours seemed to be the time point adapted for checking tumor tissue specific accumulation. After 48 hours the signal decreased in all organs and body compartments including the tumor masses.

The excision and ex vivo analysis of tumor tissue gave additional information on dye accumulation in the tumors: unlike the organs, which mostly display homogenous parenchymal diffusion of the fluorescent dyes, tumors were often only superficially vascularized and the necrotic core of many masses was not involved in drug diffusion due to the lack of functional blood vessels.

All fluorescent images were taken using ICG/ICG (excitation/emission wavelength of indocyanine green) filter combination because unspecific emissions are not present in this region (see 1.5.2). Fluorescence signal data were mostly edited as *total flux* (photons/sec; see 2.6.1) and compared utilizing a standardized “region of interest” (ROI) surface and identical color bar scales for images to be compared.

We used mostly brPEI25 (branched polyethylenimine, 25 kDa) in biodistribution experiments, sometimes as a block-copolymer with PEG. In general low acute/subacute toxicity was observed: most of the animals survived apparently without severe symptoms the first days after iv injection of PEI-based conjugates. Pulmonary erythrocyte aggregation induced by positively charged PEI is described in the literature^[21]. Acute/subacute mortality rate between 25 and 30 % was observed in some preliminary assays, we had performed using NIR 797/brPEI25-mEGF conjugates and 15-20% with QD/brPEI25-PEG and QD/brPEI25-Tf conjugates. This was most likely due to the age of the animals (>8 weeks) and particles aggregation prior to injection caused by improper particle mixing. Hence all particle preparations were analyzed prior to administration in vivo in following experiments. An average particle diameter

<250 nm was considered suitable for in vivo without inducing mortality. The size of PEI aggregate itself is a very important factor causing toxicities additional to intrinsic PEI toxicity. Similar observations were made by *Wightman et al*^[57], where aggregated polyplexes larger than 200 nm exhibited more pronounced toxicities than small particles. In the current study similar effects were observed when applying aggregates of PEI with QD. In order to prevent aggregate formation PEI was mixed with QD in a low salt buffer (*HEPES-buffered saline*, HBG) reducing aggregate formation. No death cases were observed in animals groups treated with Alexa 750/HD O thanks to reduced particle dimensions of this conjugate. This is in line with OEI and HD O low toxicity reported in a recent article^[21].

4.2 Fluorescence-based in vivo imaging

4.2.1 Fluorescent dyes (Alexa 750 and NIR 797) applications

Alexa Fluor® 750 carboxylic acid, succinimidyl ester is a fluorescent dye suitable for in vivo imaging: it has an amino reactive *succinimidyl ester* group which enables covalent bonding to primary amino groups of the PEIs. The spectral features (ex/em: 749/775 nm) of this dye make it adapted for applications in the near infrared spectrum, least disturbed by non-specific autofluorescence. Alexa 750 was first administered as free dye and then utilized to label brPEI25 and HD O (*OEI core modified with hexane-1,6-diol diacrylate and OEI*). Fifteen minutes after the injection of “free” Alexa 750 a clear signal throughout the whole organism and particularly in bladder, thyroid and liver was detected, where highest signal intensities were measured. When coupled to branched PEI25 or H DO the distribution pattern was clearly different: fluorescence was detected in lungs and liver which corresponds to the distribution patterns of positively loaded polycations when interacting with negatively charged erythrocytes and body cell surfaces. The pulmonary accumulation was lower than the hepatic one and acute/subacute toxicity due to lungs embolism seldom occurred. Hence Alexa 750 is a well suited fluorescent dye for labeling vectors like PEIs. Disadvantages are its very high cost and unpublished chemical structure.

NIR 797 isothiocyanate has spectral and chemical features adapted for in vivo imaging purposes. Excitation/emission (795/835 nm) maxima are within the NIR region and the isothiocyanate group allows covalent bonding to primary amines. When “free” injected at the same dose of Alexa 750 a strong hepatic fluorescence was detected. Unlike Alexa 750 NIR 797 tended to accumulate within the liver and scarcely in thyroid and

lungs. The signal intensity was somehow lower than Alexa 750, but the product is cheaper than Alexa 750 and its molecular structure is known.

4.2.2 Quantum dots applications

All quantum dot formulations that we tested were synthesized by Dr Andrei Susa in the *Photonics and Optoelectronics Work Group* led by Dr Andrey Rogach at the LMU, as recently described in the literature^[58]. We tested quantum dots with different surface modifications and finally selected as standard anionic QD with *Cd-Te* core, S-C3H6-COO⁻ groups on the surface and average size of 7 nm. Their fluorescence emission properties (ex/em: 500-550/750-800 nm) were compatible with our standard setup and they gave a bright fluorescent signal after illumination. After systemic administration QD widely diffused through the body compartments and fluids including bone marrow, skin, joints and salivary glands, partially reproducing the diffusion pattern observed with other small particles like fluorescently labeled OEI (HD-O). In order to reduce acute toxicity of QD/PEI particles, we standardized the mixture modalities, avoiding formation of aggregates after complexing. We verified that a strict control of particle dimensions considerably reduced mortality. In further experiments QD/PEI conjugates containing murine EGF (mEGF) or human transferrin (hTf), with or without PEG-shielding, were used for tumor targeting studies in HUH7 or N2a tumor bearing animals.

4.3 Conclusions

We assessed that PEI is a very suitable device for low-invasive in vivo transfection of tumor cells in rodents. Our findings showed that QD are cheap and reliable fluorescent markers. They were the best method of labeling PEI-based gene therapy vectors in our experience^[59]. QD displayed much stronger fluorescence at lower concentrations than organic dyes (Alexa 750 and NIR 797) and enabled low-cost experiments. In addition their inorganic structure can be easily modified and adapted to several experimental or clinical issues; they are low toxic and are designed and produced by a partner laboratory.

EGF and Tf enabled selective targeting of tumor cell lines expressing specific receptors for these molecules. Their integration into fluorescently labeled PEI-based conjugates and polyplexes positively impacted tumor targeting and enhanced fluorescent signal from tumor tissue.

We got the best results using QD/PEI-EGF and QD/PEI-Tf conjugates in HUH and N2a cell tumors in vivo. PEG-shielding displayed in both cases a positive impact on tumor targeting. A clear fluorescent signal specific for tumor tissue was detected; the imaging

software used allowed quantitative analysis of this signal. These are the best devices for fluorescent labeled gene vectors in our experience.

In the literature^{[25][26][27][28]} optical imaging methods are often compared with other imaging technologies like micro-PET, CT and MR. Controlling systems of gene delivering based on fluorescent methods enable easy application and measurement procedures, minor costs and no use of radiotracers or waiting for decay times. They require furthermore shorter scanning times and many animals can be analyzed simultaneously. Compared to PET however, they deliver semi-quantitative results and minor depth of analysis. In addition signals are often confounded by intrinsic fluorescence of biomolecules. PET and MR moreover offer quantitative analysis and tomographic images, easily transferable to clinical applications. Obtaining quantitative and reproducible informations is then a major issue for optical i.e. fluorescence and bioluminescence methods.

Future in vivo experiments with QD-labeled PEI-EGF or PEI-transferrin conjugates or polyplexes with PEG-shielding performed by our research group should focus on reproducibility, statistical relevance and standardizing all experimental procedure conditions.

5a Summary

Gene therapy is a research area where nucleic acids are transferred into cells to treat neoplastic, metabolic and hereditary diseases. Delivery of genetic material into living organisms can be achieved with viral or non-viral vectors. Viral gene carriers are very efficient but present some major disadvantages due to their pathogenicity and immunogenicity. Non-viral carriers are based on synthetic molecules binding and condensing nucleic acids into small, virus-like particles. **The aim of this thesis was to study the biodistribution and tumor targeting properties of non-viral gene vectors based on polyethylenimine (PEI) after systemic injection into mice.** The gene vectors were labeled with fluorescent dyes emitting in the near infrared (NIR), which allowed studying their bio-distribution in living animal over time. Owing to its amine groups PEI has a high positive charge density that enables electrostatic interactions with negatively charged nucleic acids and their efficient compaction into nucleic acid-PEI complexes, called *polyplexes*. The net positive surface charge of these polyplexes permits interactions with negatively charged cell surface molecules, thus leading to their internalization into the cell. To avoid unspecific interactions with blood components and non-target tissues after intravenous application, polyplexes were shielded with the hydrophilic molecule *polyethylene glycol* (PEG). PEI-based gene carrier systems were tested on two subcutaneously implanted tumor types: *Human Hepatocellular Carcinoma* (HUH7) and *Murine Neuroblastoma* (N2a). HUH7 cells express *epidermal growth factor* (EGF) receptors, while N2a cells express *transferrin* (Tf) receptors on their surfaces. To enable targeting of the polyplexes to the tumor cells, polyplexes were generated containing the ligands EGF and Tf for targeting of HUH7 cells and N2a cells respectively. The targeted polyplexes were then intravenously injected into immunodeficient, athymic *nu/nu* mice in which HUH7 or N2a tumor cells had been previously set under their skin. To monitor the biodistribution of polyplexes throughout the mouse organism and to evaluate their gene delivery capability into the neoplastic cells, polyplexes were labeled with fluorescent dyes (Alexa 750, NIR 797) or near infrared emitting quantum dots (QD), whose fluorescent expression signal was detected and analyzed with a device for imaging *in vivo*. All fluorescent molecules and quantum dots were biocompatible and non-toxic. They emitted light in the near infrared area of the spectrum, thus avoiding overlapping phenomena with autofluorescent biomolecules or absorption of light by hemoglobin. With all dyes used for polyplex labeling a fluorescent signal could be observed in organs like liver and lung being clearly distinguishable from background fluorescence. Among the fluorescent molecules tested, quantum dots were identified being the most suitable method for *in vivo* studies, showing the highest signal/noise ratios. PEG-shielding led to best tumor targeting efficiency when administering EGF or Tf-targeted polyplexes in mice bearing HUH7 and N2a tumors respectively. A clear fluorescent signal specific for tumor tissue was detected; the imaging software used allowed quantitative analysis of this signal. For this reason this system is now available for further experimental applications.

5b Zusammenfassung

Gentherapie befasst sich mit der Insertion von Nukleinsäuren in Zellen, um neoplastische, metabolische sowie hereditäre Krankheiten zu behandeln. Der Transfer von genetischem Material in einen lebenden Organismus kann durch die Verwendung viraler oder nicht viraler Vektoren erfolgen. Viren sind zwar sehr effektiv, aber ihre Anwendung birgt auch Probleme, die meist durch ihre Pathogenität und Immunogenität bedingt sind. Nicht virale Vektoren sind synthetische Moleküle, die Nukleinsäuren in kleine, virusähnliche Partikeln einbinden und kondensieren. **Das Ziel dieser Doktorarbeit war es die Bioverteilung und die gezielt gegen den Tumor gerichteten Eigenschaften von Genvektoren, die auf Polyethylenimin (PEI) basieren, nach intravenöser Injektion in Mäusen zu untersuchen.**

Die Genvektoren wurden mit fluoreszierenden Farbstoffen markiert, die Licht innerhalb des Nahinfrarot-Bereiches (NIR) emittieren und im Zeitverlauf die Beobachtung der Bioverteilung in lebenden Tieren erlauben. Dank seiner Aminogruppen hat PEI eine stark positive Ladung, die gute elektrostatische Bindungen zu negativ geladenen Nukleinsäuren erlaubt, mit denen es zum Aufbau eines Nukleinsäure-PEI-Komplexes führt, der *Polyplex* genannt wird. Die positiv geladene Oberfläche von PEI ermöglicht auch Interaktionen mit negativ geladenen Zelloberflächen mit der Folge einer Internalisierung des Komplexes. Um unspezifische Interaktionen mit Blutbestandteilen oder anderen als dem Zielgewebe zu verhindern, wurden die Polyplexe mit dem hydrophilen Molekül *Polyethylenglycol* (PEG) umhüllt. Diese auf PEI-Basis synthetisierten Gencarrier-Systeme wurden dann an der *humanen Leberzell Karzinom* Linie HUH7 und der *Maus Neuroblastom* Linie N2a getestet. Die HUH7-Zelllinie exprimiert Rezeptoren für den *epidermalen Wachstumsfaktor* (EGF) und die N2a-Zelllinie Rezeptoren für *Transferrin* (Tf) auf ihrer Oberfläche. Um ein gezieltes Tumor-Targeting von HUH7- oder N2a-Zellen zu ermöglichen, wurden Polyplexe erstellt, die EGF bzw. Transferrin an ihrer Oberfläche enthalten. Diese oberflächlich modifizierten Komplexe wurden dann intravenös in athymische *nu/nu* Mäuse verabreicht, die vorher HUH7- oder N2a-Zellen subkutan implantiert bekommen hatten. Um die Verteilung der Polyplexe als experimentelle genetische Medikamente innerhalb des murinen Organismus zu beobachten und die Akkumulation im Tumorgewebe auszumessen, waren sie mit fluoreszierenden Farbstoffen (*Alexa 750*, *NIR 797*) oder im Nahinfraroten emittierenden *Quantum Dots* (QD) markiert, deren Fluoreszenzsignalexpression mittels eines Messungsgerät für in vivo Analysen analysiert wurde.

Alle fluoreszierenden Moleküle und Quantum Dots zeigten sich biokompatibel und nicht toxisch und emittierten Licht innerhalb des nahinfraroten Bereichs des Spektrums. Damit konnte die Lichtabsorption durch Hämoglobin ebenso vermieden werden, wie sämtliche Überschneidungsphänomene mit der Fluoreszenz anderer Biomoleküle. Bei allen für die Markierung von Polyplexen verwendeten Farbstoffen und den Quantum Dots wurde ein fluoreszierendes Signal in Organen wie Leber und Lunge beobachtet, das eindeutig von der Hintergrundfluoreszenz unterschieden werden konnte. Unter den getesteten fluoreszierenden Substanzen konnten Quantum Dots als beste Methode für die Fluoreszenzmarkierung festgelegt werden. Hier war das Signal am deutlichsten von störender Hintergrundstrahlung zu unterscheiden. Das PEG-Shielding erlaubte die höchste Effizienz im Tumor-Targeting vor allem bei Applikation von EGF- bzw. Tf-markierten Polyplexen in Mäusen, die HUH7- bzw. den N2a-Tumor trugen. Ein ausgeprägtes und für Tumorgewebe spezifisches Signal konnte hier beobachtet werden. Die verwendete Imaging-Software für in vivo Applikationen ermöglichte eine quantitative Signalanalyse. Damit steht dieses System für weitere experimentelle Anwendungen zur Verfügung.

6 Appendix

6.1 Abbreviations

<i>brPEI, bPEI</i>	<i>branched polyethylenimine</i>
<i>ctrl</i>	<i>control</i>
<i>Cy</i>	<i>cyanine</i>
<i>DMSO</i>	<i>dimethyl sulfoxide</i>
<i>EDTA</i>	<i>ethylenediamin tetracetic acid</i>
<i>EGF</i>	<i>epithelial growth factor</i>
<i>EtBr</i>	<i>ethidium bromide</i>
<i>FACS</i>	<i>fluorescent-activated cell sorting</i>
<i>FCS</i>	<i>fetal calf serum</i>
<i>GFP</i>	<i>green fluorescent protein</i>
<i>HBG</i>	<i>HEPES-buffered glucose</i>
<i>HBS</i>	<i>HEPES-buffered saline</i>
<i>HCl</i>	<i>hydrochloric acid</i>
<i>HD O</i>	<i>OEI core modified with hexane-1,6-diol diacrylate and OEI</i>
<i>HEPES</i>	<i>4-(2-hydroxyethyl)-1-piperazineethanesulfonic acid</i>
<i>hTf</i>	<i>human transferrin</i>
<i>HUH7</i>	<i>Human Hepatocellular Carcinoma HuH7</i>
<i>ICG</i>	<i>indocyanine green</i>
<i>iv</i>	<i>intravenous</i>
<i>mEGF</i>	<i>murine epithelial growth factor</i>
<i>MRI</i>	<i>magnetic resonance imaging</i>
<i>mRNA</i>	<i>messenger RNA</i>
<i>Mw</i>	<i>molecular weight</i>
<i>N/P ratio</i>	<i>molar ratio of PEI nitrogen to DNA phosphate</i>
<i>N2a</i>	<i>Murine Neuroblastoma N2a</i>
<i>NaCl</i>	<i>sodium chloride</i>

<i>NIR</i>	<i>near-infrared</i>
<i>OEI</i>	<i>oligoethylenimine</i>
<i>PBS</i>	<i>phosphate-buffered saline</i>
<i>PEG</i>	<i>polyethylene glycol</i>
<i>PEI</i>	<i>polyethylenimine</i>
<i>PEI lin, lnPEI</i>	<i>linear polyethylenimine</i>
<i>PET</i>	<i>positron emission tomography</i>
<i>QD</i>	<i>quantum dots</i>
<i>ROI</i>	<i>region of interest</i>
<i>RT</i>	<i>room temperature</i>
<i>siRNA</i>	<i>small interfering RNA</i>
<i>SPECT</i>	<i>single photon emission tomography</i>
<i>Tf</i>	<i>transferrin</i>
<i>TBE</i>	<i>tris-borate EDTA</i>
<i>TNBS</i>	<i>trinitrobenzenesulphonic acid assay</i>
<i>vs</i>	<i>versus</i>

7 Acknowledgments

I am very grateful to Prof. Georg Enders for presenting my work to the Faculty of Medicine of the LMU, for his precious advice and his great helpfulness.

Many thanks to Prof. Ernst Wagner for giving me the opportunity of working in his research group and his fair way of motivating and supporting our scientific activity.

Without Dr. Manfred Ogris, who helped me with his great experience in fluorescence imaging and in vivo assays, this work would not have been possible. I thank him sincerely for his great scientific competence, his humor and patience, his kind way of being an example for all of us.

Many thanks go also to Dr. Arkadi Zintchenko for his indispensable assistance in synthesis and analysis of our gene vectors.

To all technical assistants of the Workgroup Wagner at the Department of Pharmacy for their help and sympathy, thank you!

Thank you for everything and forever

Grazie per tutto, e per sempre ...

8 References

¹ **Wagner E.**

Advances in cancer gene therapy: tumor-targeted delivery of therapeutic pDNA, siRNA, and dsRNA nucleic acids.

J BUON. 2007 Sep;12 Suppl 1:S77-82. Review.

² **Ogris M.**

Nucleic acid based therapeutics for tumor therapy.

Anticancer Agents Med Chem. 2006 Nov;6(6):563-70. Review.

³ **Meyer M, Wagner E.**

Recent developments in the application of plasmid DNA-based vectors and small interfering RNA therapeutics for cancer.

Hum Gene Ther. 2006 Nov;17(11):1062-76. Review.

⁴ **Whitehead KA, Langer R, Anderson DG.**

Knocking down barriers: advances in siRNA delivery.

Nat Rev Drug Discov. 2009 Feb;8(2):129-38.

⁵ **Gao K, Huang L.**

Nonviral Methods for siRNA Delivery.

Mol Pharm. 2008 Dec 30. Review.

⁶ **Robbins PD, Ghivizzani SC.**

Viral vectors for gene therapy.

Pharmacol Ther. 1998 Oct;80(1):35-47. Review.

⁷ **Damjanovic D, Zhang X, Mu J, Medina MF, Xing Z.**

Organ distribution of transgene expression following intranasal mucosal delivery of recombinant replication-defective adenovirus gene transfer vector.

Genet Vaccines Ther. 2008 Feb 8;6(1):5

⁸ **Beard BC, Keyser KA, Trobridge GD, Peterson LJ, Miller DG, Jacobs M, Kaul R, Kiem HP.**

Unique integration profiles in a canine model of long-term repopulating cells transduced with gammaretrovirus, lentivirus, or foamy virus.

Hum Gene Ther. 2007 May;18(5):423-34.

⁹ **Pagnotto MR, Wang Z, Karpie JC, Ferretti M, Xiao X, Chu CR.**

Adeno-associated viral gene transfer of transforming growth factor-beta1 to human mesenchymal stem cells improves cartilage repair.

Gene Ther. 2007 May;14(10):804-13. Epub 2007 Mar 8.

-
- ¹⁰ **Hassan MH, Khatoon N, Curiel DT, Hamada FM, Arafa HM, Al-Hendy A.**
Toward gene therapy of uterine fibroids: targeting modified adenovirus to human leiomyoma cells.
Hum Reprod. 2008 Jan 8.
- ¹¹ **Mancheño-Corvo P, Martín-Duque P.**
Viral gene therapy.
Clin Transl Oncol. 2006 Dec;8(12):858-67.
- ¹² **Simões S, Filipe A, Faneca H, Mano M, Penacho N, Düzgünes N, de Lima MP.**
Cationic liposomes for gene delivery.
Expert Opin Drug Deliv. 2005 Mar;2(2):237-54.
- ¹³ **Hassani Z, Lemkine GF, Erbacher P, Palmier K, Alfama G, Giovannangeli C, Behr JP, Demeneix BA.**
Lipid-mediated siRNA delivery down-regulates exogenous gene expression in the mouse brain at picomolar levels.
J Gene Med. 2005 Feb;7(2):198-207.
- ¹⁴ **Boussif O, Lezoualc'h F, Zanta MA, Mergny MD, Scherman D, Demeneix B, Behr JP.**
A versatile vector for gene and oligonucleotide transfer into cells in culture and in vivo: polyethylenimine.
Proc Natl Acad Sci U S A. 1995 Aug 1;92(16):7297-301.
- ¹⁵ **Demeneix B, Behr JP.**
Polyethylenimine (PEI).
Adv Genet. 2005;53PA:215-230.
- ¹⁶ **Kopatz I, Remy JS, Behr JP.**
A model for non-viral gene delivery: through syndecan adhesion molecules and powered by actin.
J Gene Med. 2004 Jul;6(7):769-76.
- ¹⁷ **Erbacher P, Bettinger T, Belguise-Valladier P, Zou S, Coll JL, Behr JP, Remy JS.**
Transfection and physical properties of various saccharide, poly(ethylene glycol), and antibody-derivatized polyethylenimines (PEI).
J Gene Med. 1999 May-Jun;1(3):210-22.
- ¹⁸ **Park MR, Kim HW, Hwang CS, Han KO, Choi YJ, Song SC, Cho MH, Cho CS.**
Highly efficient gene transfer with degradable poly(ester amine) based on poly(ethylene glycol) diacrylate and polyethylenimine in vitro and in vivo.
J Gene Med. 2008 Feb;10(2):198-207.
- ¹⁹ **Zhang XQ, Intra J, Salem AK.**
Comparative study of poly (lactic-co-glycolic acid)-poly ethyleneimine-plasmid DNA microparticles prepared using double emulsion methods.
J Microencapsul. 2008 Feb;25(1):1-12.
- ²⁰ **Kunath K, von Harpe A, Petersen H, Fischer D, Voigt K, Kissel Z, Bickel U.**
The Structure of PEG-Modified Poly(Ethylene Imines) Influences Biodistribution and Pharmacokinetics of Their Complexes with NF-kB Decoy in Mice.
Pharmaceutical Research, Vol. 19, No. 6, June 2002 (© 2002).

-
- ²¹ **Boeckle S, von Gersdorff K, van der Piepen S, Culmsee C, Wagner E, Ogris M.**
Purification of polyethylenimine polyplexes highlights the role of free polycations in gene transfer.
J Gene Med. 2004 Oct;6(10):1102-11.
- ²² **Chollet P, Favrot MC, Hurbin A, Coll JL.**
Side-effects of a systemic injection of linear polyethylenimine-DNA complexes.
J Gene Med. 2002 Jan-Feb;4(1):84-91.
- ²³ **Sharma VK, Thomas M, Klivanov AM.**
Mechanistic studies on aggregation of polyethylenimine-DNA complexes and its prevention.
Biotechnol Bioeng. 2005 Jun 5;90(5):614-20.
- ²⁴ **Ogris M, Brunner S, Schüller S, Kircheis R, Wagner E.**
PEGylated DNA/transferrin-PEI complexes: reduced interaction with blood components, extended circulation in blood and potential for systemic gene delivery.
Gene Ther. 1999 Apr;6(4):595-605.
- ²⁵ **Russ V, Elfberg H, Thoma C, Kloeckner J, Ogris M, Wagner E.**
Novel degradable oligoethylenimine acrylate ester-based pseudodendrimers for in vitro and in vivo gene transfer.
Gene Ther. 2008 Jan;15(1):18-29. Epub 2007 Oct 25.
- ²⁶ **Kristian Rätty J, Liimatainen T, Unelma Kaikkonen M, Gröhn O, Jumani Airene K, Ylä-Herttuala S.**
Non-invasive Imaging in Gene Therapy.
Mol Ther. 2007 Sep;15(9):1579-86. Epub 2007 Jun 19. Review.
- ²⁷ **Belmar C, So PW, Vassaux G, Moleiro-Sanemeterio V, Martín-Duque P.**
Non-invasive genetic imaging for molecular and cell therapies of cancer.
Clin Transl Oncol. 2007 Nov;9(11):703-14.
- ²⁸ **Winkeler A, Sena-Esteves M, Paulis LE, Li H, Waerzeggers Y, Rückriem B, Himmelreich U, Klein M, Monfared P, Rueger MA, Heneka M, Vollmar S, Hoehn M, Fraefel C, Graf R, Wienhard K, Heiss WD, Jacobs AH.**
Switching on the lights for gene therapy.
PLoS ONE. 2007 Jun 13;2(6):e528.
- ²⁹ **Dobrovín M, Serganova I, Mayer-Kuckuk P, Ponomarev V, Blasberg RG.**
Multimodality in vivo molecular-genetic imaging.
Bioconjug Chem. 2004 Nov-Dec;15(6):1376-88.
- ³⁰ **Rao J, Dragulescu-Andrasi A, Yao H.**
Fluorescence imaging in vivo: recent advances.
Curr Opin Biotechnol. 2007 Feb;18(1):17-25. Epub 2007 Jan 17. Review.
- ³¹ **D. C. Prasher, V. K. Eckenrode, W. W. Ward, F. G. Prendergast, M. J. Cormier**
Primary structure of the *Aequorea victoria* green-fluorescent protein.
Gene. Band 111, 1992, S. 229-233.
- ³² **Bucci E, Malak H, Fronticelli C, Gryczynski I, Laczko G, Lakowicz JR.**
Time-resolved emission spectra of hemoglobin on the picosecond time scale.
Biophys Chem. 1988 Dec;32(2-3):187-98.

-
- ³³ **Detter C, Wipper S, Russ D, Iffland A, Burdorf L, Thein E, Wegscheider K, Reichenspurner H, Reichart B.**
Fluorescent cardiac imaging: a novel intraoperative method for quantitative assessment of myocardial perfusion during graded coronary artery stenosis.
Circulation. 2007 Aug 28;116(9):1007-14. Epub 2007 Aug 7.
- ³⁴ **Koyama T, Tsubota A, Nariai K, Mitsunaga M, Yanaga K, Takahashi H.**
Novel biomedical imaging approach for detection of sentinel nodes in an experimental model of gastric cancer.
Br J Surg. 2007 Aug;94(8):996-1001.
- ³⁵ **Alacam B, Yazici B, Intes X, Nioka S, Chance B.**
Pharmacokinetic-rate images of indocyanine green for breast tumors using near-infrared optical methods.
Phys Med Biol. 2008 Feb 21;53(4):837-59. Epub 2008 Jan 15.
- ³⁶ **Unno N, Suzuki M, Yamamoto N, Inuzuka K, Sagara D, Nishiyama M, Tanaka H, Konno H.**
Indocyanine green fluorescence angiography for intraoperative assessment of blood flow: a feasibility study.
Eur J Vasc Endovasc Surg. 2008 Feb;35(2):205-7. Epub 2007 Oct 26.
- ³⁷ **Wakaiki S, Maehara S, Abe R, Tsuzuki K, Igarashi O, Saito A, Itoh N, Yamashita K, Izumisawa Y.**
Indocyanine green angiography for examining the normal ocular fundus in dogs.
J Vet Med Sci. 2007 May;69(5):465-70.
- ³⁸ **Hoshino A, Manabe N, Fujioka K, Suzuki K, Yasuhara M, Yamamoto K.**
Use of fluorescent quantum dot bioconjugates for cellular imaging of immune cells, cell organelle labeling, and nanomedicine: surface modification regulates biological function, including cytotoxicity.
J Artif Organs. 2007;10(3):149-57. Epub 2007 Sep 20. Review.
- ³⁹ **Soo Choi H, Liu W, Misra P, Tanaka E, Zimmer JP, Itty Ipe B, Bawendi MG, Frangioni JV.**
Renal clearance of quantum dots.
Nat Biotechnol. 2007 Oct;25(10):1165-70. Epub 2007 Sep 23.
- ⁴⁰ **Ballou B, Ernst LA, Andreko S, Harper T, Fitzpatrick JA, Waggoner AS, Bruchez MP.**
Sentinel lymph node imaging using quantum dots in mouse tumor models.
Bioconjug Chem. 2007 Mar-Apr;18(2):389-96. Epub 2007 Jan 31.
- ⁴¹ **Iga AM, Robertson JH, Winslet MC, Seifalian AM.**
Clinical potential of quantum dots.
J Biomed Biotechnol. 2007;2007(10):76087.
- ⁴² **Pietryga JM, Werder DJ, Williams DJ, Casson JL, Schaller RD, Klimov VI, Hollingsworth JA.**
Utilizing the Lability of Lead Selenide to Produce Heterostructured Nanocrystals with Bright, Stable Infrared Emission.
J Am Chem Soc. 2008 Mar 15;
- ⁴³ **Ogris M, Wagner E.**
Tumor-targeted gene transfer with DNA polyplexes.
Somat Cell Mol Genet. 2002 Nov;27(1-6):85-95. Review.

-
- ⁴⁴ **Ogris M, Walker G, Blessing T, Kircheis R, Wolschek M, Wagner E.**
Tumor-targeted gene therapy: strategies for the preparation of ligand-polyethylene glycol-polyethylenimine/DNA complexes.
J Control Release. 2003 Aug 28;91(1-2):173-81.
- ⁴⁵ **Kursa M, Walker GF, Roessler V, Ogris M, Roedl W, Kircheis R, Wagner E.**
Novel shielded transferrin-polyethylene glycol-polyethylenimine/DNA complexes for systemic tumor-targeted gene transfer.
Bioconjug Chem. 2003 Jan-Feb;14(1):222-31.
- ⁴⁶ **Kircheis R, Wightman L, Schreiber A, Robitza B, Rössler V, Kursa M, Wagner E.**
Polyethylenimine/DNA complexes shielded by transferrin target gene expression to tumors after systemic application.
Gene Ther. 2001 Jan;8(1):28-40.
- ⁴⁷ **Wolschek MF, Thallinger C, Kursa M, Rössler V, Allen M, Lichtenberger C, Kircheis R, Lucas T, Willheim M, Reinisch W, Gangl A, Wagner E, Jansen B.**
Specific systemic nonviral gene delivery to human hepatocellular carcinoma xenografts in SCID mice.
Hepatology. 2002 Nov;36(5):1106-14.
- ⁴⁸ **Blessing T, Kursa M, Holzhauser R, Kircheis R, Wagner E.**
Different strategies for formation of PEGylated EGF-conjugated PEI/DNA complexes for targeted gene delivery.
Bioconjug Chem. 2001 Jul-Aug;12(4):529-37.
- ⁴⁹ **Zintchenko A, Konák C.**
Interaction of DNA/polycation complexes with phospholipids: stabilizing strategy for gene delivery.
Macromol Biosci. 2005 Dec 15;5(12):1169-74.
- ⁵⁰ **Zintchenko A, Ogris M, Wagner E.**
Temperature dependent gene expression induced by PNIPAM-based copolymers: potential of hyperthermia in gene transfer.
Bioconjug Chem. 2006 May-Jun;17(3):766-72.
- ⁵¹ **Zintchenko A, Konák C.**
Interaction of DNA/polycation complexes with phospholipids: stabilizing strategy for gene delivery.
Macromol Biosci. 2005 Dec 15;5(12):1169-74.
- ⁵² **Zintchenko A, Ogris M, Wagner E.**
Temperature dependent gene expression induced by PNIPAM-based copolymers: potential of hyperthermia in gene transfer.
Bioconjug Chem. 2006 May-Jun; 17(3):766-72.
- ⁵³ **Fahrmeir J, Gunther M, Tietze N, Wagner E, Ogris M.**
Electrophoretic purification of tumor-targeted polyethylenimine-based polyplexes reduces toxic side effects in vivo
Journal of Controlled Release. 2007 Oct; 122(3):236-245.
- ⁵⁴ **Schwerdt A, Zintchenko A, Concia M, Roesen N, Fisher KD, Lindner LH, Issels RD.**
Hyperthermia induced targeting of thermosensitive gene carriers to tumors.
Hum Gene Ther. 2008 Aug 26.

⁵⁵ **Fogh J; Giovanella M.**

The Nude Mouse in Experimental and Clinical Research (Vol.1)
Academic Press, 1978.

⁵⁶ **Smrekar B, Wightman L, Wolschek MF, Lichtenberger C, Ruzicka R, Ogris M, Rödl W, Kursa M, Wagner E, Kircheis R.**

Tissue-dependent factors affect gene delivery to tumors in vivo.
Gene Ther. 2003 Jul;10(13):1079-88.

⁵⁷ **Wightman L, Kircheis R, Rössler V, Carotta S, Ruzicka R, Kursa M, Wagner E.**

Different behavior of branched and linear polyethylenimine for gene delivery in vitro and in vivo.
J Gene Med. 2001 Jul-Aug;3(4):362-72.

⁵⁸ **Rogach AL.**

Aqueous synthesis of thiol-capped CdTe nanocrystals: State-of-the-art.
Journal of Physical Chemistry C 111(2007): 14628-14637.

⁵⁹ **Zintchenko A, Susa AS, Concia M, Feldmann J, Wagner E, Rogach AL, Ogris M.**

Drug Nanocarriers Labeled With Near-infrared-emitting Quantum Dots (Quantoplexes): Imaging Fast Dynamics of Distribution in Living Animals.
Mol Ther. 2009 Aug 25.